PE&RS
August 2020
Volume 86, Number 8
PHOTOGRAMMETRIC ENGINEERING & REMOTE SENSING
The official journal for imaging and geospatial information science and technology

NEW
AWARDS UP TO $500K

INNOVATE
TRANSFORM OUR FUTURE

R&D FUNDING PROGRAM

The National Reconnaissance Office Director's Innovation Initiative (DII) Program funds cutting-edge scientific research in a high-risk, high-payoff environment to discover innovative concepts and creative ideas that transform overhead intelligence capabilities and systems for future national security intelligence needs. The program seeks the brightest minds and breakthrough technologies from industry, academia, national laboratories, and U.S. government agencies.

Visit the website for Broad Agency Announcement and Government Sources Sought Announcement requirements.

703.808.2769

NATIONAL RECONNAISSANCE OFFICE
UNITED STATES OF AMERICA

www.nro.gov/Business-Innovation-Opportunities

INDUSTRYNEWS

To have your press release published in *PE&RS*, contact Rae Kelley, rkelley@asprs.org.

ANNOUNCEMENTS

Western Carolina University has contracted with **Woolpert** for its Bob Waters Field engineering and landscape architecture project at E.J. Whitmire Stadium. The $1 million project includes the removal, demolition and replacement of the existing synthetic turf field, as well as the addition of a new synthetic turf practice area. The firm also is resurfacing the perimeter walkway and installing goal posts, fencing and concrete curbing.

Carl Armanini is a sports designer and senior landscape architect for Woolpert who specializes in the installation and design of turf athletic fields. He said Western Carolina's No. 1 objective for the field is safety, which will be supported by elements that include padding to absorb Gmax forces and appropriate drainage.

"The most important aspect of any synthetic turf or natural grass field is drainage—without it, the structural integrity of the field is compromised and can lead to athletes skating across the surface," said Armanini, who also is the construction administrator for the project. "Western Carolina wanted to go with a new type of woven turf. We were able to provide that and their other preferred products within budget. We're excited to be able to provide this for the school, and to do so on an expedited schedule."

Woolpert Project Manager Katie Thayer said the project had an accelerated timeline when it launched in January, before the COVID-19 pandemic hit. Although some short-term goals have been altered due to the crisis, the team is on target to have the field completed by Aug. 1.

"Fortunately, we got off to a quick start and were able to get the project advertised and bid ahead of our May graduation deadline," Thayer said. "Challenges surfaced while working within prescribed state orders during the pandemic and coordinating the project virtually, but we're fortunate to have an expert team in place that can pivot and react as needed."

TECHNOLOGY

GeoCue Group announces the release of their new True View® 615 and True View 620 UAS LIDAR/Imagery 3D imaging systems (3DIS). GeoCue's True View 615 & 620 are equipped with RIEGL's miniVUX-2UAV laser scanner integrated with dual photogrammetric cameras. Position and Orientation is provided by an Applanix APX-15 (True View 615) or extreme accuracy APX-20 (True View 620). All True View 3D Imaging Systems are bundled with Applanix POSPac, True View EVO post-processing software and True View Reckon data management solution.

The True View 615/620 systems are compact, survey grade 3D Imaging Sensors designed for small Unmanned Aerial Systems. The RIEGL laser scanner and dual photogrammetric cameras have been carefully configured to provide a fused LIDAR/imagery field of view of up to 120°. The system includes full post-processing software that generates a stunning ray-traced 3D colorized point cloud and geocoded images. An upgrade path will be available to promote a True View 615 to a True View 620 by adding the Applanix APX-20 external inertial measurement unit.

The True View product line gives mappers and surveyors the ability to deliver high quality analytic data with exacting accuracies. These deliverables are generated using workflows and tools within GeoCue's post-processing software, True View EVO. Examples of derived products include bare earth models, profiles, cross sections, topographic contours, volumetric analysis and more.

GeoCue's President, Lewis Graham, stated, "Our Quanergy®-based True View 410 has rapidly become the standard for general purpose drone 3D Imaging, where moderate vegetation penetration and accuracies of 5 cm RMSE are adequate. The True View 615/620 provides a solution for situations where deeper vegetation penetration, wire extraction and extreme accuracy are required. These are great new additions to the True View product line."

GeoCue is excited to expand their True View product line of 3D imaging systems. The True View 615/620 will be available for shipment late June 2020.

SPECTRAL EVOLUTION offers two versions of a pistol grip for use with our field portable spectroradiometers designed for remote sensing applications.

These pistol grips are ideal for ambient light remote sensing applications which require fiber optic data collection. They allow the user to safely hold and accurately aim the fiber at the target for more accurate measurements. Our premium version includes triggering and a Picatinny rail for the attachment of a red laser sight or laser scope for targeting. The standard pistol grip provides a value option for those who don't require a Picatinny rail or triggering.

The pistol grips are designed for high performance in field settings. They allow researchers to take the measurements they need without worrying about the size or weight of their equipment. They are an essential accessory for any remote sensing applications such as climate research, environmental studies, vegetation studies, forest canopy studies, and more.

For more information on our pistol grips, visit: https://spectralevolution.com/products/hardware/field-portable-spectroradiometers-for-remote-sensing/remote-sensing-accessories/

CALENDAR

- 9-13 November 2020, **URISA GIS Leadership Academy**, St. Petersburg, Florida. For more information, visit https://www.urisa.org/education-events/urisa-gis-leadership-academy/.
- 30 November - 4 December 2020, **Climate Change and Disaster Management — Technology and Resilience in a Troubled World**, Sydney, Australia. For more information, visit https://conference.unsw.edu.au/en/ccdm2020.

PE&RS
PHOTOGRAMMETRIC ENGINEERING & REMOTE SENSING
The official journal for imaging and geospatial information science and technology
August 2020 Volume 86 Number 8

FEATURE

See the Cover Description on Page 460

COVER DESCRIPTION

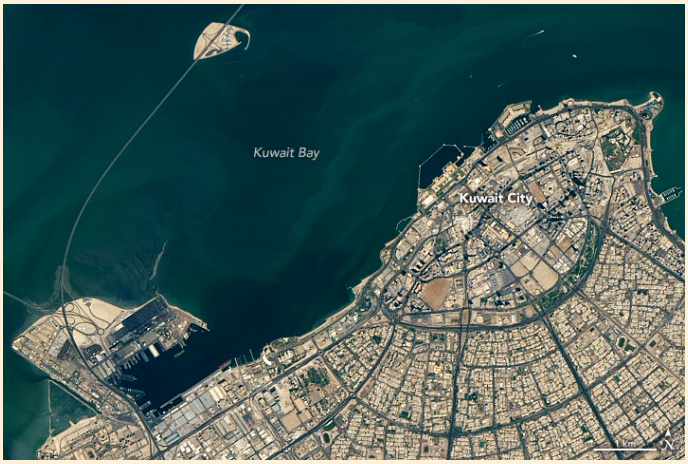

After five years of planning and construction and more than three billion dollars in construction costs, one of the world's longest bridges is complete. Opened in May 2019, the 48-kilometer (30-mile) Sheikh Jaber Al-Ahmad Al-Sabah Causeway is one of the largest construction projects in Kuwait's history.

The Operational Land Imager on Landsat 8 acquired these images of the causeway on September 8, 2019. Approximately 75 percent of the bridge (36 kilometers or 22 miles) stands over water. It also crosses two artificial islands (Bay Island North and Bay Island South) that were constructed for entertainment and tourism purposes.

Building the bridge was challenging in the coastal environment, where dangerously high temperatures and varying humidity can create extremely hot and dry conditions. Much of the construction occurred in early morning and after dark, with crews using high-powered lights or sun shields when necessary. The causeway is primarily composed of concrete piles and steel and layered with waterproofing and asphalt.

Construction companies reported that they tried to take extra care to preserve the ecosystem near the bay, specifically for green tiger shrimp. In one case, they created an alternative breeding area comprised of 1,000 rock and reef blocks in order to draw the shrimp away from the construction site.

Named after the late Sheikh Jaber Al Sabah, the causeway was built to help reshape the country into an international trade center, weening it away from an oil-dependent economy. The bridge reduces travel time by nearly an hour from the capital, Kuwait City, to the northern shore of Kuwait Bay and the proposed future site of Madinat Al-Hareer.

Meaning "Silk City" in Arabic, Madinat Al-Hareer is being proposed as a free trade zone and seaport. With development costs of more than $100 billion, the planned megacity will also include an airport, Olympic stadium, and a tower surpassing Dubai's Burj Khalifa, currently the world's tallest building. The causeway and Silk City are just a few elements in Kuwait National Development Plan 2035.

To view both images, visit https://landsat.visibleearth.nasa.gov/view.php?id=145624.

NASA Earth Observatory images by Lauren Dauphin, using Landsat data from the U.S. Geological Survey. Story by Kasha Patel.

asprs
THE IMAGING & GEOSPATIAL INFORMATION SOCIETY

PHOTOGRAMMETRIC ENGINEERING & REMOTE SENSING

JOURNAL STAFF

Publisher ASPRS
Editor-In-Chief Alper Yilmaz
Assistant Editor Jie Shan
Assistant Director — Publications Rae Kelley
Electronic Publications Manager/Graphic Artist
Matthew Austin

Photogrammetric Engineering & Remote Sensing is the official journal of the American Society for Photogrammetry and Remote Sensing. It is devoted to the exchange of ideas and information about the applications of photogrammetry, remote sensing, and geographic information systems. The technical activities of the Society are conducted through the following Technical Divisions: Geographic Information Systems, Photogrammetric Applications, Lidar, Primary Data Acquisition, Professional Practice, and Remote Sensing Applications. Additional information on the functioning of the Technical Divisions and the Society can be found in the Yearbook issue of *PE&RS*.

Correspondence relating to all business and editorial matters pertaining to this and other Society publications should be directed to the American Society for Photogrammetry and Remote Sensing, 425 Barlow Place, Suite 210, Bethesda, Maryland 20814-2144, including inquiries, memberships, subscriptions, changes in address, manuscripts for publication, advertising, back issues, and publications. The telephone number of the Society Headquarters is 301-493-0290; the fax number is 225-408-4422; web address is www.asprs.org.

PE&RS. *PE&RS* (ISSN0099-1112) is published monthly by the American Society for Photogrammetry and Remote Sensing, 425 Barlow Place, Suite 210, Bethesda, Maryland 20814-2144. Periodicals postage paid at Bethesda, Maryland and at additional mailing offices.

SUBSCRIPTION. For the 2020 subscription year, ASPRS is offering two options to our *PE&RS* subscribers — an e-Subscription and the print edition. E-subscribers can plus-up their subscriptions with printed copies for a small additional charge. Print and Electronic subscriptions are on a calendar-year basis that runs from January through December. We recommend that customers who choose both e-Subscription and print (e-Subscription + Print) renew on a calendar-year basis.

The rate of the e-Subscription (digital) Site License Only for USA and Non-USA is $1000.00 USD. e-Subscription (digital) Site License Only for Canada* is $1049.00 USD. e-Subscription (digital) Plus Print for USA is $1365.00 USD. e-Subscription (digital) Plus Print for Canada* is $1424.00 USD. e-Subscription (digital) Plus Print for Non-USA is $1395.00 USD. Printed-Subscription Only for USA is $1065.00 USD. Printed-Subscription Only for Canada* is $1124.00 USD. Printed-Subscription Only for Non-USA is $1195.00 USD. *Note: e-Subscription/Printed-Subscription Only/e-Subscription Plus Print for Canada include 5% of the total amount for Canada's Goods and Services Tax (GST #135123065). **PLEASE NOTE: All Subscription Agencies receive a 20.00 USD discount.**

POSTMASTER. Send address changes to *PE&RS*, ASPRS Headquarters, 425 Barlow Place, Suite 210, Bethesda, Maryland 20814-2144. CDN CPM #(40020812)

MEMBERSHIP. Membership is open to any person actively engaged in the practice of photogrammetry, photointerpretation, remote sensing and geographic information systems; or who by means of education or profession is interested in the application or development of these arts and sciences. Membership is for one year, with renewal based on the anniversary date of the month joined. Membership Dues include a 12-month electronic subscription to *PE&RS*. Or you can receive the print copy of *PE&RS* Journal which is available to all member types for an additional fee of $60.00 USD for shipping USA, $65.00 USD for Canada, or $75.00 USD for international shipping. Dues for ASPRS Members outside of the U.S. will now be the same as for members residing in the U.S. Annual dues for Regular members (Active Member) is $150.00 USD; for Student members $50.00 USD for USA and Canada $58.00 USD; $60.00 USD for Other Foreign members. A tax of 5% for Canada's Goods and Service Tax (GST #135123065) is applied to all members residing in Canada.

FEATURE

Natural Disasters and the Importance of Geospatial Awareness and Technologies

By Daniel Michalec, GISP, PMP, *Woolpert, Inc.*

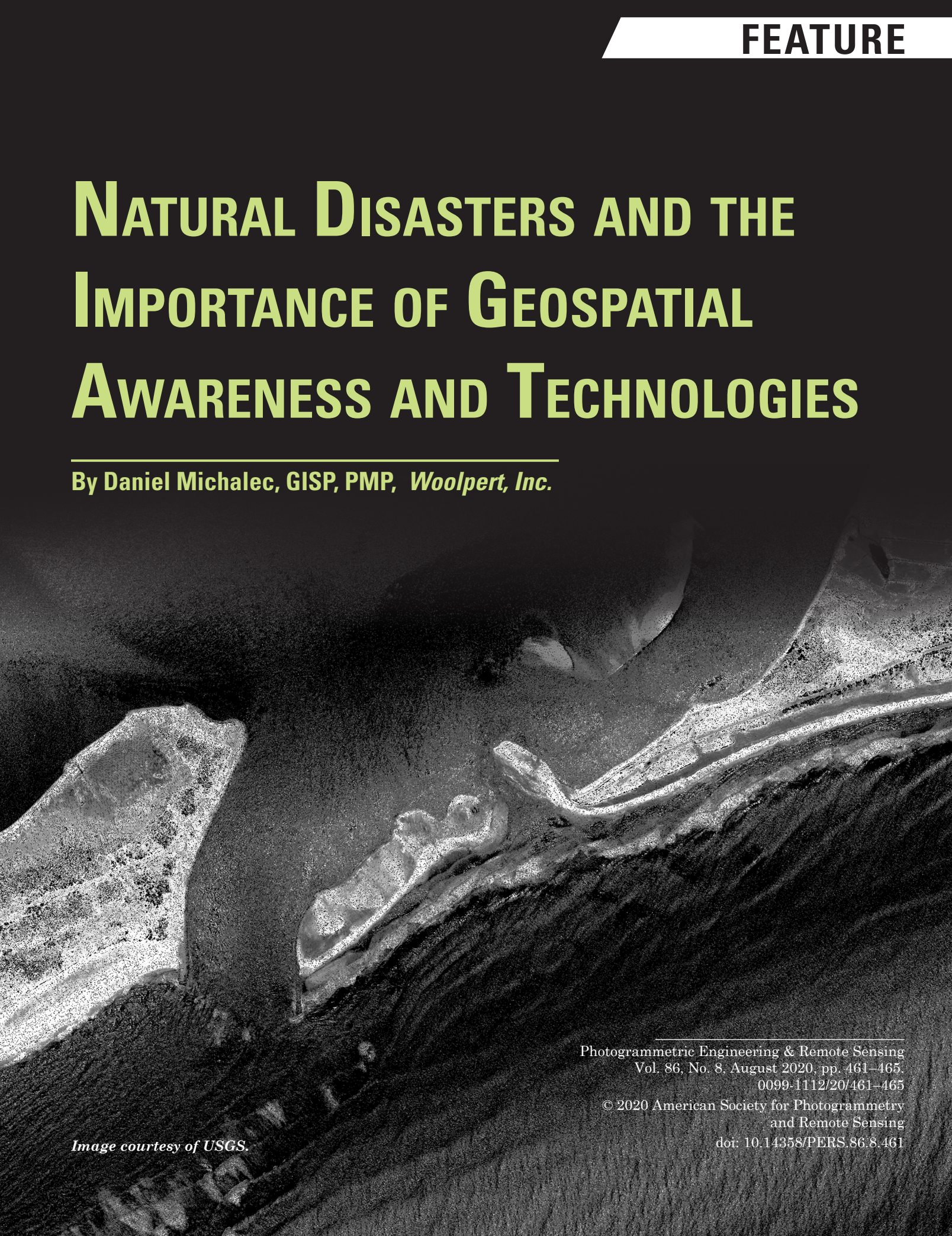

Image courtesy of USGS.

Photogrammetric Engineering & Remote Sensing
Vol. 86, No. 8, August 2020, pp. 461–465.
0099-1112/20/461–465

doi: 10.14358/PERS.86.8.461

When natural disaster strikes, few things are as important as one's sense of place and location. Immediate concerns during these events include: Who was in the path of the tornado or flood? Are any roads or highways closed? Where are shelters open for displaced residents? What does my home or business look like now? The intersection of population and infrastructure with the footprint of harm's way is critical to understanding what happened, who is impacted and what the path to recovery may look like.

Once response efforts get underway, the specifics of the impact become more challenging. How many specific properties were impacted and to what extent? How has the environment changed? Is the local infrastructure compromised, such as the soil and bedrock around bridges and pipelines? Will recovery efforts be hampered by current conditions?

And as days turn into weeks, the affected region attempts to get back to business as usual. Assessments are needed to allocate resources; physical progress must be tracked and managed. There are administrative concerns as well: The Federal Emergency Management Agency (FEMA) requires specific processes and documentation for reimbursement, property taxes may have to be re-assessed and reduced, and insurance claims need to be verified.

Thankfully, the combination of data and geospatial technologies can tell us a great deal about what happened and how to quickly and efficiently begin recovery efforts. Many federal agencies, such as the National Oceanic and Atmospheric Administration (NOAA) and the National Weather Service (NWS), have provided publicly accessible geospatial datasets to support disaster recovery for years. And this trend is increasing as the use of geospatial data by smaller city and county entities becomes more prevalent and easily integrated at the local level.

This provision of geospatial data at multiple scales will continue to enhance disaster recovery efforts by giving responders and those impacted an understanding that spans large scale planning of resources at the county level as well as specific remediation tasks needed at a property or structure. Recent examples are highlighted below.

In the Path of Tornadoes

Woolpert has provided emergency response in the wake of natural disasters for nearly 100 years. The earliest aerial imagery project in the firm's archive is of the flood of 1937 in Cincinnati. In more recent years, Woolpert has been utilizing geospatial technologies to help local, state and federal officials quickly assess damages. One of those devastating events touched close to home for Woolpert, an international architecture, engineering and geospatial firm that has been headquartered in Dayton, Ohio, since 1911.

A record-breaking 15 tornadoes roared through southwest Ohio late at night on Memorial Day 2019. Powerful EF4 and EF3 tornadoes tore paths through the Dayton area just a few miles from the Woolpert office and impacted multiple employees' homes. Two deaths and dozens of injuries were attributed to the storms, which destroyed and damaged thousands of homes, businesses, public parks and facilities.

Within 24 hours of the storms, Woolpert made available to the public an interactive map showing the paths of the tornadoes by incorporating geospatial imagery with available data

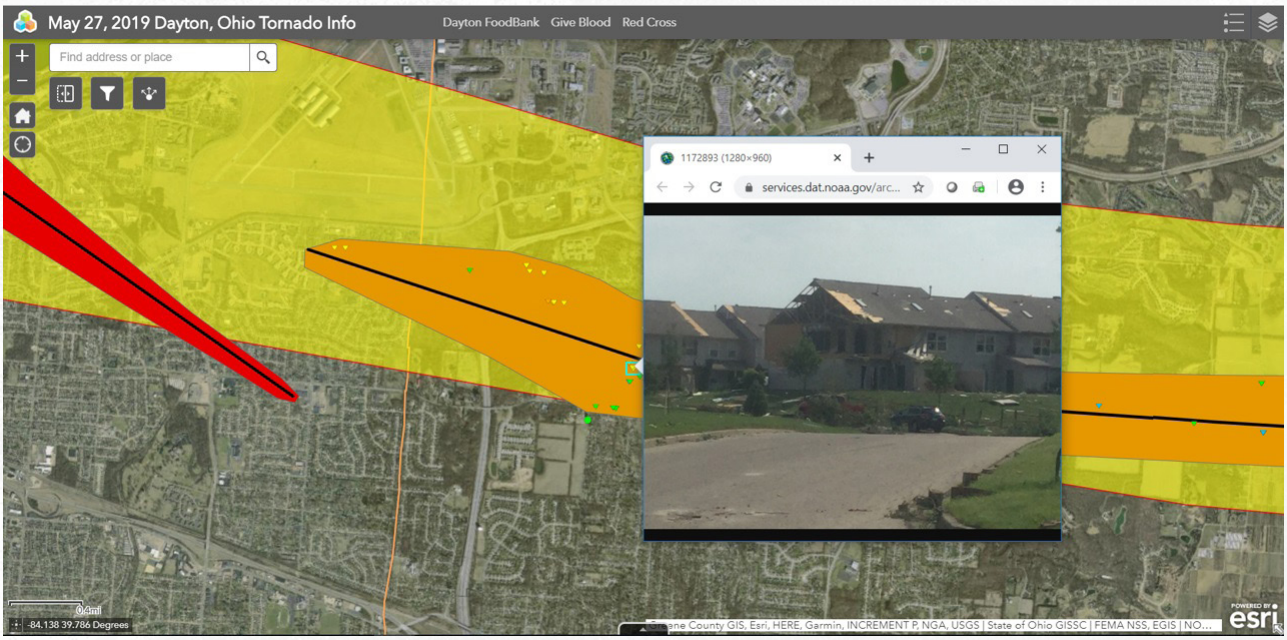

Woolpert created an interactive map showing the path of the tornadoes that blew through Dayton, Ohio, in 2019, incorporating data from NOAA and NWS. Image courtesy of Woolpert.

Imagery collected before and after the Dayton tornadoes provided useful information for assessing pre-and post-disaster conditions. These oblique images show Hara Arena, a 5,500-seat multipurpose venue located in Dayton, before and after tornado damage. Images courtesy of Lexur Associates.

from NOAA and NWS. The map was posted on the company's website and shared publicly through social media. The map illustrated where the storms likely caused the most destruction. Users could interact with the map to add or take away layers of data, which included what schools, churches and other facilities were being used as shelters. The application also integrated field-collected datapoints detailing exact damage locations beside images of affected structures and debris found.

Coincidentally in March, prior to the tornado outbreaks, aerial imagery had been collected by Woolpert in Montgomery County, where Dayton is located. While the original intent of this imagery was to support property valuations, these datasets proved useful for assessing pre- and post-disaster conditions. Updated images were acquired in June, enabling all involved to clearly understand and validate field and infrastructure conditions.

Montgomery County Auditor Karl Keith told news reporters at the time that the before-and-after images were used to help determine which properties had reduced values as a result of the damages and thus were entitled to tax reductions.

The devastation has led to ongoing recovery efforts in communities where residents and business owners continue to rebuild, and local government officials secure grant funding to replace damaged infrastructure. Even though over a year has passed since this incident, many area residents are still heavily involved in the rebuilding process.

The approach used in this response allowed first responders to review large areas, assess specific tornado paths and tracks, and then zero-in on precise damage locations—all from the safety of local offices.

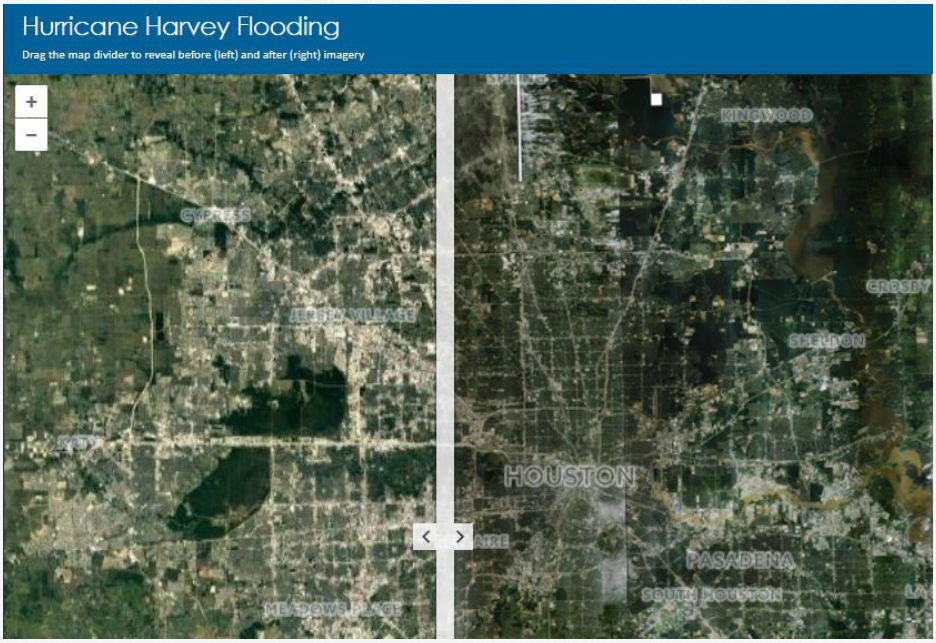

This image taken from the Woolpert website after Hurricane Harvey hit Houston, Texas, helped illustrate before and after ground conditions and document damages to identify where resources were most needed. Image courtesy of Woolpert.

Before and After the Floods

Hurricanes Harvey and Irma flooded communities along the southern coast of the U.S. in August-September 2017. And historic flooding occurred in South Carolina in 2015 as a result of record rainfall. In each of these incidents, manned aircraft were used to collect high-resolution, before-and-after aerial imagery, which was then processed to show the devastation from the storms. The acquired aerial imagery was used to produce interactive maps featuring a slider that enabled users to navigate and zoom-in on specific locations to see what their communities looked like before and after rising tides inundated coasts and torrential downpours sent rivers overflowing.

Aerial imagery collected by Woolpert as the waters crested following the 1,000-year flood that hit South Carolina in 2015 showed devastation from the storm. The imagery was shared with multiple state agencies and local governments within 24 hours to help them respond to road and dam failures and provide guidance on how to prioritize recovery efforts. Image courtesy of Woolpert.

In the days following each of those disasters, thousands of miles of aerial imagery were collected, processed and delivered in meaningful ways. The imagery helped local, state and federal officials assess and document damages, determine current flood conditions and establish where resources were needed most. The maps also gave members of the public the ability to check on specific neighborhoods and get a firsthand look at the extent of damages to their homes and businesses.

As detailed in the above scenarios, data collected immediately following a disaster can be incorporated into change-analysis products and delivered within 24 hours. Interactive maps with layers of information can be created from the geospatial imagery and shared publicly for access to anyone affected by the event. Photos of devastated areas taken before and after storms can be incorporated into interactive programs that give users a unique and valuable perspective. Such digital content is invaluable to the public and can provide local government officials, first responders, legislators and members of the public firsthand knowledge of what's happening in often hazardous environments.

COVID-19 and Disaster Recovery

2020 has presented disaster recovery concerns of an unprecedented nature. The COVID-19 pandemic has created an invisible threat, common to all countries, that appears to be controlled by precise human proximity. COVID-19 presents a footprint that is global in scale, yet extremely local in spread. While there are many unknowns, the prevailing message is to keep social distance as much as possible. The underlying geospatial complications are staggering; to keep the population of the planet six feet apart at all times is a spatial awareness problem of epic proportions. And while the current challenges are unique, the geospatial community remains committed to supporting COVID-19 disaster response by focusing on understanding available data and responder workflows.

Confirmed COVID-19 cases, death rates and other related metrics are publicly available. The integration of these data sources with location information provide visualizations of current spread, potential paths, and overarching patterns to better understand and plan for virus response. Woolpert created a county-by-county United States dashboard of case and death data over time and by location. By aggregating data geospatially, responders can review comprehensive virus status alongside population densities, multi-tenant facilities and other important metrics. Geospatial visualizations will become more important as various jurisdictions adjust and refine operational and social distancing policies along invisible administrative boundaries. Geospatial analysis of policy changes based on political boundaries may shed light on best practices for future response efforts.

And while virus tracking and monitoring will continue to provide benefit for approaches like contact tracing and Indoor Positioning Systems (IPS), the geospatial community can also support disaster response by assisting with known workflows. In events like COVID-19, response efforts are often chaotic as initial information is compiled, and those affected struggle to reprioritize processes, staff and funding. Rapid ramp-ups can be challenging, but government agencies must follow specific guidelines to be eligible for FEMA disaster reimbursement funding.

In these instances, geospatial technology is being used to provide first responders and operators with reimbursement specific field data collection tools. Woolpert is working directly with Esri to provide end-users with mobile tools to track

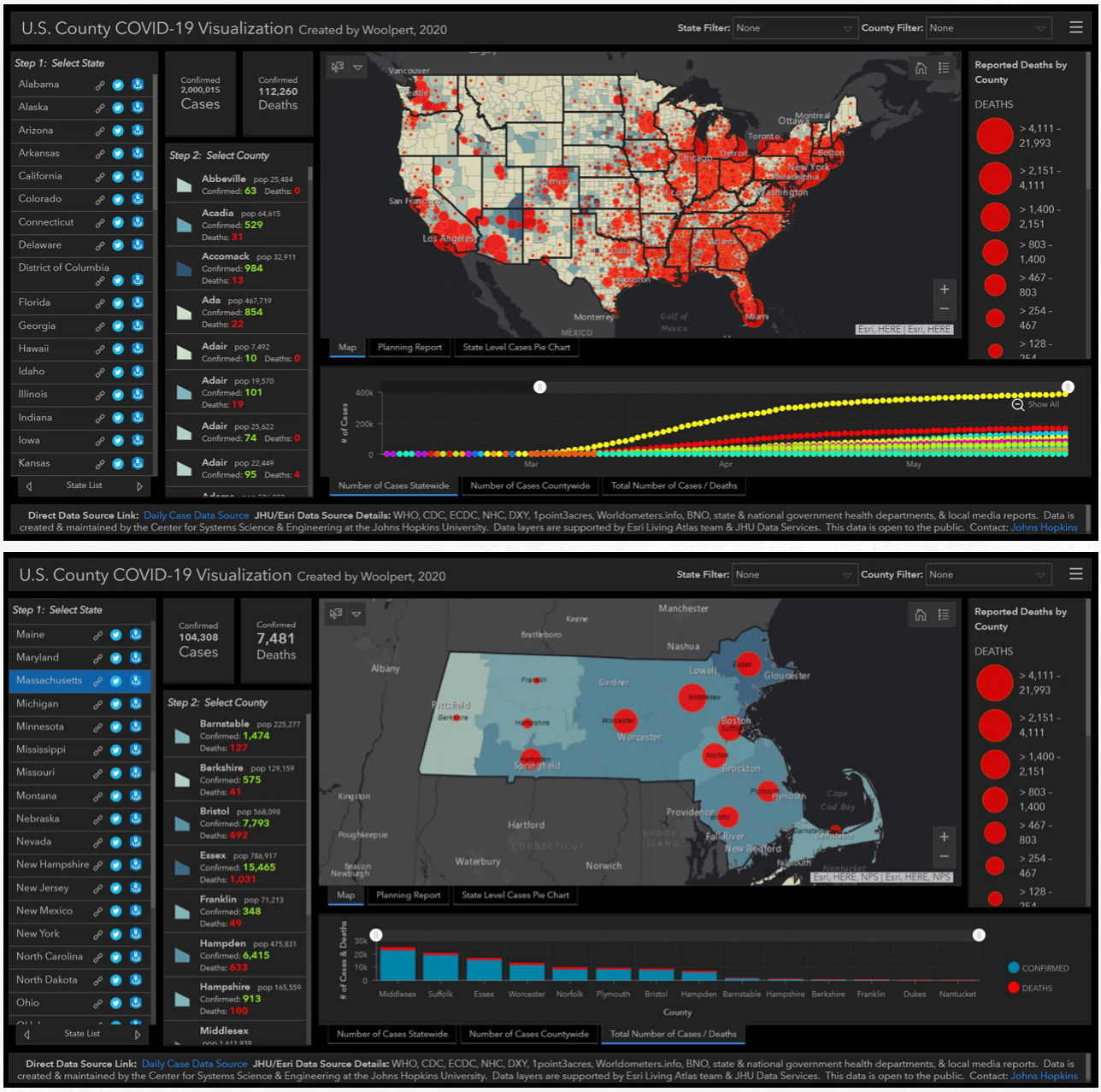

Woolpert created a county-by-county United States dashboard of COVID-19 case and death data over time and by location. By aggregating data geospatially, responders are able to review comprehensive virus status alongside population densities, political boundaries, and other important demographic metrics. Image courtesy of Woolpert.

virus response efforts in real time, on a map and to specific FEMA reimbursement standards. These process-oriented support tasks help responders focus on the tasks at hand, and the remove the guesswork on what needs to be collected and the required level of detail.

Geospatial data and technologies are invaluable tools in response to natural disasters. Benefits are being discovered every day as public and private institutions rely increasingly on geospatial approaches: aerial imagery from manned and unmanned aircraft, publicly available data feeds, process-driven response workflows and spatially aware datasets. And while proven geospatial data and approaches will continue to refine the response to recurring natural disasters—tornadoes, floods, wildfires, etc.—the industry is just beginning to define ways to address the unique challenges of COVID-19.

As we work to understand the how and why of COVID-19, the where or location of people, assets, resources and virus data will certainly be central to our success in identifying, containing and ultimately stopping the spread of this natural disaster.

Author

Daniel Michalec, GISP, PMP, is Woolpert's Innovation Portfolio Manager and a Senior Associate. He has been with Woolpert for over 14 years and works out of the firm's Dayton headquarters.

ASPRS BOOKSTORE

visit **asprs.org**

available at amazon

Digital Elevation Model Technologies & Applications, 3rd Ed
Co-Editors: David F. Maune, PhD, CP, CFM, PSM, PS, GS, SP and Amar Nayegandhi, CP, CMS-Remote Sensing
List Price: $100 | **ASPRS Members:** $80
ASPRS Student Members: $50†
Also available for Amazon Kindle
Amazon Kindle Price:** $85

Landsat's Enduring Legacy: Pioneering Global Land Observations From Space
Landsat Legacy Project Team
ISBN: ISBN 1-57083-101-7 · Hardcover · 586 pages · 2017 · Stock #4958
List Price: $95 | **ASPRS Members:** $65
Student Members: $60
Amazon Price*: $100

Manual of Airborne Topographic Lidar
Editor: Michael S. Renslow
ISBN: 1-57083-097-5 · Hardcover · 528 pages · 2012 · Stock #4587
List Price: $150 | **ASPRS Members:** $95
Student Members: $75
Amazon Price (hardcover)*: $135
Also available for Amazon Kindle
AmazonKindle Price:** $110

Manual of Photogrammetry, Sixth Edition
Editor: J. Chris McGlone
ISBN: 1-57083-099-1 · Hardcover · 1372 pages · 2013 · Stock #4737
List Price: $175 | **ASPRS Members:** $125
Student Members: $98
Amazon Price*: $175

Glossary of the Mapping Sciences
Co-published by ASPRS, ACSM and ASCE
ISBN: 1-57083-011-8
563 pp · Paperback · 1994 · Stock #5021
List Price: $50 | **ASPRS Members:** $35
Student Members: $25 | **Amazon Price*:** $50

Hyperspectral Remote Sensing for Forestry
Paul Treitz, Valerie Thomas, Pablo J. Zarco-Tejada, Peng Gong, and Paul J. Curran
ISBN: 1-57083-093-2
107 pp · Softcover · 2010 · Stock #4584
List Price: $26 | **ASPRS Members:** $21
Student Member: $21 | **Amazon Price*:** $26

Manual of Geographic Information Systems
Editor: Marguerite Madden, PhD
Foreword: Jack Dangermond, Esri
ISBN: 1-57083-086-X · Hardcover · 1352 pages + DVD · July 2009 · Stock #4650
List Price: $53 | **ASPRS Members:** $40
Student Members: $40
Amazon Price*: $55

Meeting Environmental Challenges with Remote Sensing Imagery
Editors: Rebecca Dodge & Russ Congalton
Published by American Geosciences Institute; Publishing Partners: AmericaView, USGS Land Remote Sensing Program, ASPRS
ISBN: 978-0-922152-94-0 · 82 pp · Softcover · 2013 · Stock #4589
List Price: $7.50 | **ASPRS Members:** $6
Bulk Orders (3 or more copies): $4.50 each
Amazon Price*: $9.95

MANUAL OF REMOTE SENSING, 3RD EDITION (A SERIES)

Earth Observing Platforms & Sensors
Volume 1.1
Volume Editor: Mark Jackson
ISBN: 1-57083-089-4
550 pp · Hardcover · 2009 · Stock #4582
List Price: $95 | **ASPRS Members:** $75
Student Members: $55 | **Amazon Price*:** $95

Remote Sensing of Human Settlements
Volume 5
Editor-in-Chief: Andrew B. Rencz
Volume Editors: Merrill K. Ridd & James D. Hipple
ISBN: 1-57083-077-0
747+ pp · Hardcover · 2005 · Stock # 4576
List Price: $99 | **ASPRS Members:** $80
Student Members: $60
Amazon Price*: $69.99

Remote Sensing of the Marine Environment
Volume 6
Editor-in-Chief: Andrew B. Rencz
Volume Editor: James F.R. Gower
ISBN: 1-57083-080-0 · 360 pp · Hardcover · 2006 · Stock # 4578
List Price: $95 | **ASPRS Members:** $75
Student Members: $50 | **Amazon Price*:** $95

*Member discounts are not available when ordering directly from Amazon.

**Member discounts are not available on Amazon Kindle e-books,

†Students must order via the ASPRS Bookstore & a copy of your valid student ID must be submitted to be eligible for student pricing.

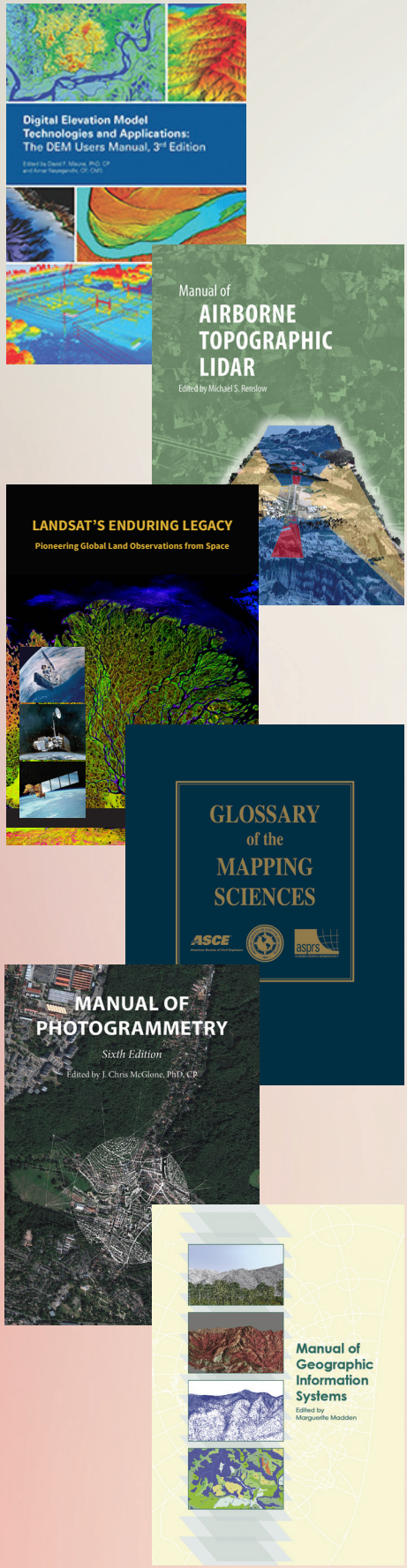

Pontus Olofsson, PhD, *Boston University*

Lessons Learned from Capacity Building Efforts in Tropical Countries

Successful capacity building is hard to achieve in less developed countries. Over a period of years we have undertaken capacity building aimed at collaborating with countries and organizations to overcome the many challenges encountered. The following descriptions provide the background and then we detail the lessons learned from the last decade of working with SilvaCarbon and NASA-SERVIR, GOFC-GOLD and the World Bank in capacity building efforts.

Tropical deforestation and forest degradation have a wide variety of environmental and societal impacts including the release of carbon to the atmosphere following forest disturbance. Carbon concentration in the atmosphere is presently at record levels and the contribution by terrestrial carbon emissions is substantial and increasing. The international community has identified enhanced forest management in tropical countries incentivized by economic compensation as a feasible means to curb greenhouse gases.

REDD+, (*Reducing emissions from deforestation and forest degradation and the role of conservation, sustainable management of forests and enhancement of forest carbon stocks in developing countries*) was negotiated under the United Nations Framework Convention on Climate Change in 2005. Under REDD+ countries receive payments for evidence of emission reductions from deforestation and forest degradation and from enhancement and conservation of forest carbon. While fine in theory, the production of evidence of reductions that meet the criteria defined by the international research community is complex. The reporting criteria, defined by the Intergovernmental Panel on Climate Change, emphasize the lack of bias and quantification of uncertainty. This implies the use of sampling techniques and unbiased estimators in a statistical inference framework, not simply making maps and counting pixels (GFOI, 2016, p. 125).

Activities on the land surface that impact the terrestrial carbon budget (primarily deforestation, forest degradation and forest recovery) tend to be small relative to the total land area. Therefore, annual or biennial accurate maps of land cover and land cover change are needed to guide the sampling and to meet other needs related to land management. Obviously those responsible for producing results for payments must be proficient in remote sensing and statistics, as well as forestry and biogeosciences.

There are further complications. The annual areal extent of forest loss and gain is often very small relative to the entire study area (typically a country), even in countries with rampant deforestation. Estimating and mapping something very small is inherently complicated and uncertain. Furthermore uncertainty in carbon parameters can influence the final estimates of the carbon emissions/removals. Complicated institutional arrangements, understaffed and underfunded agencies, and difficulties recruiting and retaining talent are other common complicating factors. The result is a situation in which the production of estimates of emissions over time, with precision sufficient to determine that reductions have occurred -- and hence to receive result-based payments -- is very difficult.

The challenges are many and complex as are the potential solutions. The quality and quantity of relevant data, software and computing power have never been greater. After Landsat data were made available for free, other relevant satellite missions followed and adopted free data policies (e.g. Sentinel-2). New spaceborne lidar and radar instruments are or will collect data of great scientific value (ICESat-2, NISAR, BIOMASS, RCM, etc.). Powerful cloud computing platforms, such as Google Earth Engine, allow remote sensing analysts to access and process large quantities of data without downloading and preprocessing the data. Deciding how to best utilize these assets for the benefit of tropical forests and people is important for capacity building.

Lesson One—Research is Required

Assessing how to best monitor terrestrial carbon emissions needs research. Capacity building programs usually do not do or sponsor research but rely on the findings and deliverables of research programs. An example of the necessary synergy between capacity building and research is provided in Figure 1. Historically remote sensing data and interpretations assessed accuracies by comparing map labels

Photogrammetric Engineering & Remote Sensing
Vol. 86, No. 8, August 2020, pp. 467–470.
0099-1112/20/467–470

doi: 10.14358/PERS.86.8.467

with ground observations. They were rarely used to estimate area bias and uncertainty in area estimates, even though such information is often more important than the measures of map accuracy. Further, the reporting criteria under REDD+ stipulate that areas are estimated by sampling and unbiased estimators. The underlying statistical framework required to satisfy these criteria has been defined in the statistical literature (Cochran 1977; Särndal et al. 1992)[1]; Olofsson et al. (2014) was written to illustrate the use of such techniques in a remote sensing context[2]. Olofsson et al. (2014) was well received by the community and featured in capacity building efforts by SilvaCarbon, UN-FAO and others[3], and many countries have implemented the recommendations provided in the article[4]. Following implementation, many studies found that certain types of errors in the maps used for stratification purposes would introduce large uncertainty in area estimates[5]. The issue needed investigating and guidance to countries was needed -- with funding from the NASA Carbon Monitoring System[6], an article was written that provides additional guidance for how to mitigate the impact of omission errors (Olofsson et al., 2020)[7]. If this article in turn is used by the community[8, 9], new issues are likely to occur which need investigation[10]. This is just one example but it highlights the importance of research programs for assisting capacity building efforts. Many of the issues that countries are wrestling with are not static and experts are not in a position to simply provide a solution. Research funding and targeted investigations that engage in country-academics and governments are required.

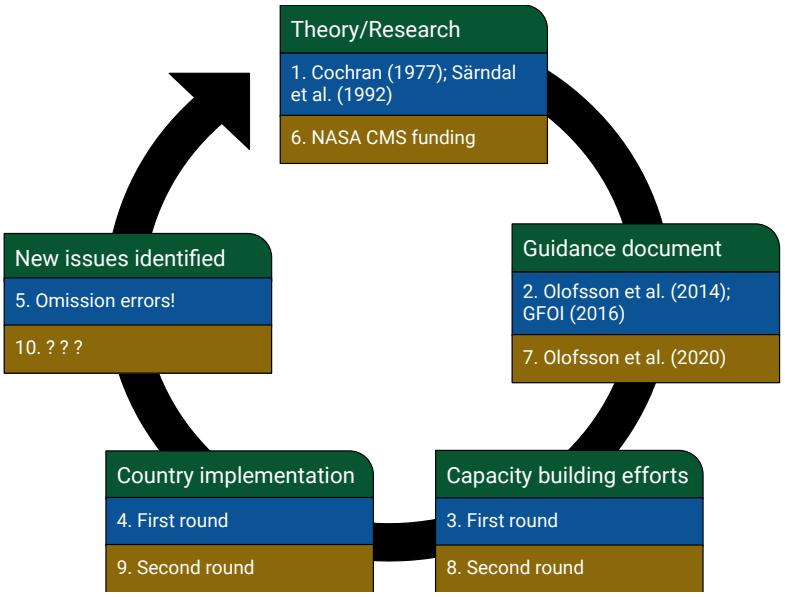

Figure 1. Example of the interdependence of capacity building efforts and research; the example shows the steps involved in popularizing sampling-based estimation of area and map accuracy.

Lesson Two—Open Source

This might be fairly obvious but unless the data and software featured in education and training sessions are available without restrictions, continuity is hard to achieve. Note that *open source* is not the same thing as *free*. The difference between open and free is best illustrated by a Government agency in charge of UNFCCC and REDD+ reporting in a tropical country in which we have been active. The agency maintains a high level of competency and has contributed to capacity building efforts in several other countries. An important reason behind the agency's ability to build and maintain talent is the re-coding of most of the software used in their national forest monitoring system. Knowledge, experience and expertise are created by coding their own versions of the software, which is greatly facilitated by keeping algorithms, tools and software open source and not just free of charge.

Lesson Three—Deliver Know-how, Not Products

We have seen that when practitioners are handed products (maps, estimates, sample data, etc.), regardless of sophistication and accuracy, maintaining continuity becomes more difficult. One-time efforts might fulfill important short-term requirements but are unlikely to build capacity. The desired outcome of capacity building is to improve the strength of the organization and enable local technical people to develop the necessary skills for sustainability. For example, if an institution or agency delivers a map product for use in forest monitoring to local practitioners, the product needs to be replicated for future monitoring which makes the process reliant on the map-making institution or agency. If the institution loses funding, changes staff, or redirects its interests, the people in charge of the local forest monitoring are back at square one. Instead, had the forest monitoring been implemented by local practitioners using open source software and data, the chances of achieving consistent monitoring would be greater. Capacity building efforts should focus on creating know-how by delivering training and educational materials while avoiding being distracted by competing methodologies, data and tools.

Lesson Four—Capacity Building Needs to be Customized for each Country

There is no global consensus on how best to conduct capacity building, although approaches that are successful in other countries are often applicable elsewhere. However, different countries present with different organization and societal structures, cultural practices, and gender roles, which in turn shape the way a country develops technical capacity. We have learned that what may work in one place or country may not work in another. Usually countries from the same geographical region share the same environmental and technical challenges but each country has their own land use priorities and land definitions. Capacity building must respond to each country's priorities and needs if capacity building is to be successful.

continued on page 470

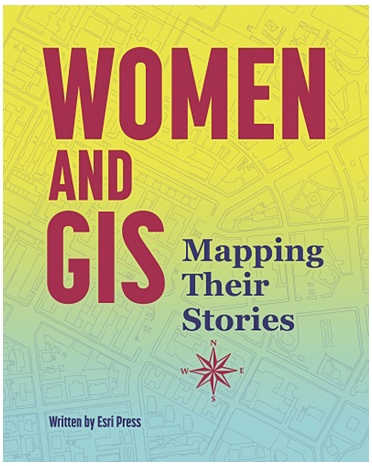

Women and GIS: Mapping Their Stories

Catherine Ortiz, Esri Press

ESRI Press, Redlands, California, 2019. ISBN: 978-1-58948-528-0. Pages: 215

Reviewed by Rebecca A Morton, ASPRS Certified Photogrammetrist, ASPRS Certified Mapping Scientist, CEO and President of GeoWing Mapping, Inc., Richmond, CA. Becky@geowingmapping.com.

As stated in its foreword, the release of *Women and GIS: Mapping Their Stories* could not come at a better time, a time when women are making their voices heard and taking leadership in exciting new ways. The book showcases the achievements and personal life stories of twenty-three remarkable women who have each changed the world for the better and have used the tools of GIS to help them achieve their goals.

The manager and publisher from ESRI Press who compiled the book, Catherine Ortiz, was impacted by her own mother and grandmother, who knew the value of math and science, and who inspired her to pursue her studies in GIS. In turn, Catherine's own desire to motivate her daughter and other young women to pursue math and science fields led to the creation of this book. The result is a collection of stories of women from all over the world with amazing accounts of personal obstacles, unique perspectives, and perseverance.

There are several common threads that run through the life stories of *Women and GIS*; among them, a love of nature, commitment to the environment, and dedication to improving the lives of our world's displaced, marginalized and vulnerable. The stories present women who dared to become leaders in their field and who were aware of the power of collaboration and team building to accomplish their dreams. Wangari Maathai, Noble Peace Price recipient, used the power of collaboration to start the Green Belt Movement in her home country of Kenya, which promoted both the sustainable use of natural resources as well as the fight for democracy. Karen E. Firehock started with a passion for playing and working outdoors and built her career around that passion, becoming an environmental planner addressing the problems in stream, river, and wetland habitats. Karen says of her collaborative work for clean water in Africa, "I had to become a part of their world first, listen, and make a difference where I could". Similarly, Kass Green, a businesswoman who founded and managed several successful technology companies using GIS and imagery, advises young women to "find solid team members to work with in your career, and continually encourage their and your intellectual growth. Then listen, listen, listen."

The book highlights women of all ages. Madison Vorva, age 23, was inspired when she was in the second grade by Jane Goodall's work with Chimpanzees. From the age of six, Madison took a leading role in conservation activism and she has since joined Jane Goodall's Institute to promote GIS within the Tapestry of Hope program. Sylvia A. Earle, age 83, was the first person to walk solo on the ocean floor; she became a NOAA Chief Scientist, and was named Time Magazine's First Hero for the Planet."

Many of these women benefited from family, mentors and teachers who spurred them to self-assurance in the face of discouragement and failures. In the story of Paulette Brown-Hinds, recognizing Paulette's disappointment in failing to land a job, her mentor stated "I don't know how to get you to see yourself the way that I see you." Shoreh Elhami grew up in Tehran and experienced challenges in obtaining her education during the Iranian Revolution and the Iran-Iraq war as well as hardships when relocating to the United States with a young family; however, the importance of life-long learning and exploration was strongly instilled in her by her mother and father and she went on to a life of mentoring female students and colleagues. In order to be taken seriously, Nancy La Vigne decided to pursue a PhD in criminal justice and found her best mentors were those she proactively sought out, people she admired and wanted to emulate. Mary Spence, a cartographer in Scotland who was honored by the Queen of England with Membership of the Order of the British Empire, was inspired as a child by a geography teacher who would load his students into his dilapidated car and explore cliffs and beaches, sharing stories of history to highlight the geography and provoke their imaginations.

Photogrammetric Engineering & Remote Sensing
Vol. 86, No. 8, August 2020, pp. 469–470.
0099-1112/20/469–470

doi: 10.14358/PERS.86.8.469

In reading these stories, one senses the joy that comes from living a self-directed, value-driven life. In the words of Molly Burhans, founder of GoodLands, an organization that manages the conservation and land use of the Catholic Church's landholdings, "It is immensely fulfilling and enjoyable if you can align your career and life in such a way that you are surrounded by people who love what they do, and the best way to achieve that is to do what you love." She also says, "Never stop being in wonder of your work." The motto of Dr. Catherine Ball, leader of the World of Drones Congress and the founder of five start-up companies is, "She who dares, learns," and she states, "I am now more fearless than ever before."

This book includes many calls to action for its readers. In the words of Sylvia A. Earle, "We have the power to change the world – the way we look at the world, the way the world goes forward henceforth- if we just use the technologies and join together with our minds and our hearts and our commitment to make a difference." Shoreh Elhami implores, "We need to educate women about gender equality and their rights, and elect lawmakers who fight for them." Kristen Kurland, Carnegie Mellon University Professor, advises, "It's clear that the cost of higher education will soon exceed an amount that many can afford. Colleges and universities will need to reinvent how they educate students while still upholding academic rigor through research and scholarship." Kathryn Sullivan, the first woman to walk in space, expresses her hopes for the future by saying, "Our world needs more, not fewer, bright and energetic people to become scientists, both to advance the frontiers of knowledge and to connect science to society."

This book has achieved the goals established by its manager and publisher, Catherine Ortiz, to highlight the importance of science, technology, engineering and math (STEM) to change our world for the better and to underscore the key role that women have played and will continue to play in the application of STEM to our world's challenges. Women who are searching for a path to realize their potential and to make a difference in the world will find inspiration and guidance from the words of wisdom and the life examples provided in this book.

SectorInsights.edu
continued from page 468

References

Cochran, W. G. (1977). Sampling techniques (3rd ed.). New York: John Wiley & Sons.

GFOI (2016). *Integration of remote-sensing and ground-based observations for estimation of emissions and removals of greenhouse gases in forests: Methods and Guidance from the Global Forest Observations Initiative*. Edition 2.0. United Nations Food and Agriculture Organization, Rome.

Olofsson, P., Foody, G. M., Herold, M., Stehman, S. V., Woodcock, C. E., & Wulder, M. A. (2014). Good practices for estimating area and assessing accuracy of land change. *Remote Sensing of Environment*, 148, 42-57.

Olofsson, P., Arévalo, P., Espejo, A. B., Green, C., Lindquist, E., McRoberts, R. E., & Sanz, M. J. (2020). Mitigating the effects of omission errors on area and area change estimates. *Remote Sensing of Environment*, 236, 111492.

Särndal, C-E., Swensson, B., & Wretman, J. (1992). Model assisted survey sampling. New York: Springer.

Author

Pontus Olofsson has a background in geography and mathematics, with a PhD in physical geography from Lund University, Sweden. He is currently a research associate professor and lecturer in the Department of Earth & Environment at Boston University, and a consultant to the World Bank. Olofsson serves on the science teams of the NASA Carbon Monitoring System, the NASA Land Cover and Land Use Change program, and NASA SERVIR. He has been supporting SilvaCarbon's capacity building efforts for almost a decade.

GIS Tips & Tricks

Al Karlin, Ph.D, CMS-L, GISP

Need to Generate Multiple Profiles Quickly?

For Engineers, Surveyors, GIS Analysts, Remote Sensors, or just about anyone who deals with Digital Elevation Models, Terrain Models, Triangular Irregular Networks (TINs), or topographic data in general, there comes a time when you want to visualize your terrain in a profile view. Engineers and Surveyors spend a lot of time generating profiles through water courses and ponds; heads-up compilers use profiles to assist in 3D-linework placement, and lidar analysts are constantly drawing profiles to assist with manual lidar classification.

Most GIS software packages have tools for extracting and viewing profiles from either raster-based DEMs, TIN-based Terrains or lidar point clouds. The general workflow includes, (1) identifying a specialized profile tool, (2) drawing a line through the area on the dataset (DEM, TIM, Terrain, pointcloud) for the profile to be generated (click-drag-click), and then (3) drag/click a line perpendicular to the profile line to specify a "width" for the profile. When this click-drag-click-drag/click sequence is completed, usually a new window, displaying the profile pops-up.

Recently, here at Dewberry, we came upon a need to construct multiple profiles, evenly spaced down the thalweg of a stream. One approach to solve this problem would be to construct a proprietary tool or, maybe use Python to customize one of the existing tools. However, we found a quick tip in GlobalMapper to save the day.

GlobalMapper (we are still running V19, but I am sure this feature has been maintained in newer versions) provides multiple ways to access the profile tool. The tool can be accessed from the Analysis Toolbar, Figure 1.

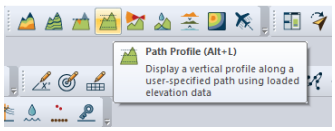

Figure 1.

from the "Tools" dropdown menu, Figure 2.

or with a keyboard shortcut, <ALT>+L (Line of Site).

Once the Profile tool is activated, the workflow is slightly different than the click-drag-click-drag/click flow. The workflow is actually simplified; to draw the profile line, left-click on the mouse to start the line, drag your line and right-click to end the line. In this example, I left-clicked on the western

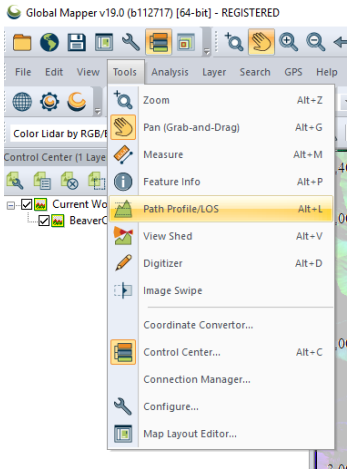

Figure 2.

portion of the line to start it, dragged to the east, and then right-clicked to stop the profile line, Figure 3.

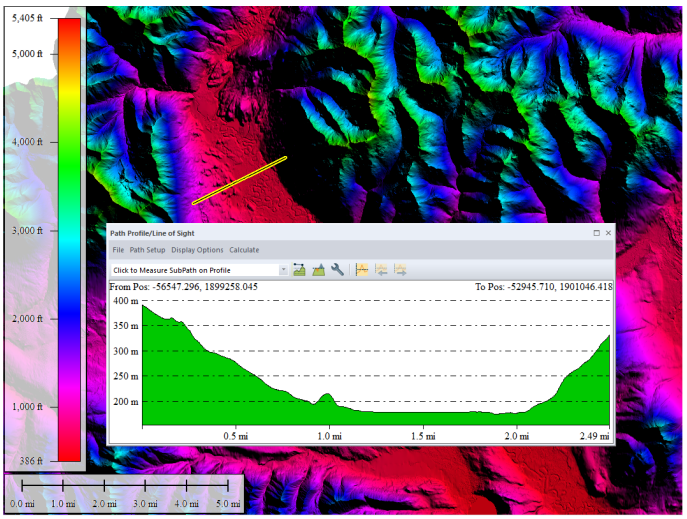

Figure 3.

But to generate multiple profile lines through this valley, there is a "trick".

Photogrammetric Engineering & Remote Sensing
Vol. 86, No. 8, August 2020, pp. 471–472.
0099-1112/20/471–472

doi: 10.14358/PERS.86.8.471

After you select the Profile tool, simply right-click anywhere on the DEM to activate the Profile Selection menu, Figure 4.

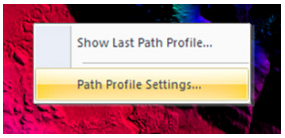

Figure 4.

And click on "Path Profile Settings", to open the "Profile Settings Menu", and make sure to check the options as seen in Figure 5.

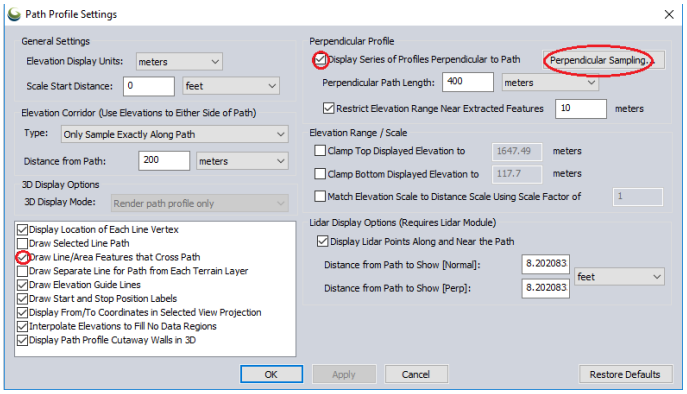

Figure 5.

Additional options are available when you click the "Perpendicular Sampling" button, as in Figure 6.

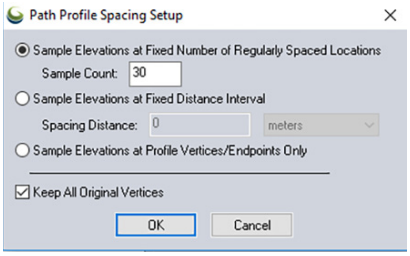

Figure 6.

Click "OK" on the Path Profile Spacing Setup menu, then "APPLY" and "OK" on the Path Profile Settings menu. Finally, back on the DEM, use the left-mouse to click the line that you want the profiles to be perpendicular to and you will see the perpendicular profile constructed with your first mouse-click. Draw as many vertices as you need and finish your line with a right mouse-click. You should see something as seen in Figure 7.

Notice the profile line perpendicular to your digitized line. The profile in the Path window represents that beginning profile. Also notice that the RIGHT ARROW in the profile window is now active. Clicking on that will move the perpendicular profile down the digitized line at the increment specified in the settings. (The LEFT ARROW will move it the opposite direction). So after a few clicks, in this case I went 5 increments, of the RIGHT ARROW, you should see something like Figure 8.

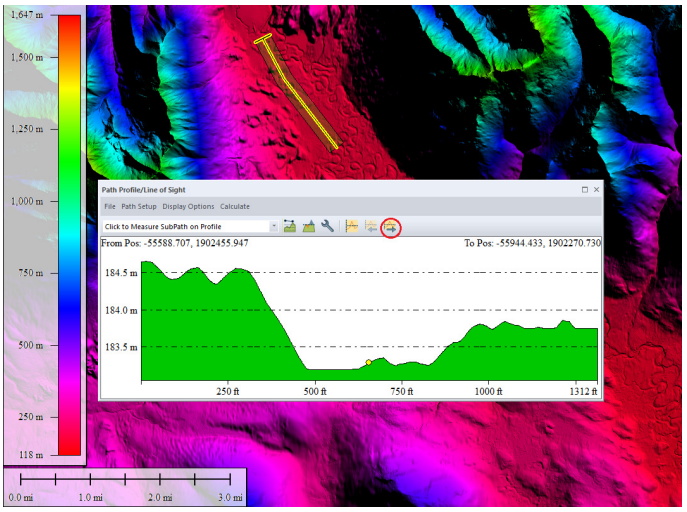

Figure 7.

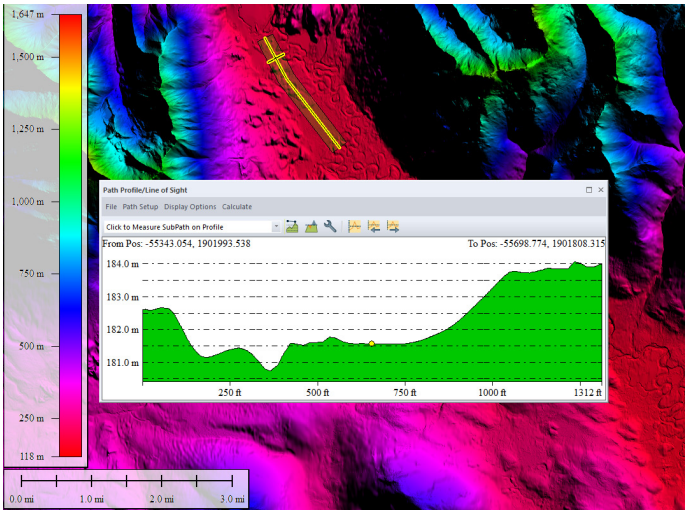

Figure 8.

Finally, if you need to export the values for the profiles, just use the "File" dropdown in the Profile Window, select "Save XYZ file" or any of the other file format options, to export the data. And there you have it.

Al Karlin, Ph.D., CMS-L, GISP *is with Dewberry's geospatial and technical services group in Tampa, Florida. As a senior geospatial scientist, he works with all aspects of lidar, remote sensing, photogrammetry, and GIS-related projects.*

GREETINGS FROM THE ASPRS STUDENT ADVISORY COUNCIL (SAC)!

This year, we are focusing on social media. Building an active social media community, that will extend the reach of ASPRS to student members and the public. Our goal is to build a powerful information channel to better serve students in a more efficient manner.

We invite every ASPRS student member to become an ASPRS SAC Brand Ambassador on social media working towards significantly boosting our audience engagement and ultimately support the original vision of ASPRS.

SAC Brand Ambassadors will

- Welcome suggestions and comments on the SAC social media pages
- Discuss ways ASPRS can serve student members
- Create student focused activities.
- Help students network, find collaborators, and share ideas on topics of their interest.
- Provide student members and the public with informative geospatial content; ASPRS Spotlight Videos etc.
- Help generate exposure to ASPRS news, achievements, opportunities and activities.
  - Conferences
  - Scholarships
  - Certifications
  - Student focused sessions
  - Volunteering
  - SAC Leadership

We understand the randomness of social media but our goal is to measure the growth in our social media accounts through different measures. Measuring this success is critical to ensure proper communication. For example, one way to validate the impact of ASPRS SAC presence on social media would be to monitor the increase in the number of applicants for ASPRS opportunity, i.e., volunteering, SAC leadership, and scholarships.

Richard Passman

CORONA Spy Satellite Engineer

Aeronautical engineer Richard Passman died in Silver Spring, Maryland on April 1, 2020 from complications from the new coronavirus. He was 94.

Mr. Passman is best known to the photogrammetry community for his contributions to the spy satellite the United States developed during the Cold War to monitor the ballistic missile capabilities of the Soviet Union, code-named CORONA. For a decade, CORONA also gave the US Intelligence community a glimpse into the USSR's economy, helping shape foreign policy with more information than the tightly controlled Soviet government would release. CORONA was the subject of the ASPRS book CORONA: Between the Earth and the Sun, published in 1997.

CORONA worked by taking photographs from orbit and ejecting them to be caught by military aircraft for developing and analysis. The ejection container, or "bucket", required extensive heat shielding to withstand re-entry through the Earth's atmosphere, and was contracted to General Electric. This heat shielding was Mr. Passman's expertise, which he previously worked on at Bell Labs before moving to GE.

Mr. Passman then went on to work as GE's general manager of space activities before retiring. The CORONA project was declassified in 1995, and only then did the world start to learn about the efforts that went into creating the very first spy satellite.

The ASPRS community would like to thank Mr. Passman, as well as the rest of his team at GE, for their work in protecting the precious photographic cargo from CORONA, so it could be safely retrieved.

Excerpt from The New York Times on April 16 2020.

Randle "Randy" Olsen

ASPRS Emeritus Member

ASPRS Emeritus Member, Randle "Randy" Olsen, age 73, passed away on June 4th in Boulder, Colorado. He was born in Tacoma, Washington to Phyllis and Robert Olsen and grew up in San Francisco, California, which he considered his home. He received both a Bachelor's and Master's degree in Civil Engineering from the University of California, Berkeley, and he worked with the United States Geological Survey as a Senior Scientist and Executive for over 40 years. In 2020, he earned an Outstanding Technical Achievement Award from ASPRS and for many years he chaired the review committee for the ASPRS Robert E. Altenhofen Memorial Scholarship. Randy married his wife, Kate Guthrie, in San Francisco and together they adopted three children. When he wasn't working, he loved to spend time outdoors with his family and was a master gardener. He is survived by his wife Kate, children Rachel, Michael, and Laurel Olsen, and grandchildren Andrew Olsen-April and Teddy Horen. Contributions in Randle's memory can be made to the Nature Conservancy in honor of his deep love for the earth.

Excerpt from The Daily Camera on Jun. 21, 2020.

JOIN ASPRS IN WELCOMING WINGTRA TO OUR FAMILY OF SUSTAINING MEMBER COMPANIES

Headquartered in the heart of Zurich, Switzerland, Wingtra is the world's leading VTOL drone producer for mapping, survey and mining industry professionals. Since its market entry in early 2017, Wingtra has partnered with more than 60 of the biggest equipment dealers and has been selling mapping drones globally ever since.

Wingtra has 80+ employees, out of which more than 30 focus on R&D. Wingtra's engineers are graduates from the world's 3rd best university for engineering and technology, ETH Zurich (Top Universities, 2019) and are among the leading research engineers in VTOL technology. Drones are assembled in-house in Zurich by their production team, and technical specialists support their customers from local offices in both North and South Americas, Europe and Asia.

Rooted in years of technological research, the WingtraOne leads the professional drone industry in high-accuracy data capture over large areas in even the most challenging environments. This is due to its VTOL tailsitter design, high-end payloads and well-engineered workflows. As its customers push it to the limit of its capabilities—reporting success across a range of use cases—Wingtra engineers work steadily to continue advancing its capabilities and bolstering its reliability.

"We would like to welcome Wingtra to the ASPRS family," said Joe Cantz,Chair of the ASPRS Sustaining Members Council. "We are glad to have you as a part of our Sustaining Members Council (SMC) and are looking forward to working with your team as you grow. SMC members are critical to our success as an organization, and we all appreciate Wingtra joining us in this capacity."

ASPRS members work in the disciplines of the mapping sciences, across the following sectors: agriculture, soils, archeology, biology, cartography, ecology, environment, forestry, range geodesy, geography, geology, hydrology, water, resources, land appraisal, real estate, medicine, transportation and urban planning/development.

For more information, visit: https://wingtra.com/.

STAND OUT FROM THE REST

EARN ASPRS CERTIFICATION

ASPRS congratulates these recently Certified and Re-certified individuals:

CERTIFIED PHOTOGRAMMETRIC TECHNOLOGIST

Matthew Peloquin, Certification #1649PT
Effective June 19, 2020, expires June 19, 2023

CERTIFIED GIS/LIS TECHNOLOGIST

Deborah Alberto, Certification #304GST
Effective June 8, 2020, expires June 8, 2023

RECERTIFIED PHOTOGRAMMETRIC TECHNOLOGIST

Jorge R. Aguayo, Certification #R1353PT
Effective March 26, 2020, expires March 26, 2023

RECERTIFIED PHOTOGRAMMETRISTS

Novica Janicijevic, Certification #R1263
Effective June 3, 2020, expires June 3, 2025

Radha Krishna Kandukuri, Certification #R1439
Effective February 16, 2020, expires February 16, 2025

Sonja Ellefson, Certification #R1450
Effective June 26, 2020, expires June 26, 2025

Brian E. Murphy, Certification #R1435
Effective December 27, 2019, expires December 27, 2024

James W. Young, Certification #R1582
Effective, April 1, 2020, expires April 1, 2025

Lindsey Galyen Certification #R971
Effective June 13, 2020, expires June 13, 2025

ASPRS Certification validates your professional practice and experience. It differentiates you from others in the profession. For more information on the ASPRS Certification program: contact **certification@asprs.org,** visit **https://www.asprs.org/general/asprs-certification-program.html**

COUNCIL OF ENGINEERING AND SCIENTIFIC SPECIALTY BOARDS CESB 1990

asprs THE IMAGING & GEOSPATIAL INFORMATION SOCIETY

NOW AVAILABLE!

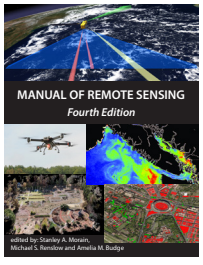

ASPRS Announces the 4th Edition of the *Manual of Remote Sensing!*

The *Manual of Remote Sensing, 4th Ed.* (MRS-4) is an "enhanced" electronic publication available online from ASPRS. This edition expands its scope from previous editions, focusing on new and updated material since the turn of the 21st Century. Stanley Morain (Editor-in-Chief), and co-editors Michael Renslow and Amelia Budge have compiled material provided by numerous contributors who are experts in various aspects of remote sensing technologies, data preservation practices, data access mechanisms, data processing and modeling techniques, societal benefits, and legal aspects such as space policies and space law. These topics are organized into nine chapters. MRS4 is unique from previous editions in that it is a "living" document that can be updated easily in years to come as new technologies and practices evolve. It also is designed to include animated illustrations and videos to further enhance the reader's experience.

MRS-4 is available to ASPRS Members as a member benefit or can be purchased by non-members. To access MRS-4, visit https://my.asprs.org/mrs4.

Ad Index

NEW ASPRS MEMBERS

ASPRS would like to welcome the following new members!

At Large
Trent Casi
Scott McTavish
Michael O'Sullivan
Paul Michael Cleary
Dr. Harald Haenisch

Cascadia
Lara Heitmeyer

Florida
Francisco J. Balsells
Todd Owen Waldorf

Heartland
Sayantan Majumdar
Mark Meirink
Curtis V. Price

Mid South
Corey Chatelain
Bobby Joe Daniel
Thomas R. Freeman, CP
Rodney Miceli, GISP
Austin Stone

Pacific Southwest
David Firman
Hersey Dan Dandini
Gaurav Juneja
Julian Magda
John William Martin
Paul Spaur
Dr. Ignacio A. Zuleta

Potomac
Dr. Matthew Gerike
John Knowlton, III

Rocky Mountain
Amy Elizabeth Larson
Drew Jurkofsky, CMS
Jonathan C. Pomeroy

Western Great Lakes
Troy D. Delmonico, CP
Jonathan Thompson

FOR MORE INFORMATION ON ASPRS MEMBERSHIP, VISIT **HTTP://WWW.ASPRS.ORG/JOIN-NOW**

Your Path To Success In The Geospatial Community

Call for Submissions

Special Issue on Urban Remote Sensing

Photogrammetric Engineering and Remote Sensing (*PE&RS)* is seeking submissions for a special issue on Urban Remote Sensing.

The formulation of the 17 Sustainable Development Goals (SDGs) is a major leap towards humankind's quest for sustainability. In recent decades, global urban areas have been rapidly expanding, especially in developing countries. The prospect is that the urbanization rate will reach 60% by 2030. Urban expansion will inevitably increase vulnerability to natural hazards, natural vegetation cover decline and arable land loss, urban heat islands, air pollution, hydrological circle alteration and biotic homogenization. Since urban ecosystems are strongly influenced by anthropogenic activities, a considerable amount of research has been conducted all around the world to understand the spatial patterns, driving forces and the ecological and social consequences of urbanization. It is not only crucial for characterizing the ecological consequences of urbanization but also for developing effective economic, social and environmental policies in order to mitigate its adverse impacts.

Remote sensing has been widely used for investigating urban environment and the associated drivers during the urbanization process, as it can quickly and frequently monitor large area surface change with lower cost, compared to filed survey or in situ measurements. Digital archives of remotely sensed data provide an excellent opportunity to study historical urban changes and to relate their spatio-temporal patterns to environmental and human factors. With the rapid development of Earth observation techniques, it has become convenient to obtain a large number of remotely-sensed imagery over a certain area at different times, from hundreds of Earth observation platforms. However, this brings challenges to researchers to timely process the remote sensing big data as well as to rapidly transfer the data into information and knowledge.

Considering this, this special issue of *PE&RS* is aimed at reporting novel studies on exploiting remote sensing big data to monitor and improve urban environment, and showing the potential of remote sensing in developing sustainable cities, including but not limited to:

- Urban remote sensing big data
- Remote sensing information interpretation
- Urban expansion, dynamics and associated environment consequences
- Remote sensing of urban water quality
- Remote sensing of urban thermal environment
- Remote sensing of urban geological environment
- Urban sustainability assessment
- Urban sustainable development
- Urban Spatiotemporal analysis
- Urban Sustainability Indicators
- Urban environmental Monitoring

Papers must be original contributions, not previously published or submitted to other journals. Submissions based on previous published or submitted conference papers may be considered provided they are considerably improved and extended. Papers must follow the instructions for authors at http://asprs-pers.edmgr.com/.

Important Dates

- July 1, 2020 Submission system opening
- October 31, 2020 Submission system closing
- Planned publication date: Dec. 2020
- Submit your manuscript to http://asprs-pers.edmgr.com/ by Oct. 31, 2020.

Guest Editors

Zhenfeng Shao, *Wuhan University*, China
Prof. Zhenfeng Shao, Professor at the State Key Laboratory of Information Engineering in Surveying, Mapping and Remote Sensing, Wuhan University, China. His research interests include urban remote sensing. He is now an associate editor of Email: shaozhenfeng@whu.edu.cn.

Orhan Altan, *Istanbul Technical University*, Turkey
Prof. Orhan ALTAN, Professor at the Department of Geomatics Engineering, Istanbul Technical University, Turkey. He is Past President and Honorary Member of ISPRS, Honorary Member of Science Academy. He has published more than 200 scientific papers in scientific journals and conferences, and editor or co-editor of more than 20 international books. Email: oaltan@itu.edu.tr

J.L.van Genderen, *University of Twente*, Netherlands
Professor J.L.van Genderen, Prof. at the Department of Earth Observation Science, Faculty of Geo-information Science and Earth Observation(ITC),University of Twente, Netherlands, he is an associate Editor of Geo-Spatial Information Science. His research interests include photogrammetry and remote sensing, urban remote sensing and computer vision. Email: Genderen@alumni.itc.nl.

A History of Laser Scanning, Part 2: The Later Phase of Industrial and Heritage Applications

Adam P. Spring

Abstract

The second part of this article examines the transition of midrange terrestrial laser scanning (TLS)–from applied research to applied markets. It looks at the crossover of technologies; their connection to broader developments in computing and microelectronics; and changes made based on application. The shift from initial uses in on-board guidance systems and terrain mapping to tripod-based survey for as-built documentation is a main focus. Origins of terms like digital twin are identified and, for the first time, the earliest examples of cultural heritage (CH) based midrange TLS scans are shown and explained. Part two of this history of laser scanning is a comprehensive analysis upto the year 2020.

Introduction

Having started out in the first part of this history of midrange terrestrial laser scanning (TLS) with space, defense, and research-driven applications (in the initial phase of its development), the second part now explores how technologies made the transition to other fields, like the nuclear industry and cultural heritage (CH). This was particularly the case in and beyond the 1990s. Building on earlier digital processing tools, new ways emerged to analyze and display the data from laser scanners. This second phase in the development of laser scanning is also one where the adoption of technology found nongovernmental organizations working as facilitators in documenting CH. Case studies were generated either to market the technologies to a wider audience or to help educate people about the technologies used. The sponsorship of such projects was supported by corporate backers wherever it proved possible. The third phase, led by tripod based systems and nonprofit corporations—which came out of California—developed and democratized its take-up. Finally, in the fourth phase, the automotive and mobile-computer industries are driving the commoditization of sensors. Phase four was still in place when this article was published.

Laser System Architecture: The Essentials

See Figure 1, next page.

Laser Scanning in Its Commercial Era (from 1979 Onward)

After the end of the first phase of development in the space and defense sectors (see part one of this article), the focus of development shifted to the commercial sector, where it still remains. The technologies that now comprise TLS in general—be it close, midrange, or long range—are all centered on measurement devices and techniques in this commercial era of use. They are geared toward the rapid documentation of scenes and objects to a high level of detail. More specifically, TLS is a form of active sensing where a laser makes contact with a surface in order to generate accurate and precise point-cloud information ("Project Development Plan" n.d.). This information is then processed using software that is compatible with the dense point clouds of 3D information thus generated (Takase *et al.* 2003). Software packages can be proprietary in nature—such as Leica Geosystems' Cyclone, Riegl's RiScan, Trimble's RealWorks, Zoller + Fröhlich's LaserControl, and Autodesk's ReCap ("Leica Cyclone" 2020; "ReCap" n.d.; "RiScan Pro 2.0" n.d.; "Trimble RealWorks" n.d.; "Z+F LaserControl" n.d.)—or open source, like CloudCompare (Girardeau-Montaut n.d.). There are even plug-ins for preexisting computer-aided design (CAD) software packages. For example, CloudWorx enables AutoCAD users to work with point-cloud information ("Leica CloudWorx" 2020; "Leica Cyclone" 2020). Like many services and solutions, AutoCAD predates the incorporation of 3D point clouds into design-based workflows (Clayton 2005). Enabling the user base of pre-existing software to work with point-cloud data in this way–in packages they are already educated in–is a gateway to increased adoption of midrange TLS. Distributed computing has also made large data sets like point clouds more accessible to a broader spectrum of people.

The term "midrange" is used to describe the rapid acquisition of 3D point-cloud data collected to known accuracies, repeatability (in terms of performance), and resolutions over a known distance (Boehler, Bordas Vicent and Marbs 2003; Spring, Peters and Minns 2010). It takes the notion of dynamic range—the ratio between the largest and smallest values (including surfaces in a scene returned as points)—into account when documenting an environment or object as a 3D image (Boehler, Heinz and Marbs 2001; Boehler and Marbs 2002; Mettenleiter *et al.* 2016). Information pertaining to its earlier uses, which are outlined later in this article, suggests that it is best viewed within a range of up to 1000 m. This updates the measurement to application parameters based on object complexity set out by Boehler *et al.* (2001; Historic England 2018)—that is, by including advancements in accuracy, repeatability, and resolution over a greater range in the period since that work was published. Current midrange TLS solutions collect up to 1 million points of data per second at optimum resolutions of millimeters up to around 5 cm—typically as a near-360° panorama of points (Mettenleiter *et al.* 2016)—depending on the size and scope of the project (also known as the *end deliverable*). Speed of data collection has continued to increase; as of July 2020, it takes anywhere from 4 to 7 min on newer units like the RTC360 and Z+F 5016 (Mettenleiter *et al.* 2016; Wujanz *et al.* 2017; Biasion *et al.* 2019)—when they are set to high accuracy, rate at which signals of points retrieved are sampled, resolution, quality, and range. Laser scanners are like still photography cameras in that they document a scene (Spring and Peters 2014). Instead of generating 2D pixels, however, they use a laser to create a 3D image commonly referred to as a point cloud (Spring 2015).

Point-cloud information is integral to a midrange TLS workflow. In this type of workflow, points are made up of x (ω), y (φ), z (κ), red, green, blue, and grayscale data (Levoy and Whitted

Remotely Interested LLC, adam@remotely-interested.com

Photogrammetric Engineering & Remote Sensing
Vol. 86, No. 8, August 2020, pp. 479–501.
0099-1112/20/479–501

doi: 10.14358/PERS.86.8.479

Laser System Architecture: The Essentials

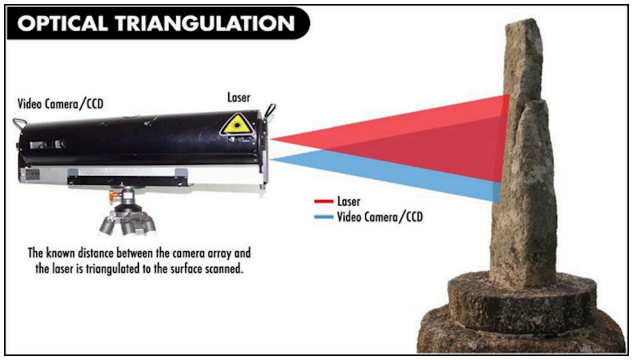

(a)

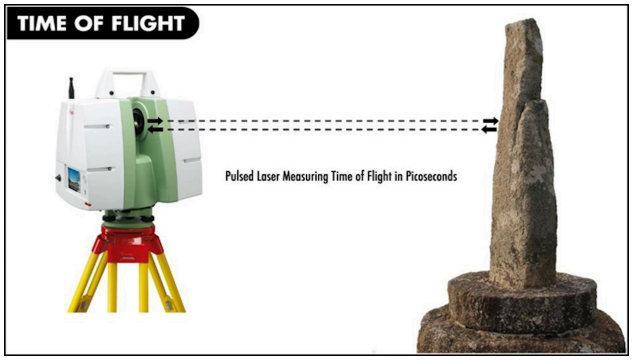

(b)

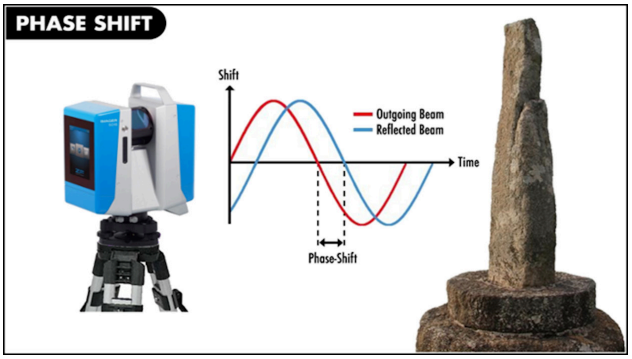

(c)

Figure 1. (a) The principle of optical triangulation was initially used in Mensi SOISIC scanners to inspect nuclear facilities owned by Électricité de France (EDF) (Fuchs *et al.* 2004). The known distance between the sensors on the scanner head and the area of overlap projected onto a surface was used to gather metrically accurate information (Learning Tools for Advanced Three-Dimensional Surveying in Risk Awareness Project [3DRiskMapping] 2008). Incorporating a laser into the system architecture of the SOISIC also extended the range at which information could be collected using this method (X. Chen & Schmitt 1992). Optical triangulation was used in low-cost consumer products by 2010 (Garcia and Zalevsky 2008; Vance 2010): For example, PrimeSense triangulation-enabling depth sensors were used in the Xbox Kinect 360 and the Project Tango prototype mobile-phone (Mantis Vision provided the structured light sensor for the tablet) ("PrimeSense Supplies 3-D-Sensing Technology" 2010; Keralia, Vyas and Deulkar 2014). PrimeSense was acquired by Apple in 2013 (Etherington 2014).

(b) 3D point-cloud data are collected by time of flight (ToF) via a pulsed beam (3DRiskMapping 2008). The Cyrax HDS 2400 and Riegl LMS-Z160/Z210 were the first ToF systems to be released when midrange terrestrial laser scanning (TLS) made the transition into commercial markets in 1997–1998 (Flatscher *et al.* 1999). Similar to the commoditization of triangulation systems via the Xbox Kinect 360, the Project Tango mobile phone-based architecture incorporated ToF sensors via the ASUS ZenFone AR phones in 2017 (Franz, Irmler and Rüppel 2018). Project Tango's failure in leading to a commercially successful product, even with ASUS's distribution network, did not stop ToF from making its way into mobile phones again (Kastrenakes 2017; Petrov 2018). Samsung introduced ToF sensors into its 10+ 5G and Note units by 2019 (Petrov 2018). Their positional use in virtual and augmented reality-based applications was the driving force behind this move (Saran, Lin and Zakhor 2019).

This trend continued to develop at Google after Project Tango was absorbed into its ARCore augmented reality system in December, 2017 (Kastrenakes 2017). The ARCore led Depth API–which created depth maps from the RGB camera in a smart phone or tablet–was announced in December, 2019 (Izadi 2019). It became available to developers, June 25th, 2020 (Hayden 2020).

(c) Phase-shift (PS) solutions collect point-cloud data via the modulation pattern of a continuous wave pattern (3DRiskMapping 2008). The use of PS in commercially available midrange TLS systems is greatly influenced by research that came out of the Robotics Institute at Carnegie Mellon University (CMU) and the Technical University of Munich (Thorpe *et al.* 1987; Hebert and Krotkov 1992; Froehlich, Mettenleiter and Haertl 1997; Flatscher *et al.* 1999; Fienup 2013). For example, K²T formed as a company in 1990 (Guzzo 2004). It produced a variety of 3D imaging solutions based around CMU research or initiatives before the Franklin Scanner evolved into SceneModeler (Shaffer 1995; Froehlich *et al.* 1998; "Project Development Plan" n.d.). These include the GFR series of short-range (up to 2 meters) light-stripe range finder and the Blitzen and Typhoon scanners—with the latter two considered for hazardous environments and vehicle-based applications (Shaffer 1995; "Project Development Plan" n.d.). SceneModeler from K²T/Quantapoint was the first PS-based midrange TLS scanner to enter the market. This was followed, however, by the Zoller and Fröhlich (Z+F) 5003 from the German team that were brought in as a core part of developing SceneModeler (Shan and Toth 2009). Z+F developed a fundamental component of the K²T scanner: the LARA rangefinder (Froehlich *et al.* 1998; Hancock, Hoffman *et al.* 1998; Hancock, Langer *et al.* 1998; Langer *et al.* 2000). iQvolution brought out its iQsun 880 PS scanners two years after the Z+F Imager 5003, in 2003 (Becker and Volz 2004)—before being acquired by FARO in 2005 (Pritchard 2005). This eventually led to the FARO Focus^{3D} line of scanners. Surphaser also produces PS systems.

Before considering the succeeding three phases of development to that of early space of defense applications (phases two to four), it is important to define the measurement systems involved in laser scanners. Both ToF and PS are time-based measurement systems in that point clouds are generated by measuring the time frame between two events (Van Genechten *et al.* 2008). For example, ToF systems - also known as pulsed systems - measure the time it takes a laser to return to the scanner against the speed of light - 299,792,458 meters per second in a vacuum and 90 km/s slower when travelling through air (Boehler *et al.* 2002; Van Genechten *et al.* 2008). As demonstrated in 1b, the pulse rates used to generate point clouds accurate and repeatable to resolutions in millimeters and centimeters are measured in picoseconds (10-12 of a second) (Van Genechten *et al.* 2008). In a PS system, the power of the continuous beam emitted from the scanner is modulated (Van Genechten *et al.* 2008; Mettenleiter *et al.* 2016). The time and difference in signal pattern returning to the scanner is used to obtain a measurement (Van Genechten *et al.* 2008). 1c shows how these phases of modulation are used to acquire measurements by comparing the outgoing and returning wave patterns of the laser as the scanner collects data (Van Genechten *et al.* 2008; Mettenleiter *et al.* 2016).

Mensi replaced their triangulation based SOISIC scanners with a longer range ToF solution called the GS 100 in 2001 (Shan and Toth 2008). This resulted in time-based measurement becoming the main solution used for data collection in commercial mid-range TLS workflows (Shan and Toth 2018; Chen et al 2005). It also brought the company more in line with Cyra Technologies and Riegl, who had successfully released commercial ToF systems by 1998 (Kacyra *et al.* 1997; Shan and Toth 2008; Gaiani *et al.* 2000; Ullrich et al 1999).

1985; Ullrich and Studnicka 1999; Levoy 2007; Spring and Peters 2014; Mettenleiter *et al.* 2016). The location of the data is fixed to a known (0,0,0) coordinate location at the point where the laser reflects from an oscillating or rotating mirror (3DRiskMapping 2008). Surfaces are reconstructed through the process of scanning, which requires the sensor to be moved to a position where at least 25% overlap exists between scans. This continues to be reduced by incorporating other sensors into scanning instruments, such as inertial measurement units (IMU) and camera tracking systems (Biasion *et al.* 2019). The captured scene can also include targets, as seen in Figure 2 and Figure 3. These are compatible with the laser systems being used, which are explained in the "Laser System Architecture: The Essentials" box.

Targets used in the act of scanning vary from black-and-white checker pattern to matte white spheres or retroreflective surfaces (Figure 2). They are used to increase the known accuracy of the data returned to the scanner, and to reference the local coordinates of the point cloud to absolute coordinate systems. For example, matte white spherical targets are used in phase-shift (PS) and time-of-flight (ToF) solutions set to a comparable wavelength on the electromagnetic spectrum (3DRiskMapping 2008). This is depicted in Figure 3, where a FARO Focus^{3D} set to a wavelength of 1550 nm was used to document the Tristan Stone, a medieval inscribed stone in Cornwall, UK (Spring and Peters 2014). As discussed in Gregory C. Walsh's (2010) patent on retro detector systems, dynamic range can also be used alongside the wavelength when developing target systems for midrange TLS. The retroreflective targets used for Riegl systems set to a near-infrared wavelength may provide some indication for this, in that the 1550-nm wavelength usually does not work well with high-reflective surfaces—not without it being compensated for within the system architecture of a laser scanning workflow.

The resolution and distance at which data are collected are also determined by the type of laser system inside the scanner (3DRiskMapping 2008; Mettenleiter *et al.* 2016). The type of scanner selected for a project should be determined by the scene being scanned, the environmental conditions in place, and the rationale for data capture (Boehler *et al.* 2001; Spring and Peters 2014; Historic England 2018). Once all point clouds have been collected, they are connected through a software-based registration process. As discussed in the "Phases of Development" box, seen in Figure 4, this is derived from the iterative closest point (ICP) algorithm-based approach, which is also optimized via other proprietary algorithms or functions when using commercial software (Besl and McKay 1992; Y. Chen and Medioni 1992). The registration process minimizes the difference between two or more point clouds (Girardeau-Montaut n.d.).

Figure 2. Retroreflective surfaces, spheres, and checkerboards are the primary types of artificial targets used in laser scanning. Note: the first set of Cyra Technologies based targets were a green retro-reflective surface, and later changed to the blue retro-reflective target surface seen above.

Variation is measured in nanometers (nm) (3DRiskMapping 2008). Wavelength in nanometers can result in different laser scanners reacting to the reflectivity of a surface in different ways (Boehler *et al.* 2003; Mettenleiter *et al.* 2016; Riquelme, Ferrer and Mas 2017). For example, the FARO family of laser scanners would not return usable data from the retroreflective targets used in Leica Geosystems scanners set to 532 nm, or Riegl scanners set to 1550 nm with a system architecture that incorporates single-photon avalanche diodes (Spring *et al.* 2010; Walsh 2010; Spring and Peters 2014).

Three laser-based solutions were originally used for midrange TLS between 1987 and 2001: optical triangulation, ToF, and PS (X. Chen and Schmitt 1992; Amann *et al.* 2001; Boehler and Marbs 2002; Shan and Toth 2009; 3DRiskMapping 2008; Mettenleiter *et al.* 2016). They are outlined in more detail in the "Laser System Architecture: The Essentials" box. Mensi replaced its triangulation-based SOISIC scanner with a longer-range ToF solution called the GS 100 in 2001 (X. N. Chen *et al.* 2005). It brought the company more in line with Cyra Technologies and Riegl, who had successfully released ToF solutions by 1998 (Kacyra *et al.* 1997; Ullrich *et al.* 1999; Gaiani *et al.* 2000). This is also discussed in more detail in the section "Transitions in Midrange TLS (Second Phase)", as well as part one of this article.

ToF- and PS-based solutions had become the primary way to collect point-cloud information with a laser by 2020 (3DRiskMapping 2008). ToF measures the time it takes a laser to return to the scanner against the speed of light (Mettenleiter *et al.* 2016). As demonstrated in the "Laser System Architecture: The Essentials" box, the pulse rates used to generate point clouds that are accurate, repeatable (in terms of performance), and to resolutions of millimeters and centimeters are measured in picoseconds (Wilson *et al.* 1999). In a PS system, the power of the continuous beam emitted from the scanner is modulated. Figure 1c shows how these phases of modulation are used to acquire measurements by comparing the outgoing and returning wave patterns of the laser as the scanner collects data. Both ToF and PS are time-based measurement solutions: The time frame between two events is integral to the collection of all information.

Figure 3. Checkerboard targets, crosshair black-and-white targets, and matte white spheres are used as targets in midrange TLS when the laser beam is set to a certain wavelength. The first-generation FARO Focus^{3D}—here being used to document the Tristan Stone, a medieval inscribed stone in Cornwall, UK—is set to a 1550-nm wavelength on the electromagnetic spectrum. Not all laser scanners are set to the same wavelength. The dynamic range of the information returned to the scanner can also be taken into account, as discussed in the section "Laser Scanning in Its Commercial Era (from 1979 Onward)."

Phases of Development

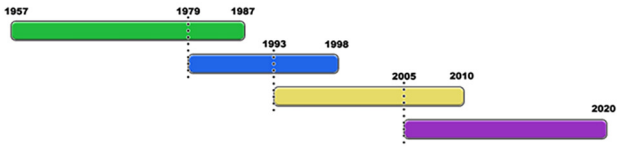

Figure 4. Four phases of development, including periods of transition, spanning 1957–2020.

Phase 1: 1957–1987

The laser was invented and Sputnik went into orbit, 1957. Sputnik immediately led to the formation of the Defense Advanced Research Projects Agency (ARPA/DARPA) in 1958 (Catmull 2014). Thus, starting the funding environment required to develop the early system architectures for midrange TLS. That is, via funding for the space and defence applications outlined in both parts of this article.

The turning point year for transition to Phase 2 starts is circa 1979 (and carries on to the formation of Mensi and favourable business acts getting passed in France and the USA by 1987). It is the year when business interest groups like the "Association pour le développement du mécénat industriel et commercial" (ADMICAL) are formed in France–by three students, who drew influence from observing the philanthropic model in the USA (Gautier *et al.* 2013). ADMICAL would soon be followed in the USA by the Stevenson-Wydler Technology Innovation Act of 1980 (Gautier *et al.* 2013). This essentially led to a number of acts that encouraged technology transfer from entities like DARPA to industry, such as the Small Business Technology Transfer Act of 1992.

Incidentally, the maintained cultural impact of applied government funded research on business cultures in the USA can be seen in phases 3 and 4. That is, via the DARPA Grand Challenge that influenced Velodyne, as well as Regina Dugan's (former Head of DARPA) role at Google running Advanced Technology and Projects (Metz 2016).

Phase 2: 1979–1998

Phase 2 has its seeds in the philanthropic movement coming out of France. It helped shape policies that encouraged business communities to contribute to projects in the cultural sphere. These policies influenced a working environment where Mensi systems could be applied to projects outside of Électricité de France (EDF). Otherwise, the SOISIC scanner was primarily being used to address their internal facility management needs by the early 1990s. This changed, however, when it was used as part of a project to upgrade parts of the city lighting of Paris–and the first CH midrange TLS scans were carried out in 1993 (Thibault, Email, July 4th, 2020; Thibault and d'Aligny 1994). This is discussed in more detail in Figure 11a.

The formation of Mensi by Auguste D'Aligny and Michel Paramythioti presents the beginnings of tripod-based systems geared to high levels of accuracy, repeatability and resolution (Bandiera *et al.* 2011; Paramythioti, M. and D'Aligny 1989). That is, for documentation and inspection as opposed to terrain mapping for autonomous vehicles. The transitional period leading to Phase 3 is seen to occur in 1993. This is the year Mensi carried out its first CH scans in Paris, as outlined in Figure 11a (Thibault, Email, July 4th, 2020; Thibault and d'Aligny 1994). Cyra Technologies was founded as a company in the same year–based on private funding and commercially derived observations. That was, for site design and inspection applications more in line with CAD based user communities of the time. Midrange TLS became the way to obtain design drawings for actual conditions of an industrial plant–using the as-built information gathered via a point-cloud (Deveau *et al.* 2005). Cyra Technologies was a "hit the ground running" scenario for Ben Kacyra and Jerry Dimsdale. Neither of these pioneers had much involvement with laser scanning prior to founding the company.

It should be noted that K²T was formed as a robotics company in 1990–to bring CMU Robotics Institute initiatives to market. Their previous involvement with DARPA projects is outlined in more detail in part one of this article. Influences from business outreach strategies built into the university system (in the USA) is discussed in Similarities to Personal-Computer Markets as well. K²T began to outline ideas for scanners like SceneModeler by 1993-94 ("Project Development Plan" n.d.; Hebert *et al.* 1992; Kweon and Kanade 1992). Like K²T, the Austrian company Riegl had strong ties to universities as well. Johannes Riegl–its namesake and founder–had been working on avalanche pulse generators at the Vienna University of Technology (VUT). This was prior to forming his company in 1978.

The Eureka PROMETHEUS Project (the largest R&D project ever in the field of driverless cars at time of publication) would also support self-driving vehicle initiatives at this phase– 1987–1995 (Dickmanns 2002; Nwagboso 1993; Maurer *et al.* 1995).

Phase 3: 1993 to 2010

The transition to Phase 3 begins when other entities to Mensi start to develop their own midrange TLS systems. It is at this point that the custom manufacture of hardware–which had been necessary in projects like the Adaptive Suspension Vehicle (ASV) and Autonomous Land Vehicle (ALV) to make them possible–can be replaced with development based around hybridization (Gage 1995; Gleichman *et al.* 1988; Waldron and McGhee 1986; Song and Waldron 1989). This is the concept of taking different available components, and bringing them together to make a new product.

Cyra Technologies, K²T and Riegl all show examples of hybridization in their early systems. For example, Cyra technologies combined the green laser from Massachusetts Institute of Technology (MIT) Lincoln Laboratory with a timing circuit repurposed from Los Alamos National Laboratory to create the Cyrax range of scanners (Wilson *et al.* 1999; Zayhowski 2010; Zayhowski 2018). K²T used a scanning mechanism they had designed at CMU–and combined it with a laser system developed by Christoph Froehlich–for the Franklin and SceneModeler units ("Project Development Plan" n.d.; Shaffer 1995; Froehlich *et al.* 1997; Langer *et al.* 2000). Riegl repurposed their own LD90-3 distance meter released for the rangefinder electronics in the LMS-Z160/Z210 (Flatscher *et al.* 1999; Riegl 2014; Studnicka 1999). This was for the European Space Agency (ESA) funded Active Surface Imaging System (ASIS) project (Flatscher *et al.* 1999; Riegl 2014; Studnicka 1999). Prior to this, they had also developed a shorter range scanner for the ESA project "Demonstrator of Advanced Laser Sensors" (DEAL) in 1996 (Riegl 2014).The ICP algorithm–developed by Besl and McKay at General Motors–made point cloud registration easier for a general user as software's also got developed.

The market that emerged by 1998 was solidified by the acquisitions of Cyra Technologies and Mensi–by Leica Geosystems and Trimble separately, 2000-2003. Two points of convergence then occurred in 2005. That is, signaling the beginning of the next era, which is greatly influenced by commoditization of sensor hardware and simultaneous and localised mapping (SLAM).

Velodyne enters the laser scanning design story via the DARPA Grand Challenge–developing a multibeam ToF system that would be adopted massively in car-based applications. They would also bring and apply their business experience in selling consumer products to the laser scanning market. PrimeSense also formed as a company at this time. This

brought triangulation-based 3D imaging to consumer products, initially via the Xbox Kinect and then tablets / smartphones.

Phase 3 stops at a point where Google invests in Velodyne (and starts to familiarize the general public to self-driving vehicles outside of the defense researcher domains); Xbox Kinect incorporate the PrimeSense triangulation unit into their gaming solution; and most midrange TLS units now have a computer and battery source built into their architecture. For the latter, this makes it easier to incorporate commercial midrange TLS units into SLAM based deliverables at Phase 4.

Incidentally, the influence of philanthropic entities on midrange TLS–first seen in France in Phase 2–is continued via The Kacyra Family Foundation in this period. That is, via the formation of CyArk and its promotion of technologies through high profile CH projects, 2003 onwards. This is discussed in more detail in the section "The Non-profit Corporations (Third Phase)."

Phase 4: 2005 to 2020

The transition to this phase began when Velodyne–a manufacturer of consumer level products at the time–entered the laser scanning market in 2005. It is a period where the emphasis on commoditization increases to where a mass market is forming around laser scanning hardware by 2020. There is also a strong influence on the market from investments and hardware coming from China (Ackerman 2016a; Shan and Toth 2018; Simai Surveying Instruments 2020; GPS World 2015).

There were, for example, significant announcements at the Consumer Electronics Show centered around low-cost laser scanning hardware from Velodyne (Velabit) and Livox (Mid-Series) in 2020 (Ohnsman 2020; "DJI Showcases" 2019). Livox was also a subsidiary of DJI (both based out of Shenzhen in China)–a company with a proven track record in bringing technologies like drones / unmanned aerial systems to a mass market of users ("Breaking Through" 2014). Amazon has also acquired the self-driving vehicle company Zoox for a rumored USD 1.2 Billion by July 2020 (Wiggers 2020).

Earlier indicators of this move to cheaper, 'plug in and develop out from' type systems could be seen by around 2015. That is, when Velodyne sensors started to get incorporated into tripod-based systems like those seen in Figure 1b of Part 1 of this article, as well as when mobile mapping solutions had started to incorporate Velodyne sensors into their hardware as well. For example, Topcon and Leica Geosystems vehicle mount systems use Velodyne scanners alongside their own systems. IQvolution had also explored a similar idea of a modular approach for midrange TLS in the article *iQsun 880 A New Modular Concept For 3D-Laser Scanning,* 2004 (Becker & Volz 2004).

This fourth phase also saw the emergence of low cost, build your own kits from companies like Scanse (Ackerman 2016b). This kind of activity–which brings down development costs and gets the technology into the hands of a broader spectrum of people–mirrors patterns of behaviour seen in the formative years of the personal computer market. It is examined in more detail in the section about "Parallels to the Personal Computing Market."

What was typically hobbyist level activity around midrange TLS via systems like the Scanse was stimulated by companies like PrimeSense. Through the notable impact platforms like Xbox Kinect had on bringing point-cloud data to a wider audience. The rise of sensors like those from PrimeSense–and later in the same decade Infineon/PMD (2019)–would also go on to influence Google projects like Project Tango in 2014 (Etherington 2014). Early examples where 3D imaging technologies in general were integrated into mobile phones and tablets. Where people could scan a room by walking through their environment with the device.

By the time this article was published, midrange TLS solutions were being increasingly influenced by developments shaped via wearable or mobile devices, as well as vehicle-based applications. Tripod based systems were increasingly being packaged to fall in line with SLAM based ideas about mapping (Biasion *et al.* 2019). For example, integration of midrange TLS systems with hardware like onboard camera tracking systems and IMU sensors–to make the scanner more aware of its position in an environment as it moved from each position–was a relatively new standard of expectation from the user (Biasion *et al.* 2019). The technology was increasingly presented as not being tethered to the tripod in the same way as it had previously. Distributed computing–either onsite via a tablet or phone, or at a desktop over the cloud or via "Edge Computing"–was also part of the zeitgeist from 2010–2020 (Spring 2015). The seeds for additional commoditization from another source were also planted when China started to develop their own tripod-based midrange TLS systems in 2015 (Simai Surveying Instruments 2020; GPS World 2015).

The Shift from US Government Space and Defense Programs to Commercialization, Set in Three Phases of Further Development in Laser Scanning Technologies

The Second Phase: Commercialization, Business Models, and Philanthropy (1979–1998)

In the second phase, it was in France that business interest groups like the Association pour le Développement du Mécénat Industriel et Commercial (ADMICAL) first started to help create the necessary working conditions (Gautier *et al.* 2013). As the leading association for corporate philanthropy in France, ADMICAL helped transform midrange TLS from applied research (funded by defense and other government grants) to a commercially viable product. As discussed later under "Application to Cultural Heritage (Second and Third Phases)," ADMICAL was the catalyst for two significant laws getting passed by the French government. Both laws supported corporate philanthropy, and in doing so, they also aided transitions in the application of midrange TLS to industrial and CH settings (Brillault, Thibault and Guisnel 1995; Pot, Thibault and Levesque 1997; Moulin *et al.* 1998).

Broader technology trends coming out of the USA also contributed to a business culture developing around the technology. The rise of the World Wide Web and the dot-com boom coincided with the development of companies like Cyra Technologies (Kacyra *et al.* 1997; Hwang and Stewart 2006; Morris and Alam 2012). This part of the story straddles both the second phase and the early years of the third phase of midrange TLS development. It spans from around 1993 through the period of commercialization to the end of the year 2000 (Phillips and Yu 2011). The dot-com boom made it easier for larger companies, such as Leica Geosystems, to see the value in digital survey tools like laser scanners. In fact, it gave them increased market value in an emerging world where information and communication technologies would play a key role (Stiroh 2002), because instruments like Cyra Technologies' original concept of a Field Digital Vision (abbreviated to FDV) machine enabled their users to collect objects and buildings as computer-based assets—used to manage, maintain, or inspect a given environment (Wilson *et al.* 1999). The acquisition of Cyra Technologies by Leica Geosystems solidified the midrange TLS market in a way, because it was the first example of a large company openly taking over the direction in which technologies would develop ("Leica Geosystems Acquires Oakland-Based Cyra Technologies" 2000). It was also shortly followed by Trimble's acquisition of Mensi in 2003 ("Trimble Navigation Acquires Mensi S.A." n.d.).

On the technical side in the second phase of development, close-range TLS also became a testing ground for the use of scan data in the reverse engineering of surface information. Companies like Cyberware and General Motors made it easier for more general users to work with point clouds and meshes

(Rioux and Bird 1993; Besl 1988). For example, the work carried out by Paul Besl and Neil McKay (1992) on iterative closest point matching, which came out of their time at General Motors, helped define the process for connecting multiple point clouds into one. It created a foundation algorithm that software packages like CloudCompare and Cyclone would later bring into their registration pipeline (Mettenleiter *et al.* 2016). This and a more detailed outline of the relationship between close-range and midrange TLS is discussed in the section "Close-Range Scanning (Second Phase)." In the third phase, a market formed around these technologies.

The Third Phase: Market Development (1993–2010)

In the third phase, market development was encouraged through nonprofit entities like CyArk promoting technologies via heritage sites. The CyArk 500 and Scottish Ten projects are two of the more notable examples linked to the California-based 501(c)(3), which was set up by Ben Kacyra in 2003 (Kacyra 2009; "New Lanark, Scotland" n.d.). The work of early adopter Kevin Cain is also outlined in the "Cultural Heritage as Marketing (Second and Third Phases)" and "Nonprofit Corporations (Third Phase)" sections. Cain formed his Institute for the Study and Integration of Graphical Heritage Techniques (INSIGHT) nonprofit corporation in 1999.

The Fourth Phase: Simultaneous and Localized Mapping (2005 Onward)

By 2020, the fourth stage of development was being shaped by applications based on simultaneous and localized mapping–otherwise referred as SLAM. Commodity sensors had emerged from efforts to make autonomous vehicles a commercially available product. Technologies had also become small enough to be worn or carried around by their users as they mapped an environment. For example, the first DARPA Grand Challenge—which was geared toward improving sensors for autonomous vehicles and took place in 2005—led to the creation of the Velodyne range of sensors (see figure 1a and 1b in part one of this article; Halterman and Bruch 2010). These went on to be integrated into hand-carried units, backpack-based systems, vehicle-based mapping systems, and even tripod-based units (Figure 5). The Grand Challenge also brought Velodyne as a developer into the midrange TLS community. Before this, it was a company with a proven track record in commodity-based business and distribution models for sound equipment like subwoofers (Robson 2017).

Handheld and wearable solutions that took the movement of their operator into account also emerged in this period. One of the more interesting systems was the Zebedee (Figure 5a), which came out of the Melbourne-based Commonwealth Scientific and Industrial Research Organization (CSIRO) in 2012 (Bosse *et al.* 2012). It used a 2D laser scanner and an inertial measurement unit mounted on a spring. A series of custom algorithms worked alongside the hardware to optimize data retrieved, including all six degrees of freedom of movement (x, y, z, ω, φ, κ) along with the laser's position in space as it captured information. Zebedee—named after the

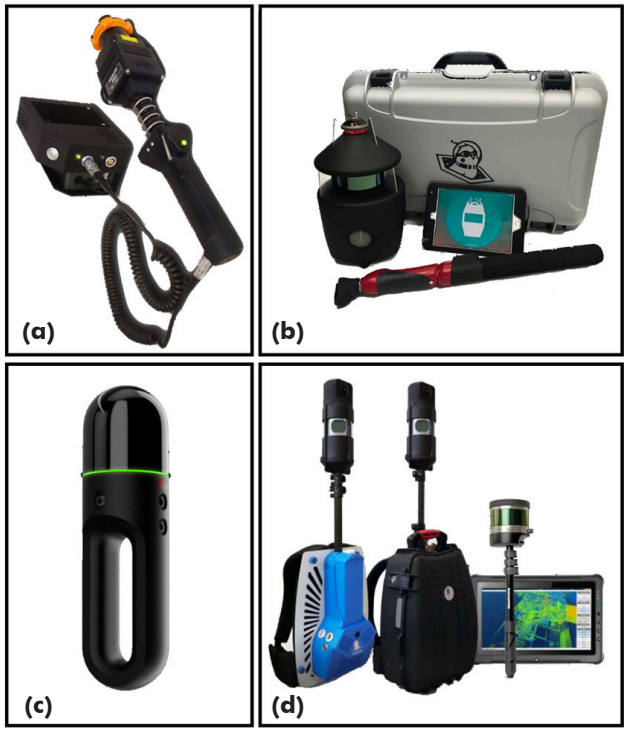

Figure 5. Handheld and wearable laser scanning technologies were being marketed in the same application areas as midrange TLS by 2020. (a) The Zebedee unit developed by the Commonwealth Scientific and Industrial Research Organization (CSIRO) was commercialized by Nottingham, UK-based 3D Laser Mapping in 2013. By 2020, it had been followed by the ZEB REVO, ZEB REVO RT, ZEB Horizon, ZEB Pano, and ZEB Discovery. Software in the form of GeoSLAM Hub was developed in 2015, and then 3D Laser Mapping merged with GeoSLAM in 2018. The ZEB Discovery unit also incorporated the iSTAR Pulsar 360-degree photography camera developed by Edinburgh-based NCTech into its system architecture. NCTech is the same company that produced the LASiris VR seen in figure 1b in part one of this article and discussed in the section "Designed for Documentation and Inspection." (b) Florida-based Paracosm was founded in 2013 and then acquired by Occipital—a San Francisco-based company that had been working on affordable 3D solutions since 2008—in 2017. The PX-80 integrated a Velodyne VLP-16 channel-based sensor into its system architecture. Users document a scene as they walk around the given object environment. Paracosm incorporated table-based computing into its workflow to work with the data collected in real time. (c) The BLK2GO was launched by Leica Geosystems in 2019. It was a handheld unit marketed around its dual-axis lidar system and suitability of use in workflows based on SLAM. It was also positioned around "adaptive reuse projects in the architecture and design industries to location scouting, pre-visualization, and VFX workflows for media and entertainment," bringing it more in line with the inspection aspects of midrange TLS (GIM International 2019). The Cyclone and Register suites of software developed by the Hexagon-owned Leica Geosystems were all compatible with the BLK2GO. (d) The HERON range of backpack and handheld solutions incorporated the Velodyne HDL-32E and Puck Lite sensors into their system architecture, along with tablet computers. They were created by Italy-based GEXCEL, which had been developing 3D image-based solutions since 2007. GEXCEL also developed software for the mining industry called Open Pit Mine Monitoring System, which was optimized for use with the Teledyne Optech Polaris systems seen in figure 1b in part one of this article. The HERON and Reconstructor software from GEXCEL also got resold by ClearEdge3D (2019), which Topcon had acquired in 2018 to help position itself in emerging "reality capture" markets. The term *reality capture* (also sometimes seen as *reality computing*) was first outlined by Cyra Technologies, brought in line with the idea of "high-definition surveying" after the brand's acquisition by Leica Geosystems, and then later reintroduced to midrange TLS communities by Autodesk (Cyra Technologies 1999; Frei *et al.* 2005; Autodesk 2013).

Explanation Box: Building Upon Navigation Based Initiatives–Who and What?

Figure 6. Midrange TLS solutions were being revisited as mobile mapping solutions in everyday life by 2020—outside the otherwise closed networks seen in the first and second phases of development. Some of the earliest examples are shown in Figure 6. (a) The Irma3D is an autonomous vehicle created by Andreas Nüchter of Jacobs University Bremen in Germany. It incorporated a Riegl VZ-400 laser scanner into its system architecture. (b) Similar solutions made it into industrial sectors via Allpoint Systems, which primarily worked with Zoller and Fröhlich scanners. The company was founded by CMU graduates and became part of Autodesk's ReCap suite of solutions in 2013. (c) Nokia acquired a company called Earthmine as part of its HERE mapping service in 2012. Earthmine was formed by John Ristevski, a former employee of CyArk, in 2006. He brought Oliver Monson (a former project manager at CyArk) into the company as a data manager a year later. Earthmine patented stereo photogrammetry-based technologies from the JPL for its early mapping solutions. HERE was acquired by Audi, BMW, and Daimler in 2015. (d) Google's self-driving cars are revisiting the concepts explored through projects like the ALV, the CMU Navigation Laboratory, and PROMETHEUS. The company has made notable investments in, and uses midrange TLS sensors from, companies like Velodyne for terrain modeling and computer-vision purposes. More detail is provided in the "Waves of Developments Driven by Its Users—How and Why?" box.

The development of midrange TLS for site documentation and survey (late 1990s) does not break away from original uses in mobile applications. It is part of a process that refines hardware and software–feeding into the infrastructures and networks established from phase one of development onwards.. For example, Cyra Technologies examined the work carried out by ERIM, employed CMU graduates like Mark Wheeler (who went on to become Chief Technology Officer of the autonomous-vehicle company DeepMap in 2016; "DeepMap" 2018), and visited the CMU Robotics Institute when the Cyrax HDS 2400, seen alongside the follow-up HDS 2500 in Figure 8, was starting to take shape. Jerry Dimsdale, the system architect for the early Cyrax systems, went on to develop the Topcon GLS series of midrange laser scanners under his company Voxis from 2003 through 2008 ("Topcon Acquires Voxis" 2008; Wan Aziz *et al.* 2012) after Cyra Technologies was acquired by Leica Geosystems in 2000 ("Leica Geosystems Acquires Oakland-Based Cyra Technologies" 2000). Launched in 2008, the Topcon scanners combined a ToF solution with a PS algorithm in order to improve the quality of scan data produced. Systems like the GLS 2000 also incorporated first- and last-pulse recording.

Gregory C. Walsh, Jerry Dimsdale's successor at Leica Geosystems, was introduced to laser scanning in 1992 when he was an engineer on a Mars rover project, funded by the ESA, called Hilare (Walsh *et al.* 1994). He went on to design five ToF systems for Leica Geosystems: the HDS 3000, ScanStation 1, ScanStation 2, ScanStation C10, and RTC360. He also contributed to the laser and photography camera systems used inside the P-series scanners developed after the P20.

jack-in-the-box from the children's television show *The Magic Roundabout*—was commercialized by companies like 3D Laser Mapping almost immediately after they saw the technology. 3D Laser Mapping later merged with its sister company GeoSLAM to place an emphasis on such solutions (GeoSLAM 2018). Robert Zlot, one of the developers of Zebedee, had received his PhD in robotics from CMU in 2006.

Transitions in Midrange TLS (Second Phase)

ToF and PS solutions had evolved by 2001. It was now possible to collect data at greater distances and accuracies. This was not the case, however, when Mensi was formed as a company in 1987 (X. Chen and Schmitt 1992). It had a close working relationship with EDF, a company that required detailed information in order to maintain its industrial power plants (Fertey *et al.* 1995; Pot *et al.* 1997). EDF acquires a stake in MENSI S.A. in 1997 ("About Us [Mensi]" n.d.). When the company was formed, however, ToF solutions were not yet accurate enough, and PS solutions could scan at the resolution needed only over a short range (Xin Chen, email to author, October 18, 2013; Fienup 2013). Mensi resolved these issues by borrowing from both passive and active sensing, with a laser increasing the range at which measurements could be collected using optical triangulation (X. Chen and Schmitt 1992). As seen in the "Laser System Architecture: The Essentials" box, the SOISIC scanner compared the known distance between the sensors inside it to the area of projected overlap on the surface being scanned.

The solution Mensi had created fed into preexisting workflows linked to "as-built" information being used by EDF (Fertey *et al.* 1995; Pot *et al.* 1997). SOISIC enabled users to gather information pertaining to actual surface conditions of the object or scene being managed. This meant it was able to give an engineer or project team working with the point-cloud information it generated a clear understanding of the actual conditions in place inside a nuclear power plant rather than design-perfect ("as-designed") conditions depicted in CAD drawings or preexisting site plans (Deveau *et al.* 2005). Early developers of the technology like Mensi recognized the shortcomings of preexisting workflows. Plan-based information alone had the potential to contain a wide level of detachment from the end product or scenes being scanned. These were predominantly design- and manufacture-based communities, driven by clearly defined metric and procedural parameters in an otherwise 2D CAD space, such as industrial pipe modeling or drafting (Pot *et al.* 1997).

As Built

Early applications of midrange TLS—whether CH, defense, space, or safety-driven workflows in environments like nuclear power plants—all shared a unifying need for the collection of "as-built" or "as is" information (Figure 7; Pot *et al.* 1997;

Figure 7. Mensi technologies were developed in order to collect as-built information. They made their way into the North American market by 1996, through Atlanta-based Catco (Kacyra, Dimsdale and Kung 2005). Then Ken Shain helped form Mensi USA in 1999 (Monroe 1999). Mensi was acquired in 2003 from EDF by Trimble.

Gentle Giant Studios used a customized purple Mensi SOISIC scanner to document props on the set of *Star Wars Episode II: Attack of the Clones*. When they traveled to Paris to scope out the technology, the Gentle Giant team discovered that the SOISIC scanner unit had originally been designed to be mounted on vehicles (Steve Chapman, email to author, November 14, 2012). It was intended for use in areas of contamination in nuclear power plants, for remote information retrieval or inspection in areas too hazardous for humans. Photograph courtesy of Steve Chapman.

Stephan *et al.* 2002). For example, as-built was how practitioners in CH measured objects (O. Coignard *et al.* 1998; Cain 2000; Cain, Sobieralski and Martinez 2003). The gathering and analysis of information was centered around physical interaction with an object or site. In essence, adaptation for commercial sectors in the late 1990s involved bringing these as-built midrange TLS solutions and workflows more in line with the needs of user communities who were more familiar with as-designed information (Kacyra *et al.* 1997; Pot *et al.* 1997).

It was only when communities driven by an as-designed mind-set started to lean toward the use of as-built information that a move toward midrange TLS, as well as other 3D imaging techniques in general, started to occur (Kacyra *et al.* 1997; Mettenleiter *et al.* 2016; "Project Development Plan" n.d.). In the case of Mensi, early adoption of midrange TLS emerged out of past experiences with photogrammetry and surface modeling. The latter is seen in this article through the Digital Karnak project, where CAD-based software was used to reconstruct the dimensions of real-world environments such as monumental architecture (Boccon-Gibod and Golvin 1990). That is in contrast to a photogrammetric or laser scanning-based solution, which depends on actual documentation of physical remains that are still available. EDF engineers had obtained 3D metric information reconstructed from 2D photographs before the Mensi scanning solution was developed.

Saisie Optique Informatisée de Structures Industrielles Complexes (SOISIC)

Midrange TLS crossed over into industrial work environments for the first time via the first Mensi scanners, called SOISIC. The French acronym SOISIC stands for "Saisie Optique Informatisée de Structures Industrielles Complexes" (Bandiera *et al.* 2011, p. 93), which means "computerized optical capture of complex industrial structures." It was used internally by EDF to map and model industrial plants in France by 1992, though work on

Figure 8. Early stages of development for the Cyrax scanners from Cyra Technologies. All photographs were kindly provided to the author by Dr. Jerry Dimsdale (Top: Email to author, January 10th, 2020; Bottom: Email to author, March 27th, 2013). The top photograph is of the early bench prototype for what was initially described as the Field Digital Vision machine (Wilson *et al.* 1999). It did not include the time-interval interpolation circuit from Los Alamos National Laboratory at this point, although the green laser from Massachusetts Institute of Technology's (MIT) Lincoln Laboratory was in use. (Prior partnering with the MIT Lincoln Laboratory, Dimsdale and Ben Kacyra visited numerous experts in the field of laser scanning, including at the Environmental Research Institute of Michigan and the CMU Robotics Institute.) Instead, a larger box pulse generator from Stanford Research Systems was used. The unit was fitted into a Volkswagen Vanagon to make it portable (bottom left). Once the time-interval interpolation circuit had been repurposed to reach the required rate of picoseconds, the hybridized system architecture of the 532-nm green laser from the MIT Lincoln Laboratory and the Los Alamos National Laboratory time circuit were used in the smaller Cyrax HDS 2400 and HDS 2500 systems (bottom right). This was prior to the 2000 acquisition of Cyra Technologies by Leica Geosystems, toward the end of the dot-com boom.

the project actually began in 1987—the same year the Digital Karnak Project took shape (Boccon-Gibod and Golvin 1990).

The accuracy of ToF systems soon increased to subcentimeter standard via the San Francisco start-up Cyra Technologies. Jerry Dimsdale, its founding Chief Technology Officer, improved upon the findings of the JPL Laser Rangefinder project (Lewis and Johnston 1977; Kacyra *et al.* 1997; Wilson *et al.* 1999). The Cyrax HDS 2400 developed was not, however, the only ToF system brought to market by 1998 (Figure 8). Riegl's LMS-Z160/Z210, released in both iterations in 1997 and 1998, had longer range but were accurate to 2.5 cm (Studnicka n.d.). Prior to its short-lived release as the LMS-Z160, Riegl had developed this Active Surface Imaging System (ASIS) for the ESA in 1997 (Flatscher *et al.* 1999).

Experience gained from the ESA project took Riegl's preexisting technology in a new direction. For example, the Riegl LD90-3 distance meter (released in 1993) was used for the range-finder electronics in the LMS-Z160/Z210 (Studnicka n.d.).

The hybridization of Riegl systems, through other technologies within the company's portfolio of sensors, laid the foundation for the range at which data could be collected (Riegl ground-based sensors can also collect data at kilometer-plus range). This started a trend in development based on integration of all airborne, vehicle, and tripod-mounted sensors (Figure 9). As a result, later technological developments like full waveform and echo digitization were devised to compensate for pulse shape deviation (Rieger, Ullrich and Reichert 2006; Ullrich and Pfennigbauer 2011).

Johannes Riegl had a background in time-based measurement linked to avalanche pulse generators—a way of producing circuits where pulses can be measured at very high speeds (nothing to do with snow and ice; "Riegl Timeline" 2014). He formed his company in 1978, after spending 10 years at the Vienna University of Technology.

Figure 9. Riegl's entry into the unmanned aerial vehicle market is an extension of its long-term multisensory approach. The company's first foray into midrange TLS—the LMS-Z160/Z210—was made possible by its work with the ESA for shuttle landing sensors. Distance-sensing technology from its preexisting portfolio of instruments was also modified to create its new laser scanning sensor.

Close-Range Scanning (Second Phase)

Close-range and midrange TLS intersect in several ways. These include attempts to commercialize sensors like those from ERIM, the emergence of robotics as a discipline running parallel to the development of 3D imaging as applied research (demonstrated in early examples like Shakey and later developments like the Robotics Institute at CMU), and the use of 3D imaging in the automotive and entertainment industries (Besl 1988; Rioux and Bird 1993; Kelly 1994). It is the latter—in the form of companies like Cyberware—that raised public awareness of 3D imaging as a way to reverse engineer surfaces in the early 1990s (Kweon, Hoffman and Krotkov 1991; Rioux and Bird 1993). More behind-the-scenes activities, especially from Perceptron and CMU, show that a consistent link to space and defense applications existed as well ("Project Development Plan" n.d.).

Perceptron

Perceptron looked to commercialize the ERIM scanning system, outlined in part one of this article, by the early 1990s (Kweon *et al.* 1991; Matthies 1999; "Project Development Plan" n.d.). University-based research like the Autonomous Planetary Rover, which resulted in the six-legged Ambler robot, is one example where the Perceptron midrange TLS system was applied (Bares *et al.* 1989; Matthies *et al.* 2007). Failure to commercialize the system, however, resulted in Perceptron continuing to focus on close-range scanners as it had done previously (Paul Besl, email to author, January 22, 2019). The company was founded in 1981, having been born out of the automotive industry and the General Motors Institute (now Kettering University; "About Us [Perceptron]" n.d.). Perceptron was still developing close-range TLS and robotic systems for CAD and manufacture at the time this article was published.

Automotive Industry

Uses of TLS outside of space and defense applications can be identified in communities working with close-range scanning, especially from the 1980s onward. It was the automotive industry that started to demonstrate a use for accurate, repeatable (in terms of performance), and high-resolution laser scans (Besl 1988, 1994; Khetan and Besl 1990). This was for the reverse engineering of surfaces, which included fully assembled vehicles. For example, synchronous scanning systems (developed by companies like Hymarc Limited) were used at General Motors as alternatives to physical models in wind-tunnel tests (Paul Besl, email to author, February 7, 2019; Lamb, Baird and Greenspan 1999). That was while Paul Besl and Neil McKay—developers of the ICP algorithm—were working on active scanning systems as an alternative to clay and RenShape 450 models. These were being used at General Motors to test vehicle aerodynamics, RenShape 450 being an easy enough material to shape using computer numeric control milling machines–as well as capable of withstanding test conditions at higher speeds in a wind tunnel.

Computer numeric control allows digital models to be converted into instructions for rapid prototyper devices such as milling machines and resin modelers. Tolerances for the digital molds created in automotive industries were typically 0.2–2 mm in the 1980s to early 1990s. Companies who had previously worked in the automotive industry, such as Callidus, became some of the first to develop midrange TLS scanners after they were commercialized ("The Callidus Precision Systems" n.d.)—that is, after 1998, when Cyra Technologies, K^2T, Mensi, and Riegl had all released units.

Digital Molds

Point-cloud and mesh information presented the opportunity for a digital mold to be created of what is described in robotics as the object environment. This is because in 3D imaging the environment being documented is literally being treated like an object from which a cast is being taken (see, e.g., Peers, Hawkins and Debevec 2006, pp. 7–8). The Coignard family discusses this in their work in terms of "la modèle numérique," "la recomposition numérique," and "reproduction numérique" (B. Coignard and Szewczyk 2016). In fact, the heritage conservation community in France (and early practitioners like Benoit Coignard) were some of the earliest, if not the first, to explore what became known in English-speaking countries as *digital surrogates* and *digital twins*. Scans of the Colossus of Ramses II in Figure 14 is one of many examples from this body of early CH based work.

In the case of manufacturing environments like General Motors, the objects of interest were automotive vehicles like cars and trucks (Khetan and Besl 1990; Besl 1994). The point clouds and meshes created from scanners like the Hymarc enabled users to refine designs on computers, because of the level of detail, quality and resolution of the as-built information collected (Besl 1988; Lamb *et al.* 1999). The algorithm for ICP-based registration stemmed from such practical applications, with elements also coming from Neil McKay's experience in the study of robotics (Paul Besl, email to author, February 18, 2020).

Cyberware

One of the most famous and important public examples of close-range scanning was produced by the California company Cyberware (Figure 10), whose laser-based triangulation systems became famous for use in visual effects for films. Mechanically, they also shared influences seen in systems like the Hymarc, which could also use a fixed-arm system where the sensor moved around the object as it collected information. Its

first film usage was in 1986, in *Star Trek IV: The Voyage Home* (Wilder 1991; Hoffmeister *et al.* 1996). Cyberware presented to the public the kind of applied research that was otherwise being carried out internally at companies like General Motors. Close-range examples like this also lay the groundwork for companies like Cyra Technologies and Mensi to capitalize on. For example, both companies had their scanning solutions on the sets of films like *Starship Troopers* and *Star Wars Episode II: Attack of the Clones* by the end of the 1990s to 2000s (Steve Chapman, email to author, November 12, 2012; Jacobs 2017).

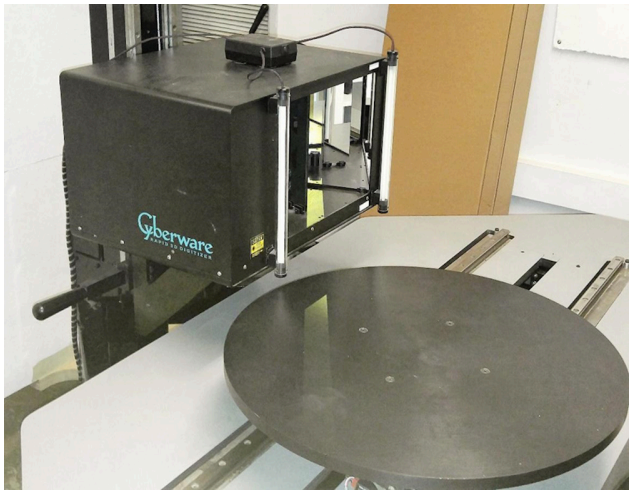

Figure 10. Artists like Dan Collins—discussed under "Commercialization in the Late 1990s (Third Phase)"—and film-industry visual-effects professionals started working with short-range Cyberware laser scanners in the early 1990s.

Lasers in Canada

The Hymarc laser scanner discussed in the section "Close-Range Scanning (Second Phase)" stemmed from research and development at the National Research Council of Canada (NRCC; Lamb *et al.* 1999). Funding came from the Canadian Space Agency (CSA) via the Strategic Technologies for Automation and Robotics Program, which also funded research conducted by Optech that was used in the development of the Laser Radar Instrument (LRI) for JPL in California (Tripp *et al.* 2003). The commercial offshoot of this was the Intelligent Laser Range Imaging System (ILRIS-3D), released in 2000.

The NRCC and CSA have helped shape and fund research and development in Canada since each was formed as a government entity (Blais 2004; Gainor 2012; Nelson 2013). Neptec, for example, is another Canadian company that has ties to the NRCC and CSA (Samson *et al.* 2004). Commercial products like the Opal-360 stemmed from research and development funded by both NASA and the CSA, in the same way as for Optech with the LRI and ILRIS-3D (Tripp *et al.* 2003; English 2010; Deslauriers *et al.* 2014). Neptec developed triangulation-based imaging first outlined in the Advanced Space Vision System prior to the Opal-360 range of scanners, shown as (r) in figure 1b of part one of this article (Blais 2004). The underlying research for these systems was started by the NRCC to examine vehicle collisions in the 1970s ("Space Vision System" 2008), then transferred to Neptec in the 1990s (Laurin 2017).

As Far Back as the First Laser Systems

The NRCC research facilities in Ottawa had been working with lasers since January 12, 1961 (Nelson 2013). There, Alexander Szabo and Boris Stoicheff demonstrated a synthetic ruby laser system in the Spectroscopy Laboratory to early laser pioneers like Arthur Schawlow. This demonstration came shortly after Theodore H. Maiman built the first working laser using this ruby-based system at California's Hughes Research Laboratories, on May 16, 1960 (Hecht 2005, 2010).

These early developments in active sensing lay the fundamental groundwork in Canada for the following:

- The formation of companies that would turn automation-driven research and development into "off the shelf" midrange TLS solutions, such as Optech in 1974 and Neptec in 1990 (Tripp *et al.* 2003)
- The formation of the CSA as a strategy-making group and funding body in 1989
- The work of notable researchers at the NRCC Institute for Information Technology, such as Marc Rioux (1984; Rioux and Bird 1993), François Blais (2004), Jean-Angelo Beraldin (Beraldin *et al.* 2011), and Michael Greenspan (Lamb *et al.* 1999)

Both the NRCC and the CSA contributed to the story of midrange TLS because of their symbiotic relationship with each other and with research and development communities in other countries, most notably France and the USA.

Multidisciplinary Application (Second Phase)

A self-sustained funding structure, whose main sponsor was EDF research and development, encouraged a multidisciplinary relationship between the Coignard family as artists and Guillaume Thibault as the principal engineer overseeing all CH projects (Figure 11a and 11b; Bommelaer and Albouy 1997; B. Coignard 1999; Thibault and Martinez 2007). Based on this work, finite element analysis (pertaining to the analysis of structures and their integrity), testing, the creation of a virtual wind tunnel, and a simulation of seismic activities were all applied to the scans of the Colossus of Ptolemy II from Alexandria, Egypt (O. Coignard *et al.* 1998; Moulin *et al.* 1998; Schmitt 1993; Schmitt *et al.* 1993). As seen in Figure 11, the Mensi team was the first to experiment with midrange TLS in CH and such a way. (The use of scan data along such lines had yet to be re-implemented into CH workflows overall at the time of publication of this article.) In the late 1990s, 2D CAD drawings and 3D visualization pipelines were used to repackage technologies for general users.

Landscapes, sites, and artifacts (the basic data types in cultural heritage) are documented from two perspectives in a CH-based workflow. The first is concerned with aesthetics and art-historical issues (Latour and Lowe 2011). The second is concerned with forensically reconstructing past actions and behaviors based on the material culture at hand (Hunter and Cox 2005; Remondino 2011). Midrange TLS can be used to obtain both sets of information, due to the resolution and range at which data are collected (Spring *et al.* 2010). It provides a way to document and inform archaeological restoration processes using quantifiable data. For example, the Delphi promotional video captured in Figure 12 demonstrates how point-cloud data were used to reconstruct the tholos at the base of Mount Parnassus (Bommelaer and Albouy 1997). Besides the use of scan data as a template for modeling the structure, fragments of sculpture and architectural remains were documented and reconstructed using 3D matching algorithms that identified fitting points between blocks. This was not wholly automated, as the software operator helped match blocks like a 3D jigsaw puzzle (O. Coignard *et al.* 1998; Lavigne 1998; R. Coignard, Coignard and Coignard 1999). It did, however, demonstrate that attribute information could be ascribed to scan data. It created more than a 3D image, showing that shapes in a scene could be extracted. As a result, the relationship between different objects could be examined. This part of the project was overseen by Guillaume Thibault (Thibault and Martinez 2007; J. L. Martinez and Thibault 2012).

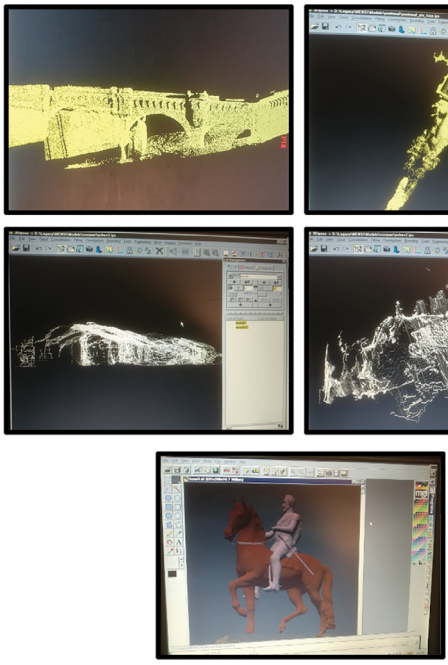

Figure 11. (a) Scans of the Pont Neuf Bridge (top, two boxes), Pont Marie Bridge and Henri IV Statue (lower box) were conducted in Paris, 1993 (Thibault, email to author, July 4th, 2020; Thibault and d'Aligny 1994). These scans were used to measure and model the bridges and statue (Thibault, Email, July 4th, 2020). The models were then run through radiosity software developed by the *Centre national de la recherche scientifique* (CNRS), as part of a computer simulation focused on how to best light the bridges and statue in the future (Thibault, email to author, July 4th, 2020). Tourism was a consideration for this project, which was part of an effort to upgrade how Paris was lit (Thibault, email to author, July 4th, 2020). It was soon followed by scans of the Vielmouly cave in the Beune Valley (France) and Cosquer Caves (middle, two boxes) in 1994 (Aujoulat *et al.* 2005; Bandiera *et al.* 2011).

The photgraphs above are of the oldest CH based midrange TLS scans still known to exist at time of publication. Shown in 3Dipsos – point cloud software developed by Mensi – the .ips (above) files demonstrate that laser based triangulaton systems like the SOISIC paved the way for midrange TLS as a site documentation and inspection tool. This is especially the case for the Cosquer Cave example, as it was only accessible by entering the cave from under water. The author would like to thank Ken Shain – former CEO of Mensi USA – for use of the photographs and data above.

(b) The Coignard family used structured light scanning to create digital molds in their early work. This eventually led to the collaboration with Mensi. (Courtesy of Coignard Family, email to author, June 12th, 2015).

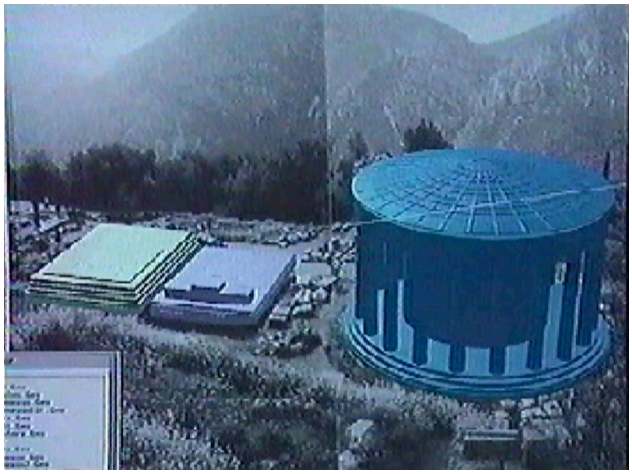

Figure 12. Mensi showcased a virtual reconstruction of Delphi at SIGGRAPH 2000, which included scans of the sculptural decorations of a circular tholos temple carried out in association with the French School at Athens in 1996. The video presentation produced by the company's Chief Executive Officer, Ken Shain, was one outcome of the high-profile cultural-heritage projects discussed in this article they were carried out by EDF and Mensi between 1993 and 1999 (Shain 2009).

There was also a document prepared by the French School at Athens called *Marmaria*. It outlined the point cloud-based work carried out at Delphi with the Mensi SOISIC scanner (Bommelaer and Albouy 1997). All information was used as attribute data, which were then fed into a vector-based modeling workflow (Albouy *et al.* 1989; Albouy 1990; Dekeyser *et al.* 2003; Vergnieux and Delevoie 2008; Homann n.d.). The latter had already been demonstrated through the Digital Karnak project (Figure 13). Architectural fragments were collected, meshed, and then introduced into the model. The Delphi video also demonstrates this, when premodeled sections of the tholos are draped onto a photograph of the site.

Trends and Influences on Development Cycles in the Fourth Phase

Lower-cost commodity sensors began to emerge because companies like Velodyne entered the midrange TLS market ("Breaking Through the Price Barrier" 2014; Ackerman 2016a; Ohnsman 2020; "Velodyne Lidar Introduces Velabit" 2020). The development cycle linked to their multibeam ToF systems made an impact within five years of having a working sensor in place (Halterman and Bruch 2010; Velodyne Lidar 2017). However, high-fidelity object documentation was not the primary driver for applied development, which is the case for most of the scanners outlined in this article. Instead, a return to autonomous vehicle development began the process of making sensors that are more affordable (Figure 5; Ohnsman 2020; "Velodyne Lidar Introduces Velabit" 2020).

For example, Velodyne entered into a partnership with Google for its self-driving car initiative (seen in Figure 6) in 2010 (Ackerman 2016a; Velodyne Lidar 2017). From this point, a development cycle began to emerge around vehicle safety applications for all sensors developed. This ultimately led to a $150 million investment in Velodyne from Ford and Baidu in 2016 (Ackerman 2016a)—that is, after the Velodyne Puck (VLP-16) was released in 2014 ("Breaking Through the Price Barrier" 2014). This sensor was priced at $7,999 and had an almost immediate impact on midrange TLS systems designed for as-built surveys.

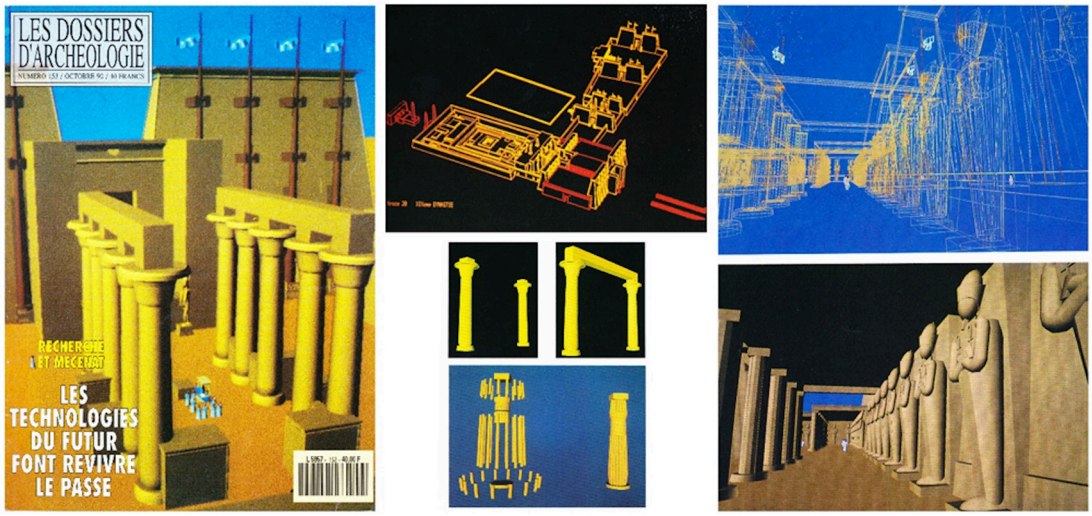

Figure 13. Mensi-based cultural-heritage applications were influenced by the computer-aided design approach developed by EDF for a digital recreation of Karnak in 1987. Henri Boccon-Gibod and Jean-Claude Golvin wrote a detailed article for the French publication *Les Dossiers d'Archéologie* in 1990. It outlined how computer-aided design models were generated–as well as informed by–the site information that was accessible to modelers at the time.

Designed for Documentation and Inspection

The Velodyne Puck was integrated into the NCTech LASiris VR and Effortless 3D laser scanners around the same time that Leica Geosystems released the more affordable BLK360 scanner, in 2016 (Tompkinson 2017). Even sensors developed by manufacturers of the first commercially available tripod-based systems repurposed their flagship hardware to include the Puck unit—a more affordable multibeam sensor, developed by Velodyne, designed to plug into a system architecture ("Breaking Through the Price Barrier" 2014). This meant that scanners could be more easily incorporated into vehicle-based applications. Primarily, for mapping based on SLAM, as seen via later midrange systems like the Leica Geosystems Pegasus, which was based on P-series scanners. Vehicle-based and wearable instruments are expanded upon in the "Building upon Navigation-Based Initiatives—Who and What?" and "Waves of Development Driven by Its Users—How and Why?" boxes.

Application to Cultural Heritage (Second and Third Phases)

The first CH applications of midrange TLS came out of France. They were supported by EDF, which was a state-owned company. University connections with EDF also encouraged the adoption of new technologies within the organization (Paramythioti and d'Aligny 1989; Bandiera *et al.* 2011). It was its corporate foundation, however, that offered up the means to legitimately support CH work. For example, philanthropic acts became more clearly defined activities in French corporate environments after a philanthropic law was passed in 1987 ("Sur le développement du mécénat et le Code général des impôts (CGI)": "On the development of philanthropy and the general code of imports"; Gautier *et al.* 2013). This law was soon followed by another, in 1990, that encouraged the creation of corporate foundations ("Sur portant création du statut de fondation d'entreprise": "On establishing the status of a corporate foundation". Both pieces of legislation came about because ADMICAL was created in 1979.

Three business students who had observed philanthropic corporations in the USA created ADMICAL to bring about similar conditions in France (Gautier *et al.* 2013). The turning point came when Jacques Rigaud—a former Chief of Staff in the Ministry of Arts and Culture—became the chairman of its board in 1980 (Guerrin and de Roux 2008). It was his passion for the arts and culture that helped make it possible for new technologies used in industry to immediately be applied to CH. In this instance, his framework for corporate philanthropy enabled midrange TLS to make the transition from industrial applications to CH from within EDF. It legitimized activities on a bureaucratic level within the organization. Industrial engineers were exposed to sites like Cosquer Cave and Delphi, and they were able to exchange their knowledge with heritage professionals (Brillault *et al.* 1995; Brunet and Vouvé 1996; Clottes *et al.* 1997; Moulin *et al.* 1998; Thibault 2001). With them came workflows geared toward as-built information—something EDF engineers had been exposed to on a daily basis.

Once access to technologies was in place, conservation professionals and geologists took an interest in midrange TLS for the documentation of in situ remains and museum collections (Schmitt 1993; Schmitt *et al.* 1993; O. Coignard *et al.* 1998; Moulin *et al.* 1998; B. Coignard 1999; Thibault 2001). They saw the potential for accurate reconstructions of an artifact or environment: reconstruction based on real-world data. Point clouds could be used to represent actual surface conditions, as well as provide more detailed overall measurements than tape measures, still cameras, and survey instruments like theodolites (Levoy and Whitted 1985; Levoy 2007). Because this early work was closely tied to the École Nationale Supérieure des Télécommunications, Paris (now Télécom Paris), ideas quickly spread to French-speaking Canada via a professor at Telecom Paris called Francis Schmitt (Baribeau, Rioux and Godin 1995; Beraldin *et al.* 2011). Schmitt's connections extended on the one hand to the École Polytechnique de Montréal in Canada (Hurtut *et al.* 2011). On the other hand, he had also published research with Xin Chen, the Chief Technology Officer at Mensi, who had obtained his PhD at the École Nationale Supérieure des Télécommunications, Paris (X. Chen and Schmitt 1992). EDF was more than large enough to support its own research and development efforts; it also worked with a network of collaborators which could disseminate its activities to a variety of professional communities all over the world.

Proof of concept for the value of technology like midrange TLS came in 1987, when EDF research and development funded the Digital Karnak project (Albouy *et al.* 1989; Albouy 1990; Dekeyser *et al.* 2003; Vergnieux and Delevoie 2008; Homann n.d.). The models produced for the project demonstrated that

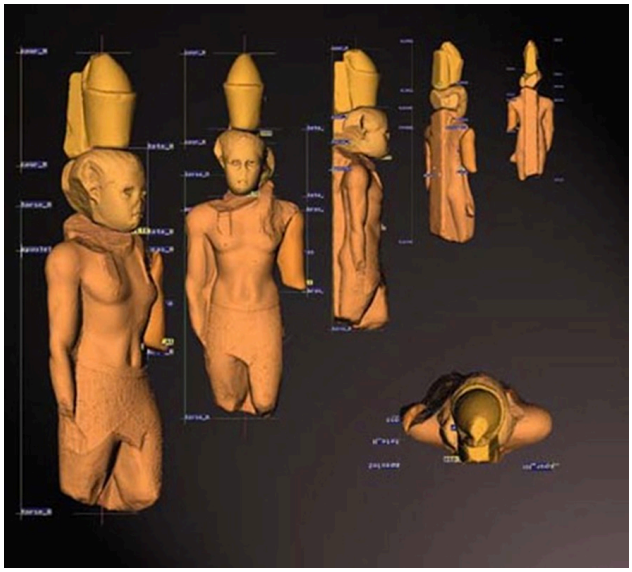

Figure 14. The Mensi SOISIC scanner quickly established that laser-based 3D point clouds could be used as an efficient way to document cultural heritage. Examples like the Colossus of Ramses II provided a more accessible way to create a digital mold or surrogate of an artifact or scene. Prior to scanning, a tape measure and the perspective of the conservator were used to preserve site and artifact information. The introduction of 3D imaging solutions like the Mensi SOISIC scanner improved any issues related to subjectivity or human error that stemmed from this process.

attribute data and primitive shapes could be created from all forms of information, including photographs and documentary evidence. It laid the groundwork for Mensi solutions to enter into CH workflows as another source of data. Marc Albouy, Deputy Director of Studies and Research at EDF, partially supported this effort in 1987 (Bommelaer and Albouy 1997). By the end of the 1990s, CH case studies also took center stage as marketing material. They were used by companies like Cyra Technologies and Riegl because of their mass appeal.

The first example of midrange scanning in CH was with a Mensi SOISIC scanner in France (Figure 11a; O. Coignard *et al.* 1998; Lavigne 1998; R. Coignard *et al.* 1999). EDF engineer Guillaume Thibault used it to document the Pont Neuf Bridge, Pont Marie Bridge and Henri IV Statue in Paris in 1993, and in 1994 it was also used at the Cosquer Cave in the Calanque de Morgiou at Marseille (Brillault *et al.* 1995; Brunet and Vouvé 1996; Clottes *et al.* 1997; Thibault, email to author, July 4th, 2020; Thibault and d'Aligny 1994; Thibault 2001). These later scans were inspired by natural relief drawings done by prehistoric artists, as well as the practical need for a realistic visitor display to compensate for waterlogged conditions inside the Cosquer Cave. Note: the Coignard family had become aware of Mensi's technology in prototype form in 1991 (Coignard Family, email to author, June 12th, 2015)

From 1993 to 1999, several CH case studies were generated through a collaboration between the Coignard family and the EDF team headed by engineer Guillaume Thibault (Schmitt 1993; Schmitt *et al.* 1993; O. Coignard *et al.* 1998; Moulin *et al.* 1998; B. Coignard 1999). These included a statue of a Gallic warrior, the Hindu god Harihara from Cambodia, a centaur, the Colossus of Ptolemy II from Alexandria, Egypt, an epigraphy-based example from the Louvre in Paris, and a statue of the Emperor Augustus. The Emperor Augustus statute was used as the first attempt at creating a digital surrogate of a scene with computer-based technologies—or, as Benoit Coignard described it, "clones numériques" (B. Coignard 1999). Prior to scanning, tape measure and the perspective of the conservator were used to preserve site and artifact information. The introduction of 3D imaging solutions like the Mensi SOISIC scanner resolved any issues related to subjectivity or human error that stemmed from this process.

Cultural Heritage as Marketing (Second and Third Phases)

Kevin Cain, who is discussed in more detail later under "Nonprofit Corporations (Third Phase)," had used a prototype Field Digital Vision machine developed by Cyra Technologies by 1995 (Kevin Cain, email to author, August 23, 2015; "Reimagining Maybeck's Palace," 2002), on the Palace of Fine Arts in San Francisco (Kacyra *et al.* 1997; Loedeman 1999). Samples of the modeling work produced from this data are seen in Figure 15. Unlike the Mensi system, the FDV used a ToF-based solution, which had increased accuracy and range based on specifications for improvement identified through the JPL Laser Rangefinder project (see part one of this article). A time-interval interpolation integrated circuit, which had been developed for underground blast monitoring at the Los Alamos National Laboratory, was linked to a Q-switched or pulsed laser developed by the MIT Lincoln Laboratory (Howe and Auchampaugh 1992; Kacyra *et al.* 1997; Wilson *et al.* 1999; Shan and Toth 2009; Spring *et al.* 2010). The increased pulse rate created from this solution meant that a data resolution of 2–6 mm could be achieved over distances of 0.5–50 m (Gaiani *et al.* 2000). Solutions based on Field Digital Vision and CGP (Computer Graphics Perception)—the first point-cloud registration and modeling software, created by Cyra Technologies—were also strategically marketed to sectors such as architecture, engineering, and construction. They were positioned around pre-existing 2D CAD and 3D visualization pipelines (Kacyra *et al.* 1997).

In the spring of 1997, Cyra Technologies carried out more historic building work by scanning the facade of the Hearst Memorial Mining Building at the University of California, Berkeley (Addison and Gaiani 2000; Addison *et al.* n.d.). The scans were conducted as part of an earthquake-proofing retrofit of the building, which would subsequently involve dismantling parts of the historic facade to add structural reinforcements. A similar retrofitting project occurred at San Francisco City Hall in February 1998 ("Renovation of Historic

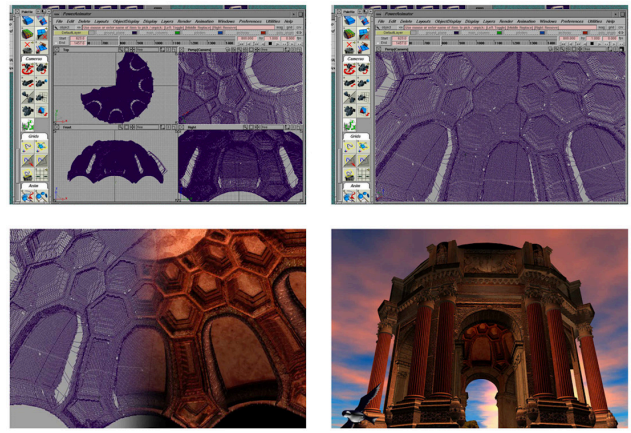

Figure 15. The Palace of Fine Arts in San Francisco was used by Cyra Technologies to market early midrange laser scanners like the HDS 2400. Modeling work of the point-cloud data was carried out by Kevin Cain and his team at the Academy of Art University in San Francisco. All photographs were kindly provided to the author by Kevin Cain (Email to author, September 17th, 2013).

Building" 1998). Marc Levoy followed on from this in 1999 by using a Cyrax HDS 2400 for in situ scans of Michelangelo's David as part of the Digital Michelangelo Project in Rome (Levoy *et al.* 2009).

From 1998 to 2001, several examples were presented by Riegl using data from the LMS-Z160/Z210 (Ullrich and Studnicka 1999; "3D Imaging Sensor LMS-Z210" 2001; Pfeifer and Rottensteiner 2001). These included the Assemblée Nationale in Paris; the ruins of Burg Kollmitz in Lower Austria; the Kirche am Hof in Vienna (the inside vaulting and outside facade of the church); and Schönbrunn Palace and the State Opera in Vienna. The Riegl system was explained by using polychromatic scales for the representation of height data, with grayscale used to represent surface reflectance (Nitzan *et al.* 1977; Pfeifer and Rottensteiner 2001; Riegl 2001; Ullrich and Studnicka 1999). These CH examples were also used to explain the relationship of the laser echo returned to the scanner and the point cloud generated, and to emphasize the difference between a depth image, a conventional 2D photograph, and basic 3D models (Ullrich and Studnicka 1999; Pfeifer and Rottensteiner 2001). Case studies were disseminated using VRML 3D interactive vector models displayed on the Riegl website (Ullrich and Studnicka 1999; Riegl 2001; Pfeifer and Rottensteiner 2001). As with the EDF Digital Karnak project, CAD modeling played an important role in the data-processing workflow adopted for early Riegl CH examples.

Nonprofit Corporations (Third Phase)

Having acquired a Mensi scanner in 2000, Kevin Cain turned the California nonprofit Egyptian Cultural Heritage Organisation into the Institute for the Study and Integration of Graphical Heritage Techniques (INSIGHT) and continued to enlist the skills of Philippe Martinez (Cain 2000; P. Martinez 2001; Cain, Martinez and Munn 2002; Cain and Martinez 2003; Cain *et al.* 2003; P. Martinez and Cain 2011). Martinez was an archaeologist who had been part of the Mensi-based Delphi project seen in Figure 12. He would also go on to work with Paul Debevec at the Parthenon using a SceneModeler scanner in 2003 (Debevec *et al.* 2005).

Mensi also showcased this virtual reconstruction of Delphi at SIGGRAPH 2000, including scans of the sculptural decorations of a circular tholos temple done in association with the French School at Athens in 1996 (Bommelaer and Albouy 1997; Flaten and Gill 2007; Thibault and Martinez 2007; J. L. Martinez and Thibault 2012). The video presentation produced by the company's Chief Executive Officer, Ken Shain, was one outcome of the high-profile CH projects already discussed that were carried out by EDF and Mensi between 1993 and1999 (Saint-Aubin 1995; Brillault *et al.* 1995; Brunet and Vouvé 1996; Bommelaer and Albouy 1997; Clottes *et al.* 1997; O. Coignard *et al.* 1998; Lavigne 1998; Moulin *et al.* 1998; B. Coignard 1999; Thibault 2001). Meanwhile, after selling Cyra Technologies to Leica Geosystems in 2001, Ben Kacyra turned from commercial applications to CH by forming his own nonprofit corporation, CyArk, in 2003 (Dawson *et al.* 2013). This San Francisco-based archive for scan data was his response to the destruction of the Bamiyan Buddhas in Afghanistan in 2001.

Both INSIGHT and CyArk went on to achieve success in the 2000s. For example, Cain worked with members of the EDF team on the omphalos in the museum at Delphi discussed in part one of this article. INSIGHT helped with the development of the registration process in CloudCompare, which in 2009 became an open-source platform for working with point-cloud

Waves of Development Driven by Its Users—How and Why?

Developments in midrange TLS now follow general consumer trends and markets. Two waves of development have taken place under these conditions, both driven by how much laser scanning solutions cost and in reaction to developments in other technology-driven markets. Included in this melee is the adaptation of business models used to monetize personal computing. For example, the same iTunes service-as-a-solution (SaaS) model used by Apple for MP3 files was applied to point-cloud data by 2013 (Spring 2015). The ReCap range of software packages from Autodesk were the first to adopt and promote this form of content management (Spring 2015). One of their pricing options even included a credit-based system to process point-cloud and mesh data via their distributed computing-based services.

It is, however, the commoditization of sensor technologies—the process of turning products of value into objects of trade—that ultimately created the second, third, and fourth waves of sensor development. For example, the Velodyne Puck has been used across both mobile and terrestrial mapping solutions. It was incorporated into hardware like the Pegasus mobile mapping unit from Leica Geosystems as well as tripod-based products like the NCTech LASiris VR and Effortless 3D seen in figure 1b of the first part of this article. Leica Geosystems also announced the BLK360 solution, which, along with the Puck-based LASiris VR and Effortless 3D, created another layer to the TLS market that was promoting midrange TLS solutions for professional uses at prices below $15,000 (Tompkinson 2017).

Arguably, the fourth wave of development—signaled by plug-and-use sensors and low-cost kit-based solutions—had fully emerged by 2016. ToF-based kits like the Scanse unit, for example, incorporated low-cost computers like the Raspberry Pi into their system architecture, making them easier for nontechnical users to build (Ackerman 2016b). Velodyne released a $100 sensor called the Velabit in January 2020 (Ohnsman 2020). It was introduced at the Consumer Electronics Show, immediately positioned for clash detection in cars, and was described as "designed to be easy to manufacture at mass production level" ("Velodyne Lidar Introduces Velabit" 2020). This kind of development in hardware is similar to kits seen in the period building up to the mass adoption of the personal computer, such as the Altair 8800 kit or Sinclair kits.

FARO Technologies, Inc

In terms of sensors and software, the FARO Focus^{3D} scanner and Scene software are the prime example of the way the technology is shaped or packaged in the commercial era of laser scanning. FARO packages midrange TLS along similar lines to tablets or smartphones—smaller, powerful, and yet easy to use (Spring 2012). The FARO Focus^{3D} was designed to be like other all-in-one systems. Midrange TLS scanners had contained all the components required of a solution—sensors, onboard computer, data storage, and power supply—since the Z+F 5006 was released in 2006 (Shan and Toth 2009). The Focus^{3D} was, however, miniaturized to fall in line with consumer technologies such as handheld computing devices like the iPhone. Software variations like Scenect—an Xbox Kinect-capable version of Scene—and the creation of a FARO app store in 2012 were also developments geared to broader "prosumer" markets (Kotler 1986). These are markets that are composed of user communities working with 3D imaging technologies, whether laser scanner or app-equipped smartphone, in their personal and professional lives (Spring 2015). Midrange TLS had entered a stage of development where more socially driven business models were being considered by the time this article was published. Technologies shaped by user experiences were the next big thing.

information (Duguet *et al.* 2004; Thibault and Martinez 2007). CyArk quickly refined its business model for heritage documentation around the same time. It was predominately geared toward capitalizing on the points of synergy between private- and public-sector entities. In fact, the turning point for CyArk came in 2010, when Mount Rushmore was scanned in collaboration with the Scottish government using five midrange TLS scanners (Lee 2010; "New Lanark, Scotland" n.d.). Point clouds that were generated fed into both the Scottish Ten and CyArk 500 projects. Mass media exposure from the scanning of Mount Rushmore helped corporate partners like Leica Geosystems, as well as the US National Park Service and the CyArk 500 initiative—a reflection of Ben Kacyra's ambition to document 500 heritage sites over a five-year period (Kacyra 2009). FARO was listed as the main contributing midrange TLS partner on CyArk's website by 2020 ("Partners" 2020). There was also an ongoing collaboration between CyArk and Google Arts & Culture via the Open Heritage initiative (Watkin 2018; "Open Heritage" n.d.).

Commercialization in the Late 1990s (Third Phase)

Developments in personal computing enabled TLS to make the transition from applied research communities like robotics into applied markets, such as design, engineering, and as-built survey (Kacyra *et al.* 1997; Roland and Shiman 2002; Markoff 2005; "Project Development Plan" n.d.). This link is a fundamental reason why 1997 and 1998 were turning-point years for a broader commercialization of laser scanning: years when personal computers finally became ubiquitous technology. In fact, the miniaturization and increased efficacy of both computers and TLS are intertwined. This is because integrated circuits are one of the key components driving their development.

For example, microelectronics and microchip-based timing were fundamental in the development of both Riegl and Cyra Technologies laser scanning hardware (Wilson *et al.* 1999; Studnicka n.d.). Riegl optimized its preexisting LD90-3 laser distance meter to create its early ToF scanners, whereas Cyra Technologies combined a passively Q-switched microchip green laser—which stemmed from a collaboration with John Zayhowski from the MIT Lincoln Laboratory—with a time-interval interpolator integrated circuit that was originally designed to monitor nuclear blasts (Kacyra *et al.* 1997; Zayhowski 2010, 2018; Wilson *et al.* 1999). That was in order to create a ToF system specified to accuracy and resolution in millimeters, with a range of up to 100 m.

Even throughout the 1990s, the main computers used to develop point cloud-enabled software like CGP were specialist graphics machines. Silicon Graphics or Sun Microsystems hardware was used to create point-based software capable of running on Windows NT microcomputers (Kacyra *et al.* 1997). It was not until the advent of dedicated graphics processing unit (GPU) cards—which led the way to affordable high-performance computer graphics—that processor-intensive point-cloud and polygon-based rendering became accessible to a wider consumer base (Tarini, *et al.* 2003). As seen in the "CloudCompare" box in part one of this article, for example, GPU-based computation made it easier to perform otherwise processing-intensive tasks, such as light-field simulation. This development was in favor of faster GPU-based functions like the Poisson shading of the Tristan Stone photograph in that box (Spring and Peters 2014). Users outside of large corporations, government agencies, and research institutions were relatively small in number before dedicated GPUs (Palacios and Triska 2011). They would have needed a clear application for the use of such technologies to justify absorbing the costs associated with information processing and development requirements (Kotler 1986).

Expanding the User Community

Once TLS started to emerge as a coherent solution in this way, different types of users began to take the technology in a diverse range of applied directions. In industrial sectors like automotive engineering, for instance, CAD and computer-aided manufacture presented clearly defined incentives for the continued development of TLS in general (see the use of computer numeric control and rapid prototypers by Besl and McKay mentioned earlier under "Automotive Industry"). Along with close-range scanners, which were made popular by companies such as Cyberware, industrial applications like machine-part design bridged a gap in terms of awareness. New users and skill sets were brought into communities where point-cloud information would change the way they approached a

(a) (b)

Figure 16. (a) Dan Collins started to incorporate full-body scanning into his sculptures as the technology developed. (b) *Twister* was the most successful piece of art to come out of Collins's collaboration with Cyberware. The point clouds generated provided a level of detail not seen before. Collins had to wait for an affordable computer to be released before he could work with his point clouds in the way he had originally intended.

project (Lavigne 1998). Early adopters like sculptor Dan Collins, who outlined his scan to computer-aided manufacture creations in *The Challenge of Digital Sculpture* in 1997, serve as good examples (Figure 16a and 16b; Collins 1994, 1997; "ISC Web Special" n.d.).

By 1998, midrange TLS and digital photogrammetry solutions began to unlock the potential of point cloud-driven workflows (Pot *et al.* 1997). Software like 3Dipsos (Mensi), Architect (K^2T/Quantapoint), CGP (Cyra Technologies), and RiScan (Riegl) worked with point-cloud information from midrange TLS systems (Kacyra *et al.* 1997; Debevec *et al.* 2005; X. N. Chen *et al.* 2005; Ullrich and Pfennigbauer 2011). They used the information provided to solve real-world problems. In industrial applications, for example, the as-built condition of a structure could now be compared to the as-designed specifications from which it was constructed in order to look for variation between the two. 3D point clouds were used to inform and refine future projects as well as help formulate management strategies for existing structures (Addison *et al.* n.d.). This was touched upon earlier in this article, when Cyra Technologies used its midrange TLS solutions on buildings that were retrofitted to withstand the effects of earthquakes in San Francisco ("Renovation of Historic Building" 1998).

The ability to easily connect individual point clouds together was also a key selling point for laser scanning. ICP-based registration took stitching from a three-point process to an actual all-point process (Besl and McKay 1992; Y. Chen and Medioni 1992). It gave users the ability to connect overlapping scenes by picking common points of overlap, which would inform any statistical analysis performed by the software used. It also led the way for other point cloud-based processes to take on a more user-friendly form. These included solid meshing for processes like volume analysis, georeferencing scan data to real-world coordinate systems, and packaging files in ways that were more compatible with CAD solutions like AutoCAD (Kacyra *et al.* 1997). For the first time, data were repackaged to be accessible to users whose skill sets were not overtly linked to otherwise specialist computer practices.

Parallels to the Personal-Computing Market

Cheaper systems like the Scanse Sweep also started to emerge around the period of 2014–2016 (Ackerman 2016b). The $349 Sweep unit was also available in kit form, so that users could build their own laser scanners. This kit-based approach—along with the plug-in integration with an individual's own systems and own practices—as validated by Velodyne, parallel's activities seen in the early days of the personal-computer market (Markoff 2005). It suggests that midrange TLS sensors will continue to make a transition to become commodity items, much like microchips and semiconductors did after the mass adoption of personal computers (Figure 17).

Similarities to Personal-Computer Markets

The midrange TLS systems outlined in parts one and two of this article would not be possible without the microcomputer revolution started by the Intel 8080 microprocessor. In fact, midrange TLS currently feeds into the infrastructures built up around smartphones, tablets, and powerful desktop- or carry case-sized computers (as outlined in the section "Trends and Influences on Development Cycles in the Fourth Phase" and the "Waves of Development Driven by its Users—How and Why?" box). The development of markets around midrange TLS hardware and software presents its own examples of hybridization and commoditization as well—patterns of development related to repurposing or adding value to objects, which was fundamental to the creation of a user community and market based around early examples like personal computers.

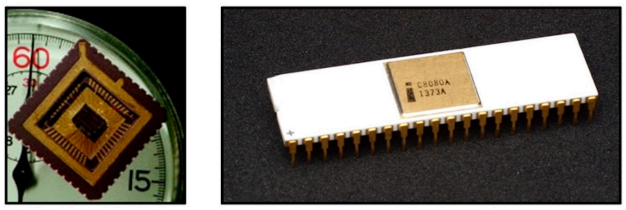

Figure 17. (Left) The time-interval interpolator integrated circuit created by Los Alamos National Laboratory for its nuclear-weapons program. It was later repurposed for the Cyrax scanners produced by Cyra Technologies to reach the millimeter and centimeter levels of accuracy they required. (Right) The Intel 8080 8-bit microprocessor, originally used in calculators, cash registers, computer terminals, and industrial robots. It was more famously repurposed for the Altair 8800, the first successful personal or microcomputer.

For example, the first wave of Cyra Technologies (later Leica Geosystems) scanners were developed by repurposing the time-interval interpolator integrated circuit created by Los Alamos National Laboratory (Figure 17). It was used alongside a green eye-safe laser from MIT's Lincoln Laboratory to create what was initially called the Field Digital Vision machine. Its associated software, CGP, was designed on specialist graphics workstations from Silicon Graphics (Kacyra *et al.* 1997; Wilson *et al.* 1999). But the software was developed to run on Windows NT workstations of the time, so that a wider user community had access to the scanner and its data. This act of commoditization came in the added value brought by a growing user base. Having a working product and proven value would later help establish a midrange TLS market—especially when coupled with the dot-com boom in the mid to late 1990s, first when Leica Geosystems acquired Cyra Technologies in 2000 ("Leica Geosystems Acquires Oakland-Based Cyra Technologies" 2000), and then when Trimble acquired Mensi in 2003 ("Trimble Navigation Acquires Mensi S.A." n.d.).

This type of activity around the technology is similar to what happened during the formative years of the personal-computer market (Markoff 2005). That is, once the Altair 8800 provided the proof of concept required to make personal computers a reality to a broader spectrum of people—like the Homebrew Computer Club in the San Francisco Bay Area, and Microsoft's co-founders Bill Gates and Paul Allen.

The Altair 8800 computer proved to be a nexus for both hybridization and commoditization to take place around personal-computing technologies (Rustad and Onufrio 2012). Hybridization via the way its 8080 microprocessor had been repurposed–taking the idea of the computer from room-size mainframes to a desktop box (Markoff 2005). Commoditization via the scale and cost at which the hardware could be produced. This and the fact that people could afford access to the Altair 8800 grew the market that formed around it by adding layers, such as discovering ways to add hardware via software. Well-known examples where the latter occurred include the Homebrew Computer Club and what went on to become Microsoft.

The first proven use for the Altair 8800—which began to demonstrate its potential through hobbyist users—came from the Homebrew Computer Club (Markoff 2005). Steve Dompier programmed it to play "The Fool on the Hill" by the Beatles using static from a radio next to it. Gates and Allen then extended its use further by creating Altair Basic, an interpreter that essentially enabled users to add a keyboard and monitor to the system. This made the Altair 8800 easier to use and usable for a broader range of applications, such as word processing and gaming. Prior to Altair Basic, the 8800 had no display monitor or keyboard and could execute commands only via a number of switches on the front of its box—hence why a radio

had to be put next to it to play music. Altair Basic was also the foundation upon which Gates and Allen formed Microsoft.

Parallel example in mid-range TLS: the multibeam system architecture developed by Velodyne for self-driving vehicles in the Grand Challenge quickly got repurposed for tripod-based and mapping systems (Halterman and Bruch 2010; Tompkinson 2017). Its success as a platform to integrate into or build new system architectures on led to a new wave of sensor companies as well, including Cepton, Hella, Innoluce, Ouster, and many more (Davies 2020). These happenings—the development of a sensor for one purpose getting used for another, then a market forming around it to the point where other companies are formed to produce similar technologies—mirror events that played out around the Intel 8080 microchip in the 1970s (Markoff 2005).

Components like the 8080 microchip were repurposed from use in sequencing in hardware like traffic lights and calculators to create the Altair 8800—the first personal computer (Markoff 2005). This same process of hybridization, repurposing existing materials to create something new, can also be seen in the years building up to midrange TLS becoming a commercially viable product (Rustad and Onufrio 2012). Cyra Technologies is a prime example of this process in action. A laser system from MIT's Lincoln Laboratory and a time-interpolation circuit from Los Alamos National Laboratory were core components for all Cyra-based laser scanners up to 2009 (Kacyra *et al.* 1997; Zayhowski 2010, 2018; Wilson *et al.* 1999). This and other examples have already been outlined in more detail in the section "Commercialization in the Late 1990s (Third Phase)."

On the business side, the formation of K²T also follows the template set out by Ivan Sutherland and David Evans at the University of Utah in the 1960s ("Evans & Sutherland" n.d.; "Project Development Plan" n.d.). Evans and Sutherland formed a company of the same name as part of their agreed-upon move to Salt Lake City (Gaboury 2016). This not only commercialized their research in computer graphics at the university—where they made one of the main nodes for ARPA/DARPA's research in computing—but set out the template most universities now use in commercializing their research in the USA: finding a commercial niche for research, then using the application to develop the technology out and expand a market. Ed Catmull, one of the founders of Pixar, is even on record as saying that his time as a student at the University of Utah School of Computing helped inform how he structured Pixar Animation Studios (Catmull 2014). Companies formed by former students of Evans and Sutherland include Adobe, Netscape, Pixar, and Silicon Graphics (Gaboury 2016). Nolan Bushnell, founder of Atari, was also a student at the University of Utah when Evans and Sutherland were there (Gaboury 2016).

Summary

This history of midrange TLS was born out of curiosity and crafted via perseverance. It stemmed from questions about what was largely a black-box technology when the author started working with it in 2006. Putting together all the pieces of the puzzle grew into a project that evolved for well over a decade. A multilingual literature review was part of the process—comprising media written or produced in Chinese, English, French, German, Japanese, Italian, and Russian—as were many lessons learned in network literacy and cultures.

It is a history defined by constant change that is, at certain times, forged from what superficially appear to be otherwise disjointed threads or happenings—events that are woven together at turning-point moments in intricate and incidental ways. Take the ICP algorithm as an example: Besl had just gotten some success (if slow) with the Nelder–Mead downhill simplex algorithm from *Numerical Recipes in C*. He stopped by McKay's office to chat about it, and McKay said it would be interesting to try matching with the closest point for each model point and then repeat that iteratively. Besl modified his existing code by the next day, found he was getting monotonic convergence, and then proved the local convergence theorem. This is just one of many examples of the importance of having the personalities in the appropriate—usually applied—research settings for major breakthroughs to happen in the long term. It also highlights that the technologies and solutions which will continue to evolve beyond this publication were forged out of a rich and complex web of events.

Events that shaped technologies also feed into a history born out of applied research—from space and defense guidance systems to site documentation and inspection. The funding sources that fueled this research and work environments are equally as important as how technologies were being applied, because funding helped frame the progress being made, whether it was DARPA, the ESA, corporate funds or grants, via ADMICAL, or business models based on consumer uptake from the late 1990s onward.

Funding sources have a fundamental impact on how further changes to both hardware and software are shaped. For example, companies like Velodyne demonstrate that funding sources remain one of the constant agents of change in the commercial period of use and development of midrange TLS. The volume of commentary about the lidar market around the time this history was published supports this idea as well.

The term *lidar*—light detection and ranging—was avoided in both parts of this article due to the broad and sometimes vague ways in which it can be used. This was especially the case around the time of publication: a period when a gold rush was playing out in the sensor market. Lidar had become an all-encompassing term in the automotive industry and in associated media output tethered to events like the Consumer Electronics Show. This was, in part, largely due to the impact that sensors from companies such as Velodyne were having on collision detection and driver safety–and, in bringing the cost of technologies down so that a larger community of developers now had access to them. Marketing and associated press related to the iPad Pro from Apple (released around the time this article was published) emphasize this further as well. A central element to the iPad Pro announcement—which came in March 2020, shortly after the Consumer Electronics Show and during the COVID-19 pandemic—highlighted that a lidar sensor was included in this new tablet.

Overall, the term *midrange* TLS was used to be more specific to the subject matter at hand—that is, to focus on the intricacies linked to devices of measurement tethered to dynamic range and ranging. Or, in other words, the retrieval of entire surfaces of varying sizes in a scene as clouds of measurable points as opposed to just single points of measurement. As a term, *midrange* firmly cemented where the technologies sat as a method of data collection: those designed for building-scale documentation, sitting between small to medium-size object scanners and landscape-scale scanning instruments that can collect data from over a kilometer away.

The act of scanning was also considered an active imaging process, where a point cloud was generated by a laser beam making contact with a surface. Accuracy, repeatability, and resolution were seen as overarching variables to consider in working with point-cloud information. Accuracy pertained to the perceived scale of measurement (within centimeters over a distance up to a kilometer away); repeatability (examples include the ability to rescan a site with the same instrument and workflow to compare to previous results and / or baseline, or features of the system architecture of the instrument, such as number of times the signal of points returned are sampled to help improve data quality); and resolution was considered in terms of data quality or the visual level of detail represented in the 3D image generated via the point cloud.

Acknowledgements

The author would like to thank the many leaders in their field who enthusiastically waited for these articles to make it to publication. This includes core people from Cyra Technologies, K²T, Mensi and Riegl. Both articles pay homage to them and many other pioneers in 3D imaging.

The articles are dedicated to Rebecca, Fonzie, Harvey, Poppy and Willow. This article was made open access by Remotely Interested LLC.

Note: The author discovered the JPL Research Robot–which had the scanning laser rangefinder on it–had been mislabeled as the 'Stanford Refined Cart Robot' at the Computer History Museum (CHM) in Mountain View, California. This discovery came in between the final edits for part one and part two. Its starting point are in part one though: 'This took a similar form to the JPL Laser Rangefinder by 1979.' Dr Spring contacted the CHM and the catalogue was corrected to 'Jet Propulsion Laboratory (JPL) Research Robot' on June 22nd, 2020.

The author would also like to correct a typo made in the melee of final edits for part one. The Amiga based Scannerless Range Imager was an early example of a phase shift system.

References

3D Imaging Sensor LMS-Z210. 2001. <http://web.archive.org/web/20010306013840/http://www.riegl.com/lms-z210/e_lms-z210.htm> Accessed 8 February 2020.

3D LiDAR Technology Brought to Mass-Market with a $599 Livox Sensor. 2019. <https://www.livoxtech.com/news/1> Accessed 8 February 2020.

#MWC19 Landing Page. n.d. <https://pmdtec.com/mwc/> Accessed 8 February 2020.

About Us [Mensi]. n.d. <http://mensi.free.fr/english/aboutus.html> Accessed 20 February 2020.

About Us [Perceptron]. n.d. <https://perceptron.com/about-us/> Accessed 29 March 2020.

Ackerman, E. 2016a. Ford and Baidu Invest $150 Million in Velodyne for Affordable Lidar for Self-Driving Car. <https://spectrum.ieee.org/cars-that-think/transportation/sensors/ford-and-baidu-invest-150-million-in-velodyne-for-affordable-automotive-lidar> Accessed 20 February 2020.

Ackerman, E. 2016b. Sweep Is a $250 LIDAR with Range of 40 Meters That Works Outdoors. <https://spectrum.ieee.org/automaton/robotics/robotics-hardware/sweep-lidar-for-robots-and-drones> Accessed 11 February 2019.

Addison, A. C., D. Chudak, M. Gaiani, R. Marchetti and F. Uccelli. n.d. Facciata di Hearst Memorial Mining Building. <http://web.archive.org/web/19991008084802/http://dns.unife.it/architettura/labs/OFF/Pomposa_Berkley/pag2.htm> Accessed 12 July 2020.

Addison, A. C. and M. Gaiani. 2000. Virtualized architectural heritage: New tools and techniques. *IEEE MultiMedia* 7 (2):26–31.

Albouy, M. 1990. Les technologies du futur font revivre le passé. *Dossiers d'Archéologie* 153:2–7.

Albouy, M., H. Boccon-Gibod, J.-C. Golvin, J.-C. Goyon and P. Martinez. 1989. *Karnak: Le temple d'Amon restitué par l'ordinateur*. Paris: M. A. Éditions.

Amann, M.-C., T. Bosch, M. Lescure, R. Myllylae and M. Rioux. 2001. Laser ranging: A critical review of usual techniques for distance measurement. *Optical Engineering* 40 (1):10–19.

Aujoulat, N., Perazio, G., Faverge, D. and F. Peral, 2005. Contribution de la saisie tridimensionnelle à l'étude de l'art pariétal et de son contexte physique. *Bulletin de la Société préhistorique française,* pp.189-197.

Autodesk. 2013. Autodesk Reality Capture Technology Rapidly Evolving, No Longer Science Fiction. <https://adsknews.autodesk.com/news/autodesk-reality-capture-technology-rapidly-evolving-no-longer-science-fiction> Accessed 8 February 2020.

Bandiera, A., J. A. Beraldin and M. Gaiani. 2011. Nascita ed utilizzo delle tecniche digitali di 3D imaging, modellazione e visualizzazione per l'architettura dei beni culturali, in *Ikhnos: Annale di Analisi Grafica e Storia della Rappresentazione* 2011, 81–134.

Bares, J., M. Hebert, T. Kanade, E. Krotkov, T. Mitchell, R. Simmons and W. Whittaker. 1989. Ambler: An autonomous rover for planetary exploration. *Computer* 22 (6):18–26.

Baribeau, R., M. Rioux and G. Godin. 1995. Three dimensional object modeling towards improving access to collections by virtualizing reality. Pages 170–177 in *Multimedia Computing and Museums: Selected Papers from the Third International Conference on Hypermedia and Interactivity in Museums (ICHIM '95–MCN '95), San Diego, California, October* 9–13, 1995, held in San Diego, Calif., 9–13 October 1995. Edited by D. Bearman. Pittsburgh, Penn.: Archives & Museum Informatics.

Becker, R. and H. Volz. 2004. IQSUN 880 a new modular concept for 3d-laser scanning. Pages 30–32 in *Proceedings of the ISPRS Working Group VIII/2: Laser-Scanners for Forest and Landscape Assessment*, held in Freiburg, Germany, 3–6 October 2004. International Archives of Photogrammetry, Remote Sensing and Spatial Information Sciences Vol. XXXVI-8/W2. Edited by M. Thies, B. Koch, H. Spiecker and H. Weinacker. Freiburg, Germany: Institute for Forest Growth, Institute for Remote Sensing and Landscape Information Systems.

Beraldin, J.A., M. Picard, A. Bandiera, V. Valzano and F. Negro. 2011. Best practices for the 3D documentation of the Grotta dei Cervi of Porto Badisco, Italy. *Proceedings of SPIE* 7864: 78640J.

Besl, P. J. 1988. Active, optical range imaging sensors. *Machine Vision and Applications* 1 (2):127–152.

Besl, P. J., 1994. *SURFSEG: A Geometric Signal Processor*. Report No. AP-40. Warren, Mich.: General Motors Research and Development Center.

Besl, P. J. and N. D. McKay. 1992. A method for registration of 3-D shapes. *IEEE Transactions on Pattern Analysis and Machine Intelligence* 14 (2):239–256.

Biasion, A., T. Moerwald, B. Walser and G. Walsh. 2019. A new approach to the Terrestrial Laser Scanner workflow: The RTC360 solution, in *FIG Working Week 2019: Geospatial Information for a Smarter Life and Environmental Resilience*, held in Hanoi, Vietnam, 22–26 April 2019. <https://pdfs.semanticscholar.org/ae37/099c6560bb93392ae4496169f1ae4c7d1ce6.pdf> Accessed 20 February 2020.

Blais, F. 2004. Review of 20 years of range sensor development. *Journal of Electronic Imaging* 13 (1):231–243.

Boccon-Gibod, H., & J.-C. Golvin. 1990. Le grand temple d'Amon-Rê à Karnak reconstruit par ordinateur. *Dossiers d'Archéologie* 153:8–19.

Boehler, W., M. Bordas Vicent and A. Marbs. 2003. Investigating laser scanner accuracy. pp. 696–702 in *Proceedings of CIPA Symposium 19*, held in Antalya, Turkey, 30 September–4 October 2003. Edited by M. Orhan Altan, Antalya, Turkey: CIPA 2003 organising committee.

Boehler, W., G. Heinz and A. Marbs. 2001. The potential of non-contact close range laser scanners for cultural heritage recording. pp. 430–436 in *XVIII CIPA Symposium*, held in Potsdam, Germany, 18–21 September 2001. ISPRS Archives Vol. XXXIV-5/C7. Edited by J. Albertz, Berlin, Germany: CIPA.

Boehler, W. & A. Marbs. 2002. 3D scanning instruments. Pages 9–12 in *Proceedings of the CIPA WG 6 International Workshop on Scanning for Cultural Heritage Recording*, held in Corfu, Greece, 1–2 September 2002. Edited by W. Boehler. Thessaloniki, Greece: Publishing Ziti.

Bommelaer, J.-F. and M. Albouy. 1997. *Marmaria: le sanctuaire d'Athéna à Delphes*. Paris: Ecole française d'Athènes.

Bosse, M., R. Zlot and P. Flick. 2012. Zebedee: Design of a spring-mounted 3-D range sensor with application to mobile mapping. *IEEE Transactions on Robotics* 28 (5):1104–1119.

Breaking Through the Price Barrier for LiDAR Sensors, Velodyne Introduces 3D Real-Time 'LiDAR Puck at $7999. 2014. <https://www.suasnews.com/2014/09/breaking-through-the-price-barrier-for-lidar-sensors-velodyne-introduces-3d-real-timelidar-puck-at-7999/> Accessed 11 February 2019.

Brillault, B., G. Thibault and F. Guisnel. 1995. La grotte Cosquer au plus près du réel. *Collection de notes internes de la Direction des études et recherches. Production d'énergie (hydraulique, thermique et nucléaire)*.

Brunet, J. and J. Vouvé. 1996. *La Conservation des grottes ornées*. Paris: Éditions CNRS.

Cain, K. 2000. Drawing accurate ground plans from laser scan data. In SIGGRAPH *Campfire: Graphics and Archaeology*, edited by K. Akeley, 20–23. New York: ACM.

Cain, K. and P. Martinez. 2003. Drawing accurate ground plans using optical triangulation data. Pages PP–PP in *2003 Conference on Computer Vision and Pattern Recognition Workshop*, held in Madison, Wis., 16–22 June 2003. Los Alamitos, Calif.,: IEEE Computer Society.

Cain, K., P. Martinez and J. Munn. 2002. *Digital Documentation for the Zawya and Sabil of Sultan Farag Ibn Barquq, Cairo*. <http://www.insightdigital.org> Accessed 12 July 2020.

Cain, K., C. Sobieralski and P. Martinez. 2003. Reconstructing a colossus of Ramesses II from laser scan data, in SIGGRAPH *'03: ACM* SIGGRAPH *2003 Sketches & Applications*, held in San Diego, Calif., 7–31 July 2003. Edited by A. Rockwood. New York: Association for Computing Machinery.

The Callidus Precision Systems. n.d. <https://web.archive.org/web/20001025152839/http://www.callidus.de/PAGES_EN/wir.htm> Accessed 29 March 2020.

Catmull, E. 2014. *Creativity Inc.: Overcoming the Unseen Forces That Stand in the Way of True Inspiration*. New York: Random House.

Chen, X. and F. Schmitt. 1992. Intrinsic surface properties from surface triangulation. In *Computer Vision—ECCV '92*. Lecture Notes in Computer Science vol. 588. Edited by G. Sandini, 739–743. Berlin: Springer.

Chen, X. N., Q. Xia, S. H. Zhang and Y. Zhou. 2005. 3D laser scanner system for surveying and engineering. Pages 14–16 in *Proceedings of the ISPRS Joint Conference: 3rd International Symposium Remote Sensing and Data Fusion Over Urban Areas (URBAN 2005) and 5th International Symposium Remote Sensing of Urban Areas (URS 2005)*, held in Tempe, Ariz., 14–16 March 2005. Edited by M. Moeller and E. Wentz.

Chen, Y. and G. Medioni. 1992. Object modelling by registration of multiple range images. *Image and Vision Computing* 10 (3):145–155.

Clayton, M. J. 2005. Computational design and AutoCAD: Reading software as oral history. Pages 103–107 in *Proceedings of the 9th Iberoamerican Congress of Digital Graphics*, held in Lima, Peru, 21–23 November 2005.

Clottes, J., J. Courtin, J. Collina-Girard, M. Arnold and H. Valladas. 1997. News from Cosquer Cave: Climatic studies, recording, sampling, dates. *Antiquity* 71 (272):321–326.

Coignard, B. 1999. Rapport de Restauration du Colosse d'Alexandrie. <http://www.sculpt.fr/RESTAURATION/PDF/Anastylose-du-colosse-d-Alexandrie.pdf> Accessed 12 July 2013.

Coignard, B. and M. Szewczyk. M. 2016. Reconstruction virtuelle et restauration d'ensembles sculptés fragmentaires: Le cas d'une statue d'époque impériale du musée départemental Arles antique. Pages 143–158 *in Les Préalables à la Restauration: Journées d'Étude*, held in Nancy, France, 13–14 October 2016. <http://technologies.c2rmf.fr/c2rmf/JDNNancy_C2RMF.pdf> Accessed 29 March 2020.

Coignard, O., R. Coignard, B. Coignard and S. Zamia. 1998. La restauration du colosse d'Alexandrie. *Archéologia* 349: 34–41.

Coignard, R., O. Coignard and B. Coignard. 1999. Infosculpture: Un Art Millénaire à l'Ère Numérique. <http://www.sculpt.fr/SUITE/INFOSCULPT/UP/MAIN.htm> Accessed 12 July 2013.

Collins, D. 1994, December. Searching for virtue in a virtual landscape. New Art Examiner 22: 24–31. <http://www.public.asu.edu/~dan53/Virtue.html> Accessed 12 July 2013.

Collins, D. 1997. The challenge of digital sculpture: Or how to become better tool users, in *Proceedings of the Sixth Biennial Symposium on Art and Technology*, held in New London, Conn., 27 February–2 March 1997. Edited by L. Friedman. New London, Connecticut;: Center for Arts and Technology, Connecticut College. <http://www.public.asu.edu/~dan53/digital_sculpt.html> Accessed 12 July 2013.

Cyra Technologies. 1999. The Cyrax Reality Capture Process. <https://web.archive.org/web/19990125094610/http://www.cyra.com/> Accessed 8 February 2020.

Davies, A. 2020. There are too many lidar companies. They can't all survive. *Wired*. <https://www.wired.com/story/too-many-lidar-companies-cant-all-survive/> Accessed 3 April 2020.

Dawson, P. C., M. M. Bertulli, R. Levy, C. Tucker, L. Dick and P. L. Cousins. 2013. Application of 3D laser scanning to the preservation of Fort Conger, a historic polar research base on northern Ellesmere Island, *Arctic* Canada. *Arctic* 66 (2):147–158.

Debevec, P., C. Tchou, A. Gardner, T. Hawkins, C. Poullis, J. Stumpfel, A. Jones, P. Einarsson, M. Fajardo and P. Martinez. 2005. Making "The Parthenon": Digitization and reunification of the Parthenon and its sculptures, in *VAST 2005: The 6th International Symposium on Virtual Reality, Archaeology and Cultural Heritage*, held in Pisa, Italy, 8–11 November 2005. Edited by M. Mudge. Aire-la-Ville, Switzerland: Eurographics Association.

DeepMap. 2018. <https://www.deepmap.ai> Accessed 11 February 2019.

Dekeyser, F., F. Gaspard, L. de Luca, M. Florenzano, X. Chen and P. Leray. 2003. Cultural heritage recording with laser scanning, computer vision and exploitation of architectural rules. *International Archives of the Photogrammetry, Remote Sensing and Spatial Information Sciences* 34 (5/W12):145–149.

Deslauriers, A., S. Zhu, M. Sekerka and E. Trickey. 2014. Technology transfer for a 360 scanning lidar, in *i-SAIRAS 2014: The 12th International Symposium on Artificial Intelligence, Robotics and Automation in Space*, held in Montreal, Canada, 17–19 June 2014. Edited by É. Dupuis. Montreal, Canada: Canadian Space Agency.

Deveau, M., N. Paparoditis, M. Pierrot-Deseilligny, X. Chen and G. Thibault. 2005. Strategy for the extraction of 3D architectural objects from laser and image data acquired from the same viewpoint, in *3D-ARCH 2005: Virtual Reconstruction and Visualization of Complex Architectures*, held in Mestre-Venice, Italy, 22–24 August 2005. ISPRS Archives Vol. XXXVI-5/W17. Edited by S. El-Hakim, F. Remondino and L. Gonzo. Mestre-Venice, Italy: ISPRS.

Dickmanns, E. D. 2002. The development of machine vision for road vehicles in the last decade. Pages 268–281 in *IEEE Intelligent Vehicle Symposium 2002*, held in Versailles, France, 17–21 June 2002. New York: IEEE.

DJI Showcases Wide Product Portfolio at CES 2020 Including new Incubated Livox Lidar Technology. 2020. <https://www.suasnews.com/2020/01/dji-showcases-wide-product-portfolio-at-ces-2020-including-new-incubated-livox-lidar-technology/> Accessed 20 February 2020.

Duguet, F., G. Drettakis, D. Girardeau-Montaut, J.-L. Martinez and F. Schmitt. 2004. A point-based approach for capture, display and illustration of very complex archaeological artefacts. Pages 105–114 in VAST 2004: *The 5th International Symposium on Virtual Reality, Archaeology and Intelligent Cultural Heritage*, held in Brussels, Belgium, 7–10 December 2004. Edited by Y. Chrysantou, K. Cain, N. Silberman and F. Niccolucci. Goslar, Germany: Eurographics Association.

English, C. 2010. Smart sensing for real-time pose estimation, assembly, and inspection using 3D laser scanning systems. Pages 277–284 in *PerMIS '10: Proceedings of the 10th Performance Metrics for Intelligent Systems Workshop*, held in Baltimore, Md., September 2010. Edited by E. Messina. New York: Association for Computing Machinery.

Etherington, D. 2014. Google's Project Tango Includes Tech Apple-Acquired 3D Imaging Company PrimeSense. <https://techcrunch.com/2014/04/17/googles-project-tango-includes-tech-apple-acquired-3d-imaging-company-primesense/> Accessed 14 January 2015.

Evans & Sutherland Computer Corporation History. n.d. <http://www.fundinguniverse.com/company-histories/evans-sutherland-computer-corporation-history/> Accessed 20 February 2020.

Fertey, G., G. Thibault, T. Delpy and M. Lapierre. 1995. *An Industrial Application Virtual Reality: An Aid for Designing Maintenance in Nuclear Plants*. Publication No. EDF--96-NJ-00021. Clamart, France: Électricité de France.

Fienup, J. R. 2013. Phase retrieval algorithms: A personal tour. *Applied Optics* 52 (1):45–56.

Flaten, A. R. and A. A. Gill. 2007. Virtual Delphi: Two case studies. Pages 780–785 in *Proceedings of the 21st CIPA Symposium: AntiCIPAting the Future of the Cultural Past*, held in Athens, 1–6 October 2007. ISPRS Archives Vol. XXXVI-5/C53. Edited by A. Georgopoulos. Athens, Greece: ISPRS.

Flatscher, R., A. Ullrich, G. Paar and G.-J. Ulbrich. 1999. Active surface imaging system (ASIS). Pages 379–384 in *Proceedings of the Fifth International Symposium, Artificial Intelligence, Robotics and Automation in Space*, held in Noordwijk, the Netherlands, 1–3 June 1999. Edited by M. Perry. Paris: European Space Agency.

Franz, S., R. Irmler and U. Rüppel. 2018. Real-time collaborative reconstruction of digital building models with mobile devices. *Advanced Engineering Informatics* 38:569–580.

Frei, E., J. Kung and R. Bukowski. 2005. High-definition surveying (HDS): A new era in reality capture. Pages 262–271 in *Proceedings of the ISPRS Working Group VIII/2: Laser-Scanners for Forest and Landscape Assessment*, held in Freiburg, Germany, 3–6 October 2004. International Archives of Photogrammetry, Remote Sensing and Spatial Information Sciences Vol. XXXVI-8/W2. Edited by M. Thies, B. Koch, H. Spiecker and H. Weinacker. Freiburg, Germany: Institute for Forest Growth, Institute for Remote Sensing and Landscape Information Systems.

Froehlich, C., M. Mettenleiter and F. Haertl. 1997. Active laser radar (lidar) for measurement of corresponding height and reflectance images. *Proceedings of SPIE* 3101: 292–305.

Froehlich, C., M. Mettenleiter and F. Haertl. 1998. Imaging laser radar for high-speed monitoring of the environment. *Proceedings of SPIE* 3207: 50–64.

Fuchs, A., E. Alby, R. Begriche, P. Grussenmeyer and J.-P. Perrin. 2004. Confrontation du relevé laser 3D aux techniques de relevé conventionnelles et développement d'outils numériques pour la restitution architecturale. *Revue Française de Photogrammétrie et Télédétection* 173/174: 36–47.

Gaboury, J. 2016. Other places of invention: Computer graphics at the University of Utah. In *Communities of Computing: Computer Science and Society in the ACM*, edited by T. J. Misa, 259–285. Williston, Vt.: Morgan & Claypool.

Gage, D. W. 1995. UGV history 101: A brief history of unmanned ground vehicle (UGV) development efforts. *Unmanned Systems Magazine* 13 (3):9–32.

Gaiani, M., M. Balzani and F. Uccelli. 2000. Reshaping the Coliseum in Rome: An integrated data capture and modeling method at heritage sites. *Computer Graphics Forum* 19 (3):369–378.

Gainor, C. 2012. Canadian Lidar Technology. <https://spaceq.ca/canadian_lidar_technology/> Accessed 20 February 2020.

Garcia, J. and Z. Zalevsky. 2008. Range mapping using speckle decorrelation. US Patent 7,433,024.

Gautier, A., A.-C. Pache and I. Chowdhury. 2013. *Nonprofit Roles in For-profit Firms: The Institutionalization of Corporate Philanthropy in France*. ESSEC Business School Working Paper 1319. Paris: ESSEC Business School.

GeoSLAM. 2018. 3D Laser Mapping & GeoSLAM Global Merger Announced. <https://geoslam.com/3d-laser-mapping-geoslam-global-merger-announced/> Accessed 20 February 2020.

GIM International. 2019. H*exagon Expands Leica BLK Series to Enhance 3D Reality Capture.* <https://www.gim-international.com/content/news/hexagon-expands-leica-blk-series-to-enhanced-3d-reality-capture> Accessed 04 July 2020.

Girardeau-Montaut, D. n.d. CloudCompare. <https://www.danielgm.net/cc/> Accessed 14 September 2018.

Gleichman, K., L. Harmon, T. Miciek, C. Miller and D. Zuk.1988. *Sensor Support for the* DARPA *Autonomous Land Vehicle Program*. Publication No. ERIM-176600-12-F. Arlington, VA: DARPA.

GPS World. 2015. Hi-Target Introduces Laser Scanner. <https://youtu.be/Tzea3hHIW40> Accessed 20 February 2020.

Guerrin, M. and E. de Roux. 2008. "Un désengagement de l'Etat dans la culture pénaliserait le mécénat." *Le Monde*. <https://www.lemonde.fr/culture/article/2008/02/13/jacques-rigaud-un-desengagement-de-l-etat-dans-la-culture-penaliserait-le-mecenat_1010823_3246.html> Accessed 20 February 2020.

Guzzo, M. 2004. Quantapoint Could Double Annual Sales. *Pittsburgh Business Times*. <https://www.bizjournals.com/pittsburgh/stories/2004/07/12/story6.html> Accessed 20 February 2020.

Hancock, J., E. Hoffman, R. M. Sullivan, D. Ingimarson, D. Langer and M. Hebert. 1998. High-performance laser range scanner. *Proceedings of SPIE* 3207: 40–49.

Hancock, J., D. Langer, M. Hebert, R. Sullivan, D. Ingimarson, E. Hoffman, M. Mettenleiter and C. Froehlich. 1998. Active laser radar for high-performance measurements. Pages 1465–1470 in *Proceedings, 1988 IEEE International Conference on Robotics and Automation*, held in Leuven, Belgium, 16–20 May 1998. Piscataway, N.J.: Institute of Electrical and Electronics Engineers.

Halterman, R. and M. Bruch. 2010, May. Velodyne HDL-64E lidar for unmanned surface vehicle obstacle detection. *Proceedings of SPIE* 7692: 76920D.

Hayden, S. 2020. Google ARCore Depth API Now Available, Letting Devs Make AR More Realistic. *RoadToVR* https://www.roadtovr.com/google-depth-api-arcore-augmented-reality/ Accessed 04 July 2020.

Hebert, M. and E. Krotkov. 1992. 3D measurements from imaging laser radars: How good are they? *Image and Vision Computing* 10 (3):170–178.

Hecht, J. 2005. *Beam: The Race to Make the Laser*. Oxford, UK: Oxford University Press.

Hecht, J. 2010. A short history of laser development. *Applied Optics* 49 (25): F99–F122.

Historic England. 2018. *3D Laser Scanning for Heritage: Advice on the Use of Laser Scanning in Archaeology and Architecture*. Swindon, UK: Historic England. <https://historicengland.org.uk/images-books/publications/3d-laser-scanning-heritage/heag155-3d-laser-scanning/> Accessed 20 February 2020.

Hoffmeister, J. W., M. McPohlenz, D. A. Addleman, M. A. Kasic and K. M. Robinette. 1996. *Functional Description of the Cyberware Color 3-D Digitizer 4020 RGB/*PS*-D*. Publication No. AL/CF-TR-1996-0069. Wright-Patterson Air Force Base, Ohio: Air Force Materiel Command.

Homann, G. n.d. Le Jeu des 7 Erreurs avec "Karnak Restitué par l'Ordinateur." <http://gerard.homann.free.fr/WEB_EGYPTE/erreurs_kro.htm> Accessed 12 July 2013.

Howe, S. D. and G. Auchampaugh. 1992. Nuclear data needs for the Space Exploration Initiative. In *Nuclear Data for Science and Technology*, edited by S. M. Qaim, 692–695. Berlin: Springer.

Hunter, J. and M. Cox. 2005. *Forensic Archaeology: Advances in Theory and Practice*. London: Routledge.

Hurtut, T., Y. Gousseau, F. Cheriet and F. Schmitt. 2011. Artistic line-drawings retrieval based on the pictorial content. *Journal on Computing and Cultural Heritage* 4 (1): 3.

Hwang, H. S and C. Stewart. 2006. Lessons from dot-com boom and bust. In *Encyclopedia of E-Commerce, E-Government, and Mobile Commerce*, edited by M. Khosrow-Pour, 698–702. Hershey, Penn.: Idea Group Reference.

ISC Web Special: Dan Collins. n.d. <http://www.sculpture.org/documents/webspec/digscul/collins/collins.shtml> Accessed 12 July 2013.

Izadi, S. 2019. Blending Realities with the ARCore Depth API. Google Developers. https://developers.googleblog.com/2019/12/blending-realities-with-arcore-depth-api.html Accessed 04 July 2020.

Jacobs, G. 2017. The GeoDude on the Adoption of Laser Scanning Today. <https://www.xyht.com/lidarimaging/the-geodude-on-the-adoption-of-laser-scanning-today/> Accessed 29 March 2020.

Kacyra, B. 2009. CyArk 500—3D documentation of 500 important cultural heritage sites. Pages 315–320 in *Photogrammetric Week '09*, held in Stuttgart, Germany, 7–11 September 2009. Edited by D. Fritsch. Heidelberg, Germany: Wichmann.

Kacyra, B. K., J. Dimsdale, M. Brunkhart, J. A. Kung and C. R. Thewalt. 1997. Integrated system for imaging and modeling three-dimensional objects. WIPO Patent WO/1997/040342.

Kacyra, B. K., J. Dimsdale and J. A. Kung. 2005. Integrated system for quickly and accurately imaging and modeling three-dimensional objects. US Patent 6,847,462.

Kastrenakes, J. 2017. Google's Project Tango Is Shutting Down Because ARCore Is Already Here. <https://www.theverge.com/2017/12/15/16782556/project-tango-google-shutting-down-arcore-augmented-reality> Accessed 20 February 2020.

Kelly, A. 1994. *Concept Design of a Scanning Laser Rangefinder for Autonomous Vehicles*. Publication No. CMU-RI-TR-94-21. Pittsburgh, Penn.: Carnegie Mellon University Robotics Institute.

Keralia, D., K. K. Vyas and K. Deulkar. 2014. Google Project Tango—A convenient 3D modeling device. *International Journal of Current Engineering and Technology* 4 (5):3139–3142.

Khetan, R. P. and P. J. Besl. 1990. *Surface Coordinate Measurement and Mathematical Surface Representation of a Concept Seat for the Impact Vehicle*. Report No. EM-759/CS-626. Warren, Mich.: General Motors Research Laboratories.

Kotler, P. 1986. 'Prosumers: A New Type of Consumer.' *The Futurist* 20: 24–9.

Kweon, I. S., R. Hoffman and E. Krotkov. 1991. *Experimental Characterization of the Perceptron Laser Rangefinder*. Publication No. CMU-RI-TR-91-1. Pittsburgh, Penn.: Carnegie Mellon University Robotics Institute.

Kweon, I. S. and T. Kanade. 1992. High-resolution terrain map from multiple sensor data. *IEEE Transactions on Pattern Analysis and Machine Intelligence* 14 (2):278–292.

Lamb, D. G., D. L. Baird and M. A. Greenspan. 1999. An automation system for industrial 3-D laser digitizing. Pages 148–157 in *Second International Conference on 3-D Digital Imaging and Modeling*, held in Ottawa, Canada, 8 October 1999. Los Alamitos, Calif.: Institute of Electrical and Electronics Engineers.

Langer, D., M. Mettenleiter, F. Härtl and C. Fröhlich. 2000. Imaging ladar for 3-D surveying and CAD modeling of real-world environments. *The International Journal of Robotics Research* 19 (11):1075–1088.

Latour, B. and A. Lowe. 2011. The migration of the aura, or how to explore the original through its facsimiles. In *Switching Codes*, edited by T. Bartscherer and R. Coover, 275–298. Chicago: University of Chicago Press.

Laurin, D. 2017. Technology development in active optical instrumentation at Canadian Space Agency, Space Technologies. *Proceedings of SPIE* 10313: 1031310.

Lavigne, C. 1998. Digital sculpture. Translated by M.-P. Jiccio and R. M. Smith. <http://www.sculpture.org/documents/webspec/magazine/wsenglis.shtml> Accessed 8 February 2020.

Learning Tools for Advanced Three-Dimensional Surveying in Risk Awareness Project. 2008. *Theory and Practice on Terrestrial Laser Scanning: Training Material Based on Practical Applications*. <https://lirias.kuleuven.be/retrieve/122640> Accessed 8 February 2020.

Lee, E., 2010. Digitizing the legacy. *American Surveyor* 7 (7):10–17.

Leica CloudWorx Digital Reality Plugins for CAD. 2020. <https://leica-geosystems.com/en-us/products/laser-scanners/software/leica-cloudworx> Accessed 20 February 2020.

Leica Cyclone 3D Point Cloud Processing Software. 2020. <https://leica-geosystems.com/en-us/products/laser-scanners/software/leica-cyclone> Accessed 20 February 2020.

Leica Geosystems Acquires Oakland-Based Cyra Technologies, Inc., World Leader in Emerging Field of 3D Laser Scanning. 2000. <https://web.archive.org/web/20010204011700/http://cyra.com:80/leicamerge.html> Accessed 11 February 2019.

Levoy, M. 2007. The early history of point-based graphics. In *Point-Based Graphics*, edited by M. Gross and H. Pfister, 9–18. Amsterdam: Morgan Kaufmann. <http://graphics.stanford.edu/papers/points/levoy-pointbook-ch2.pdf> Accessed 17 July 2017.

Levoy, M., M. Curless, B. Curless, J. Gerth, S. Marschner, L. Pacelle, D. Piturro and K. Pulli. 2009. The Digital Michelangelo Project. <https://graphics.stanford.edu/projects/mich/> Accessed 12 July 2020.

Levoy, M. and T. Whitted. 1985. *The Use of Points as a Display Primitive*. Technical Report 85-022. Chapel Hill, N.C.: University of North Carolina, Department of Computer Science. <http://citeseerx.ist.psu.edu/viewdoc/download?doi=10.1.1.89.1180&rep=rep1&type=pdf> Accessed 17 July 2017.

Lewis, R. A. and A. R. Johnston. 1977. A scanning laser rangefinder for a robotic vehicle. Pages 762–768 in *IJCAI'77: Proceedings of the 5th International Joint Conference on Artificial Intelligence*, held in Cambridge, Mass., 22–25 August 1977. San Francisco: Morgan Kaufmann.

Loedeman, J. H. 1999. Methods of capturing reality can be improved: Interview with Ben Kacyra, CEO of Cyrax. *GIM International* 13 (10):48–51.

Lucic, K. 2014. Mantis Vision Unveiled Their 3D Project Tango-like Aquila Tablet And An SDK For Developers. *Android Headlines*. https://www.androidheadlines.com/2014/09/mantis-vision-unveiled-3d-project-tango-like-aquila-tablet-sdk-developers.html Accessed 04 July 2020.

Markoff, J. 2005. *What the Dormouse Said…: How the 60s Counterculture Shaped the Personal Computer Industry*. New York: Penguin.

Martinez, J.-L. and G. Thibault. 2012. La reconstitution de la colonne des danseuses de Delphes. <https://www.inrap.fr/la-reconstitution-de-la-colonne-des-danseuses-de-delphes-9244> Accessed 12 July 2013.

Martinez, P. 2001. Digital realities and archaeology: A difficult relationship or a fruitful marriage? Pages 9–16 in *VAST '01: Proceedings of the 2001 Conference on Virtual Reality, Archeology, and Cultural Heritage*, held in Glyfada, Greece, November 2001. New York: Association for Computing Machinery.

Martinez, P. and K. Cain. 2011. Ramses II: The Great Voyage. Research Paper. INSIGHT, Available in: http://www.insightdigital.org .

Matthies, L. H. 1999. Robotic perception for autonomous navigation of Mars rovers. In *Frontiers of Engineering: Reports on Leading Edge Engineering from the 1998 NAE Symposium on Frontiers of Engineering*, 99–105. Washington, DC: National Academies Press.

Matthies, L., M. Maimone, A. Johnson, Y. Cheng, R. Willson, C. Villalpando, S. Goldberg, A. Huertas, A. Stein and A. Angelova. 2007. Computer vision on Mars. *International Journal of Computer Vision* 75:67–92.

Maurer, M., R. Behringer, D. Dickmanns, T. Hildebrandt, F. Thomanek, J. Schiehlen and E. D. Dickmanns. 1995. VaMoRs-P: An advanced platform for visual autonomous road vehicle guidance. *Proceedings of SPIE* 2352: 239–248.

Mettenleiter, M., F. Härtl, S. Kresser and C. Fröhlich. 2016. *Laserscanning: Phasenbasierte Lasermesstechnik für die hochpräzise und schnelle dreidimensionale Umgebungserfassung*. Munich: Süddeutscher Verlag.

Metz, C. 2016. Ex-Darpa Head Regina Dugan Leaves Google for Facebook. *Wired*. <https://www.wired.com/2016/04/regina-dugan-leaves-google-for-facebook/> Accessed 20 February 2020.

Monroe, M. 1999. 3-D Scanner a Tool to Update Archaic Facilities. *Atlanta Business Chronicle*. <https://www.bizjournals.com/atlanta/stories/1999/12/13/focus13.html> Accessed 11 February 2019.

Morris, J. J. and P. Alam. 2012. Value relevance and the dot-com bubble of the 1990s. *The Quarterly Review of Economics and Finance*, 52 (2):243–255.

Moulin, S., F. Voldoire, G. Nicolas and G. Thibault. 1998. Ptolémée: le Colosse d'Alexandrie ressuscité. Aster Échos 28: PP–PP. <http://www.code-aster.org/documents/fiches_etudes_ae/AE_28_1.pdf> Accessed 8 February 2020.

Nelson, R. 2013. How did we get here? An early history of forestry lidar. *Canadian Journal of Remote Sensing* 39 (suppl. 1):S6–S17.

New Lanark, Scotland. n.d. <http://www.scottishten.org/index/property2.htm> Accessed 25 June 2012.

Nitzan, D., A. E. Brain and R. O. Duda. 1977. The measurement and use of registered reflectance and range data in scene analysis. *Proceedings of the IEEE*, 65 (2):206–220.

Nwagboso, C.O., ed. 1993. *Automotive Sensory Systems*. Dordrecht, the Netherlands: Springer Science+Business Media.

Ohnsman, A. 2020. Lidar Pioneer Velodyne Debuts $100 Auto Safety Sensor as Self-Driving Cars' Pace to Market Slows. *Forbes*. <https://www.*forbes*.com/sites/alanohnsman/2020/01/07/lidar-pioneer-velodyne-debuts-100-auto-safety-sensor-as-self-driving-cars-pace-to-market-slows> Accessed 20 February 2020.

Open Heritage. n.d. <https://artsandculture.google.com/project/openheritage> Accessed 8 February 2020.

Palacios, J. and J. Triska. 2011. A Comparison of Modern GPU and CPU Architectures: And the Common Convergence of Both. <https://cours.do.am/ParadigmeAgent/final.pdf> Accessed 04 May 2013.

Paramythioti, M. and A. d'Aligny. 1989. Process and apparatus for three-dimensional surveying. US Patent 4,873,449.

Partners. 2020. <https://cyark.org/about/partners> Accessed 2 April 2020.

Peers, P., T. Hawkins and P. Debevec. 2006. *A Reflective Light Stage*. Technical Report ICT-TR-04.2006. Los Angeles: USC Institute for Creative Technologies.

Petrov, D. 2018. Galaxy S10 and 2019 iPhones May Don a 3D-Sensing Camera, Native Support Expected in Snapdragon 855. <https://www.phonearena.com/news/Galxy-S10-iPhone-3D-depth-sensing-cameras-Qualcomm-snapdragon-855_id111580> Accessed 20 February 2020.

Pfeifer, N. and G. Rottensteiner. 2001. The Riegl Laser Scanner for the Survey of the Interiors of Schönbrunn Palace. <https://photo.geo.tuwien.ac.at/media/filer_public/9f/89/9f89b5c4-f5b4-4891-94af-959e79988458/np_vienna_terrestrialls_2001.pdf> Accessed 04 May 2014.

Phillips, P.C.B. and J. Yu. 2011. Dating the timeline of financial bubbles during the subprime crisis. *Quantitative Economics* 2 (3):455–491.

Pot, J., G. Thibault and P. Levesque. 1997. Techniques for CAD reconstruction of "as-built" environments and application to preparing for dismantling of plants. *Nuclear Engineering and Design* 178 (1):135–143.

PrimeSense Supplies 3-D-Sensing Technology to "Project Natal" for Xbox 360. 2010. <https://news.microsoft.com/2010/03/31/primesense-supplies-3-d-sensing-technology-to-project-natal-for-xbox-360/> Accessed 20 February 2020.

Pritchard, C. 2005. FARO Technologies Buys iQvolution. <https://www.marketwatch.com/story/faro-technologies-buys-iqvolution-for-12-million> Accessed 20 February 2020.

Project Development Plan. n.d. <http://www.cs.cmu.edu/afs/cs/project/lri/members/lalit/doc/proposals/BenFranklin/alonzo2/project_development_plan.txt> Accessed 20 February 2020.

ReCap. n.d. <https://www.autodesk.com/products/recap/overview> Accessed 20 February 2020.

Reimagining Maybeck's Palace. 2002. <https://web.archive.org/web/20030510210205/http://www.insightdigital.org/pfa.htm> Accessed 29 March 2020.

Remondino, F. 2011. Heritage recording and 3D modeling with photogrammetry and 3D scanning. *Remote Sensing* 3 (6):1104–1138.

Renovation of Historic Building: San Francisco City Hall, San Francisco, CA. 1998. <http://www.leica-geosystems.us/downloads123/zz/general/general/TruStories/City%20Hall%20TRU_en.pdf> Accessed 01 December 2014.

Rieger, P., A. Ullrich and R. Reichert. 2006. Laser scanners with echo digitization for full waveform analysis. Pages 215–221 in *Proceedings: International Workshop, 3D Remote Sensing in Forestry*, held in Vienna, Austria, 14–15 February 2006. Edited by T. Koukal and W. Schneider. Vienna: Institute of Surveying, Remote Sensing and Land Information, University of Natural Resources and Applied Life Sciences.

Riegl Timeline: Pulsed Laser Radar and Laser Scanning Since 1968. 2014. <http://www.riegl.com/uploads/tx_pxpriegldownloads/RIEGL-Timeline_since-1968_asper_30-06-2014_view.pdf> Accessed 01 December 2014.

Rioux, M. 1984. Laser range finder based on synchronized scanners. *Applied Optics* 23 (21):3837–3844.

Rioux, M. and T. Bird. 1993. White laser, synced scan (3D scanner). *IEEE Computer Graphics and Applications* 13 (3):15–17.

Riquelme, A. J., B. Ferrer and D. Mas. 2017. Use of high-quality and common commercial mirrors for scanning close-range surfaces using 3D laser scanners: A laboratory experiment. *Remote Sensing 9* (11): 1152.

RiScan Pro 2.0. n.d. <http://www.riegl.com/products/software-packages/riscan-pro/> Accessed 20 February 2020.

Robson, W. 2017. LiDAR: Velodyne Shifts from Subwoofers to Self-Driving Cars. <https://www.audioholics.com/news/lidar-velodyne-shifts-from-subwoofers-to-self-driving-cars> Accessed 20 February 2020.

Roland, A. and P. Shiman. 2002. *Strategic Computing:* DARPA *and the Quest for Machine Intelligence, 1983–1993*. Cambridge, Mass.: The MIT Press.

Rustad, M. L. and M. V. Onufrio. 2012. Reconceptualizing consumer terms of use for a globalized knowledge economy. *University of Pennsylvania Journal of Business Law* 14: 1085–1190.

Saint-Aubin, J. P. 1995. *The survey of caves and their surroundings, their return by computer*. CNRS Editions, URL: http://www.culture.gouv.fr/culture/conservation/fr/cours/aubin.htm#Note_1

Samson, C., C. English, A. Deslauriers, I. Christie, F. Blais and F. Ferrie. 2004. The Neptec three-dimensional laser camera system: From space mission STS-105 to terrestrial applications. *Canadian Aeronautics and Space Journal* 50 (2):115–123.

Saran, V., J. Lin and A. Zakhor. 2019. Augmented annotations: Indoor dataset generation with augmented reality, in *Proceedings Title*, held in Enschede, the Netherlands, 10–14 June 2019. *International Archives of the Photogrammetry, Remote Sensing and Spatial Information Sciences* Vol. XLII-2/W13. Edited by G. Vosselman, S. J. Oude Elberink and M. Y. Yang. <https://d-nb.info/1187931217/34> Accessed 20 February 2020.

Schmitt, F. 1993. *Traitement des Objets*. Rapport scientifique 1991-1992 du département image de l'École Nationale Supérieur des Télécommunication, Paris.

Schmitt, F., F. Polycarpe, J. C. André, S. Corbel and R. Coignard. 1993. Traitement tridimensionnel d'objets de musées. Pages 123–143 in *Moulages, copies, fac-similés: actes des IXèmes journées des restaurateurs en archéologie*, held in Soissons, France, 14–15 June 1993. Paris, France: CEPMR.

Shaffer, G. 1995. *2D Mapping of Expansive Unstructured Areas*. Pittsburgh, Penn.: Carnegie Mellon University Robotics Institute. <https://www.ri.cmu.edu/pub_files/pub3/shaffer_gary_1995_1/shaffer_gary_1995_1.pdf> Accessed 20 February 2020.

Shain, K. 2009. Delphi, Greece: A Virtual Reconstruction. <https://www.youtube.com/watch?v=Hl4Y_85qaMw> Accessed 30 March 2016.

Shan, J. and C. K. Toth, eds. 2009. *Topographic Laser Ranging and Scanning: Principles and Processing*. Boca Raton, Fla.: CRC Press.

Shan, J. and C. K. Toth, eds. 2008. *Topographic Laser Ranging and Scanning: Principles and Processing*, 2nd ed. Boca Raton, Fla.: CRC Press.

Simai Surveying Instruments. 2020. SMG Laser Scanner. <http://www.smartmaxgeosystems.com/Products-VS10-VS30.html> Accessed 20 February 2020.

Song, S.-M. and K. J. Waldron. 1989. *Machines That Walk: The Adaptive Suspension Vehicle*. Cambridge, Mass.: The MIT Press.

Space Vision System Helps Astronauts See in Space. 2008. <https://web.archive.org/web/20080603143525/http://www.nrc-cnrc.gc.ca/eng/education/innovations/discoveries/svs.html> Accessed 20 February 2020.

Spring, A. P. 2012. The Third Industrial Revolution. *GeoInformatics* 15 (7):32–34.

Spring, A. P. 2015. Creating substance from a cloud: Low-cost product generation. *Computer* 48 (2):67–74.

Spring, A. P. and C. Peters. 2014. Developing a low cost 3D imaging solution for inscribed stone surface analysis. *Journal of Archaeological Science* 52: 97–107.

Spring, A. P., C. Peters and T. Minns. 2010. Using mid-range laser scanners to digitize cultural-heritage sites. *IEEE Computer Graphics and Applications* 30 (3):15–19.

Stephan, A., M. Mettenleiter, F. Härtl, I. Heinz, C. Fröhlich, G. Dalton and G. Hines. 2002. Laser-sensor for as-built documentation. Pages 396–403 in *2nd Symposium on Geodesy for Geotechnical and Structural Engineering*, held in Berlin, Germany, 21–24 May 2002. Edited by H. Kahmen, W. Niemeier and G. Retscher. Vienna: Department of Applied and Engineering Geodesy, Institute of Geodesy and Geophysics, Vienna University of Technology.

Stiroh, K. J. 2002. Are ICT spillovers driving the new economy? *The Review of Income and Wealth* 48 (1):33–57.

Studnicka, N. n.d. 3D Imaging Sensor LMS-Z210. <https://books.ub.uni-heidelberg.de/arthistoricum/reader/download/264/264-17-77812-1-10-20170522.pdf> Accessed 20 February 2020.

Takase, Y., Y. Sasaki, M. Nakagawa, M. Shimizu, O. Yamada, T. Izumi and R. Shibasaki. 2003. Reconstruction with laser scanning and 3D visualization of Roman monuments and remains in Tyre, Lebanon. Pages 325–329 in *International Workshop on Vision Techniques for Digital Architectural and Archaeological Archives*, held in Ancona, Italy, 1–3 July 2003. International Archives of Photogrammetry, Remote Sensing and Spatial Information Sciences Vol. XXXIV-5/W12. Edited by G. Fangi and E. S. Malinverni.

Tarini, M., P. Cignoni and R. Scopigno. 2003. Visibility based methods and assessment for detail-recovery. Pages 467–464 in *IEEE Visualization 2003*, held in Seattle, Wash., 19–24 October 2003. Los Alamitos, Calif.: IEEE Computer Society.

Thibault, G. 2001. 3D modeling of the Cosquer Cave by laser survey. *INORA: International Newsletter on Rock Art* 28: 25–29. <http://www.icomos.org/centre_documentation/inora/inora28/inora-28-6.pdf> Accessed 20 July 2014.

Thibault, G. and A. d'Aligny 1994. Numérisation 3D au plus proche du réel–Scannérisation du Pont Neuf. Actes d'Imagina 94, Bry-sur-Marne, INA–Centre National de la Cinématographie, pp. 98-105. https://www.mediaport.net/CP/CyberScience/BDD/fich_030.fr.html Accessed 04 July 2020.

Thibault, G. and J.-L. Martinez. 2007. La reconstitution de la colonne des danseuses de Delphes. Pages 231–238 in *Actes du colloque Virtual Retrospect 2007*, held in Pessac, France, 14–16 November 2007. Edited by R. Vergnieux and C. Delevoie. Bordeaux, France: Editions Ausonius.

Thorpe, C., M. Hebert, T. Kanade, S. Shafer and the Strategic Computing Vision Lab. 1987. Vision and navigation for the Carnegie-Mellon NavLab. *Annual Review of Computer Science* 2: 521–556.

Tompkinson, W. 2017. SPAR 2017 Preview: A New Kind of Low-Cost Reality Capture. <https://www.spar3d.com/blogs/measuring-the-value/spar-2017-preview-new-kind-low-cost-reality-capture/> Accessed 20 February 2020.

Topcon Acquires Voxis, Inc., Scanner Technology Leader. 2008. <http://www.businesswire.com/news/home/20080829005621/en/Topcon-Acquires-Voxis-Scanner-Technology-Leader> Accessed 27 February 2014.

Trimble Navigation Acquires Mensi S.A. n.d. <https://mergr.com/trimble-navigation-acquires-mensi-s.a> Accessed 20 February 2020.

Trimble RealWorks. n.d. <https://geospatial.trimble.com/products-and-solutions/trimble-realworks> Accessed 20 February 2020.

Tripp J, Ulitsky A, Pashin S, Mak N, Hahn J (2003) Development of a compact, high-resolution 3D laser range imaging system. *ProcSPIE Int Soc Opt Eng* 5088:112–122

Ullrich, A., R. Reichert, N. Studnicka and J. Riegl. 1999, May. High-performance 3D-imaging laser sensor. *Proceedings of SPIE 3707*: 658–664.

Ullrich, A. and N. Studnicka. 1999. 3D-Laser-Entfernungsbildaufnahme. Pages 49–56 in *Current Developments of Microelectronics: Proceedings of the Seminar "Aktuelle Entwicklungen der Mikroeletronik,"* held in Bad Hofgastein, Austria, 3–6 March 1999. Edited by K. Riedling. Vienna: Gesellschaft für Mikroelektronik. <http://gme.tuwien.ac.at/hofg99/report.pdf> Accessed 27 February 2014.

Ullrich, A. and M. Pfennigbauer. 2011. Echo digitization and waveform analysis in airborne and terrestrial laser scanning. Pages 217–228 in *Photogrammetric Week '11*, held in Stuttgart, Germany, 5–9 September 2011. Edited by D. Fritsch. Berlin: Wichmann/VDE. <https://phowo.ifp.uni-stuttgart.de/publications/phowo11/220Ullrich.pdf> Accessed 20 February 2020.

Van Genechten, B., Quintero, M.S., De Bruyne, M., Poelman, R., Hankar, M., Barnes, S., Caner, H., Budei, L., Heine, E., Reiner, H., García, J.L.L. and Taronger, J. M. B. 2008. 3D RiskMapping. *Theory and practice on Terrestrial Laser Scanning: Training material based on practical applications*. URL: http://jllerma.webs.upv.es/pdfs/Leonardo_Tutorial_Final_vers5_ENGLISH.pdf (last date accessed April 2nd 2020)

Vance, A. 2010. With Kinect, Microsoft Aims for a Game Changer. *New York Times*. <https://www.nytimes.com/2010/10/24/business/24kinect.html> Accessed 20 February 2020.

Velodyne Lidar. 2017. It Began With a Race…16 Years of Velodyne LiDAR. <https://velodynelidar.com/blog/it-began-with-a-race16-years-of-velodyne-lidar/> Accessed 08 April 2018.

Velodyne Lidar Introduces Velabit. 2020. <https://velodynelidar.com/press-release/velodyne-lidar-introduces-velabit/> Accessed 05 April 2020.

Vergnieux, R. and C. Delevoie, eds. 2007. *Actes du colloque Virtual Retrospect 2007*, held in Pessac, France, 14–16 November 2007. Bordeaux, France: Editions Ausonius.

Waldron, K. J. and R. McGhee. 1986. The Adaptive Suspension Vehicle. *IEEE Control Systems Magazine* 6 (6):7–12.

Walsh, G. C. 2010. Retro detector system.US Patent 7,649,617.

Walsh, G., D. Tilbury, S. Sastry, R. Murray and J. P. Laumond. 1994. Stabilization of trajectories for systems with nonholonomic constraints. *IEEE Transactions on Automatic Control* 39 (1):216–222.

Wan Aziz, W. A., M. Z. Syahmi, A. Anuar and N. T. Khairul. 2012. Terrain slope analyses between terrestrial laser scanner and airborne laser scanning. Pages 242–247 in *2012 IEEE Control and System Graduate Research Colloquium*, held in Shah Alam, Malaysia, 16–17 July 2012. Piscataway, N.J.: Institute of Electrical and Electronics Engineers.

Watkin, H. 2018. Open Heritage Project by CyArk and Google Helps Preserve Monuments in 3D. <https://all3dp.com/open-heritage-project-cyark-google-helps-preserve-monuments-3d/> Accessed 09 September 2019.

Wiggers, K.2020. Amazon acquires autonomous vehicle startup Zoox. https://venturebeat.com/2020/06/26/amazon-acquires-autonomous-vehicle-startup-zoox/ Accessed 04 July 2020.

Wilder, C. 1991. Digitizing enters third dimension: Using a digitizer and a PC, 3-D models are being created for various applications. *Computerworld* 25 (35):14.

Wilson, K., C. Smith, D. Neagley, B. Kacyra, J. Dimsdale and J. J. Zayhowski. 1999. Cyrax: A portable three-dimensional laser-mapping and imaging system. In *1997–1998 Physics Division Progress Report*, Los Alamos National Laboratory Report LA-13606-PR.

Wujanz, D., M. Burger, M. Mettenleiter and F. Neitzel. 2017. An intensity-based stochastic model for terrestrial laser scanners. *ISPRS Journal of Photogrammetry and Remote Sensing* 125: 146–155.

Zayhowski, J. J. 2010. Passively Q-switched microchip lasers and applications. *The Review of Laser Engineering* 26 (12):841–846.

Zayhowski, J. J. 2018. Microchip lasers. In *Encyclopedia of Modern Optics*, 2nd ed., edited by R. Guenther and D. Steel, vol. 2, 415–423. Amsterdam: Elsevier.

Z+F LaserControl. n.d. <https://www.zf-laser.com/Z-F-LaserControl-R.laserscanner_software_1.0.html?&L=1> Accessed 20 February 2020.

WHO'S WHO IN ASPRS

BOARD OF DIRECTORS

BOARD OFFICERS

President
Jeff Lovin
Woolpert

President-Elect
Jason M. Stoker, Ph.D
U.S. Geological Survey

Vice President
Christopher Parrish, Ph.D
Oregon State University

Past President
Thomas Jordan, Ph.D.
University of Georgia

Treasurer
Stewart Walker, Ph.D.

Secretary
Lorraine B. Amenda, PLS, CP

BOARD MEMBERS

Sustaining Members Council – 2021
Chair: Joe Cantz
www.asprs.org/About-Us/Sustaining-Members-Council.html

Early-Career Professionals Council – 2021
Chair: Bobby Arlen
Vice Chair: Melissa Martin

Region Officers Council – 2021
Chair: Lorraine B. Amenda, PLS, CP
Vice Chair: Demetrio Zourarakas

Student Advisory Council – 2021
Chair: Youssef Kaddoura
http://www.asprs.org/Students/Student-Advisory-Council.html

Technical Division Directors Council – 2021
Chair: Bandana Kar, Ph.D
Vice Chair: Denise G. Theunissen

TECHNICAL DIVISION OFFICERS

Geographic Information Systems Division – 2021
Director: Xan Fredericks
Assistant Director: Denise G. Theunissen
www.asprs.org/Divisions/GIS-Division.html

Lidar Division – 2022
Director: Joshua Nimetz, CMS
Assistant Director: Ajit Sampath
www.asprs.org/Divisions/Lidar-Division.html

Photogrammetric Applications Division – 2022
Director: Kurt Rogers
Assistant Director: Benjamin Wilkinson
www.asprs.org/Divisions/Photogrammetric-Applications-Division.html

Primary Data Acquisition Division – 2021
Director: Jon Christopherson
Assistant Director: J. Chris Ogier
www.asprs.org/Divisions/Primary-Data-Aquisition-Division.html

Professional Practice Division – 2022
Director: Harold W. Rempel, III, CP
Assistant Director: Bill Swope
www.asprs.org/Divisions/Professional-Practice-Division.html

Remote Sensing Applications Division – 2022
Director: Raechel A. Portelli, Ph.D.
Assistant Director: Amr Abd-Elrahman
www.asprs.org/Divisions/Remote-Sensing-Applications-Division.html

Unmanned Autonomous Systems (UAS) – 2022
Director: Megan Ritelli, Ph.D.
Assistant Director: Dan Hubert

REGION PRESIDENTS

Alaska Region
David Parret
http://www.asprsalaska.org/

Cascadia Region
Robert Hairston-Porter

Eastern Great Lakes Region
Shawana P. Johnson, Ph.D, GISP
http://egl.asprs.org/

Florida Region
Xan Fredericks
http://florida.asprs.org/

Heartland Region
Whit Lynn
http://heartland.asprs.org/

Mid-South Region
https://www.asprs.org/all-regions/mid-south.html

Northeast Region
(representing the merger of The New England and Central New York Regions)
Trevis Gigliotti, Interim President

North Atlantic Region
Richard W. Carlson, Jr., P.L.S., C.P.
http://natlantic.asprs.org/

Pacific Southwest Region
Omar G. Mora
https://pswasprs.org/

Potomac Region
Dave Lasko
http://www.asprspotomac.org/

Rocky Mountain Region
http://www.asprs-rmr.org/

Western Great Lakes Region
Brandon Krumwiede
http://wgl.asprs.org/

Study on Global Burned Forest Areas Based on Landsat Data

Zhaoming Zhang, Tengfei Long, Guojin He, Mingyue Wei, Chao Tang, Wei Wang, Guizhou Wang, Wenqing She, and Xiaomei Zhang

Abstract

Forests are an extremely valuable natural resource for human development. Satellite remote sensing technology has been widely used in global and regional forest monitoring and management. Accurate data on forest degradation and disturbances due to forest fire is important to understand forest ecosystem health and forest cover conditions. For a long time, satellite-based global burned area products were only available at coarse native spatial resolution, which was difficult for detecting small and highly fragmented fires. In order to analyze global burned forest areas at finer spatial resolution, in this study a novel, multi-year 30 meter resolution global burned forest area product was generated and released based on Landsat time series data. Statistics indicate that in 2000, 2005, 2010, 2015, and 2018 the total area of burned forest land in the world was 94.14 million hm², 96.65 million hm², 59.52 million hm², 76.42 million hm², and 83.70 million hm², respectively, with an average value of 82.09 million hm². Spatial distribution patterns of global burned forest areas were investigated across different continents and climatic domains. It was found that burned forest areas were mainly distributed in Africa and Oceania, which accounted for approximately 73.85% and 6.81% of the globe, respectively. By climatic domain, the largest burned forest areas occurred in the tropics, with proportions between 88.44% and 95.05% of the world's total during the study period. Multi-year dynamic analysis shows the global burned forest areas varied considerably due to global climate anomalies, e.g., the La Niña phenomenon.

Introduction

Forests are very important for human beings. Forest monitoring and management are of great significance for the implementation of the United Nations 2030 Agenda for Sustainable Development. As a common disturbance in many forest systems in the world, forest fires have significant impact on both forest cover and forest productivity. Satellite remote sensing technology can provide valuable information on burned land. In the past decade, several remote sensing-based global burned area (BA) products were released, including Global Burned Area 2000 (GBA2000) (Tansey *et al.* 2004), GLOBSCAR (Simon *et al.* 2004), L3JRC (Tansey *et al.* 2008), GlobCarbon (Plummer *et al.* 2006), Fire_CCI41(Chuvieco *et al.* 2016), Fire_CCI51 (Chuvieco *et al.* 2018), Global Fire Emissions Database (GFED) 4 (Giglio, Randerson, Werf 2013), GFED4s (Van der Werf *et al.* 2017), MCD45 (Roy *et al.* 2005), and MCD64 (Giglio *et al.* 2018). These BA products were used in a variety of fields, such as forest disturbance study (Lierop *et al.* 2015), biomass burning emissions estimate (Randerson *et al.* 2012), and fire hazard assessment (Mouillot *et al.* 2014). However, a major limitation of the aforementioned global BA products is their relatively coarse native spatial resolution, which ranged from 250 m (FireCCI51) to 0.25 degrees (GFED4). BA with such resolution is generally not adequate for resolving small and highly fragmented fires (Chuvieco *et al.* 2019). To resolve this problem, a novel Global Annual Burned Area Mapping (GABAM) product was proposed based on Landsat time series data (Long *et al.* 2019). GABAM is the highest spatial resolution (30 m) global BA product to date and the GABAM product of 2015 was publicly released and can be freely accessed (https://vapd.gitlab.io/post/gabam2015/). Up to now, research associated with the GABAM product were scarcely reported. In order to explore applications of the new GABAM product, in this paper a study on 30 m resolution global burned forest areas was performed based on the GABAM algorithm and Landsat time series data. For this purpose, first 30 m global burned forest area products in the years of 2000, 2005, 2010, 2015, and 2018 were generated and released; based on these products, spatial distribution patterns of burned forest areas were investigated across different continents and climatic domains, then temporal variation characteristics of global burned forest areas among the five years were analyzed by statistics data, and finally some conclusions were made.

Methodology

GABAM products were produced using dense time series Landsat land surface reflectance (SR) and the Google Earth Engine platform. The Landsat data have been geometrically rectified with less than 12 m root-mean-square error and atmospherically corrected, including a quality assessment mask (cloud, shadow, water, snow, and saturation). After masking pixels of low quality, two years of cloud-free Landsat SR time series were used to compute several BA sensitive features, including Normalized Burned Ratio, Normalized Burned Ratio 2, the Burned Area Index, the Mid-InfraRed Burn Index, etc. Based on high quality global BA and no BA samples, a machine learning algorithm (random forest) and these sensitive features were employed in model training and per-pixel burned probability calculation. Annual MODIS Vegetation Continuous Fields 250 m Collection 5.1 (MOD44B) products of the current and previous year, which contain the tree-cover percent layer and nontree vegetation layer, were utilized to determine whether the pixel was dominated

Zhaoming Zhang, Tengfei Long, Guojin He, Mingyue Wei, Chao Tang, Wei Wang, Guizhou Wang, Wenqing She, and Xiaomei Zhang are with the Aerospace Information Research Institute, Chinese Academy of Sciences, Beijing 100094, China (longtf@radi.ac.cn, hegj@radi.ac.cn).

Zhaoming Zhang, Tengfei Long, Guojin He, Wei Wang, Guizhou Wang, and Xiaomei Zhang are with the Key Laboratory of Earth Observation Hainan Province, Sanya 572029, Hainan, China.

Zhaoming Zhang, Tengfei Long, Guojin He, Wei Wang, Guizhou Wang, and Xiaomei Zhang are with the Sanya Institute of Remote Sensing, Sanya 572029, Hainan, China.

Mingyue Wei, Chao Tang, and Wenqing She are with the University of Chinese Academy of Sciences, Beijing 100049, China.

Photogrammetric Engineering & Remote Sensing
Vol. 86, No. 8, August 2020, pp. 503–508.
0099-1112/20/503–508

doi: 10.14358/PERS.86.8.503

by trees or by herbaceous vegetation. Together with the tree domination, spectral indices statistics of two years, and the burned probability, some logical filters were used for candidate BA seeds selection, then a region growing algorithm was utilized to map the global BA distribution. More details about the GABAM algorithm can be found in the work of Long *et al.* (2019).

The GABAM product includes forest, grassland, and cropland burned areas. In order to obtain burned forest areas, the GABAM burned area was spatially intersected with the 30 meter resolution global forest cover map, which was also developed using Landsat satellite data (Zhang *et al.* 2020). The workflow for burned forest area mapping is shown in Figure 1.

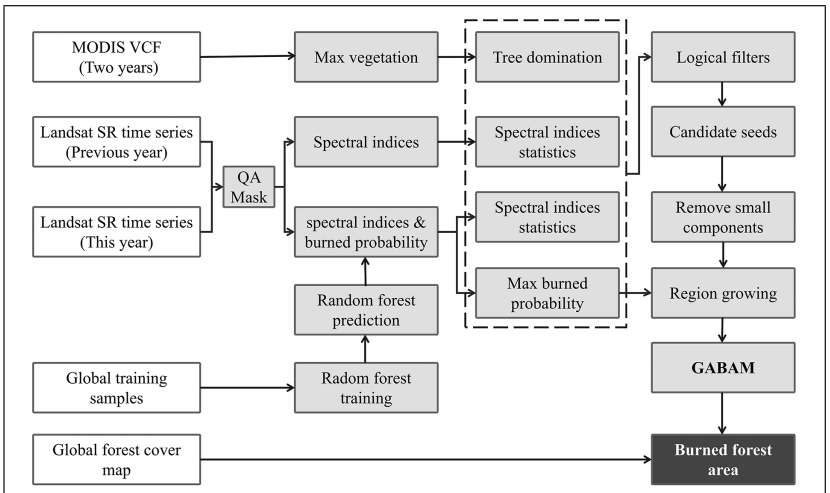

Figure 1. Workflow for burned forest area mapping.

All the obtained 30 m global burned areas and global burned forest area products in 2000, 2005, 2010, 2015, and 2018 can be freely downloaded from the website: https://vapd.gitlab.io/post/gabam. These products were projected in geographic (Lat./Long.) projection at 0.00025 degrees (approximately 30 m) resolution, with the WGS84 horizontal datum and the EGM96 vertical datum. The global products were divided into 10 × 10 degree tiles ranging from 180 W–180 E and 80 N–60 S.

Results and Analysis

Spatial Distribution Analysis of Burned Forest Areas

Statistics indicate that in 2000, 2005, 2010, 2015, and 2018 the total area of burned forest land in the world was 94.14 million hm², 96.65 million hm², 59.52 million hm², 76.42 million hm², and 83.70 million hm², respectively, with an average value of 82.09 million hm² (Table 1). The spatial distribution of global burned forest areas in the five years were demonstrated in Figures 2–6. In order to better display the spatial distribution of global burned forest areas, in Figures 2–6 burned density, i.e., percentage of burned pixels in each 0.25 degrees × 0.25 degree grid was used instead of directly drawing the burned pixels on a global map. We can see from Figures 2–6 that on the global scale, the spatial distribution of burned forest areas was rather scattered. The relatively concentrated areas of forest fires were mainly in central and southern Africa, northern Australia, and central South America. Most of the aforementioned areas are located near the equator, with high temperature and sufficient fuel, and fires are prone to occur in dry seasons. On the contrary, these regions had very sparse burned forest areas, like very humid regions (e.g., interior Amazon rainforest), very cold regions (e.g., Tibet plateau), or areas with strict fire management (e.g., national forest park or city forest).

Statistics of burned forest areas in each continent are shown in Table 1. It can be seen from Table 1 that Africa had the largest burned forest area. In 2000, 2005, 2010, 2015, and 2018, burned forestland in Africa was 69.28 million hm², 72.71 million hm², 36.22 million hm², 62.51 million hm², and 65.12 million hm², respectively, accounting for 73.59%, 75.23%, 60.85%, 81.79%, and 77.80% of the world's total, with a five-year average of 73.85%. Followed by Oceania, the Oceanian burned forest area in the five years was 7.52 million hm², 7.95 million hm², 3.12 million hm², 4.40 million hm², and 5.37 million hm², respectively, which accounted for 7.99%, 8.22%, 5.24%, 5.76%, and 6.42% of the world. By detailed analysis, it was observed that the spatial distribution of burned forest areas was in close agreement with ecosystems that experience large and frequent fires, including savannas across southern Africa and northern Australia.

In this study, climatic domains were delineated into four global ecological zones including tropical, subtropical, temperate, and boreal (FAO 2012; MacDicken 2015). As shown in Table 2, the distribution of burned forest areas exhibited obvious differences in different climatic domains. The largest area of burned forest was in the tropics, where more than 56.36 million hm² of forest burned annually, with proportions between 88.44% (2018) and 95.05% (2015) of the global burned forest area. Subtropical was next; the subtropical burned forest area over five years was 3.57 million hm², 3.10 million hm², 1.99 million hm², 1.25 million hm², and 1.91 million hm², accounting for 3.79%, 3.21%, 3.34%, 1.63%, and 2.28% of the world, respectively. Results from the Global Forest Resources Assessment 2015 (FAO 2015) of the Food and Agriculture Organization of the United Nations indicated that 44% of global forest area was in tropical and 8% was in subtropical climatic domains (Keenan *et al.* 2015). Tropical and subtropical areas have lush vegetation, sufficient fuels, and high temperature all the year round, resulting in the vast majority of forest burning areas in the world. Although temperate climatic domain accounted for 26% of global forest areas and boreal for 22% (Keenan *et al.* 2015), burned forest areas in these two climatic domains were relatively small. During the study period, burned forest areas in temperate climates accounted for 3.36%, 2.06%, 1.39%, 1.53%, and 2.52% of the world's total, and proportions for the boreal domain were only 0.95%, 0.60%, 0.56%, 1.79%, and 6.76%, respectively. It should be mentioned that the burned forest areas in boreal

Table 1. Statistics of burned forest areas of each continent (1000 hm²).

Year	Africa	Asia	Oceania	Europe	North America	South America	Total
2000	69 276.47	6146.47	7524.51	2906.94	2224.22	6065.62	94 144.24
2005	72 705.47	5993.69	7951.28	1635.02	2082.49	6279.83	96 647.76
2010	36 216.33	6549.10	3121.43	396.18	645.71	12 588.39	59 517.14
2015	62 508.63	3822.58	4401.72	333.80	1464.19	3892.21	76 423.14
2018	65 120.21	7959.31	5371.17	249.31	2603.99	2399.92	83 703.90

Table 2. Statistics of burned forest area in different climatic domains (1000 hm²).

Year	Boreal area	Temperate area	Subtropical area	Tropical area	Total
2000	895.76	3161.62	3565.81	86 557.05	94 144.24
2005	576.03	1986.66	3099.77	90 985.29	96 647.76
2010	335.54	830.21	1987.77	56 363.62	59 517.14
2015	1368.75	1167.86	1248.53	72 638.00	76 423.14
2018	5657.63	2107.30	1908.12	74 030.84	83 703.90

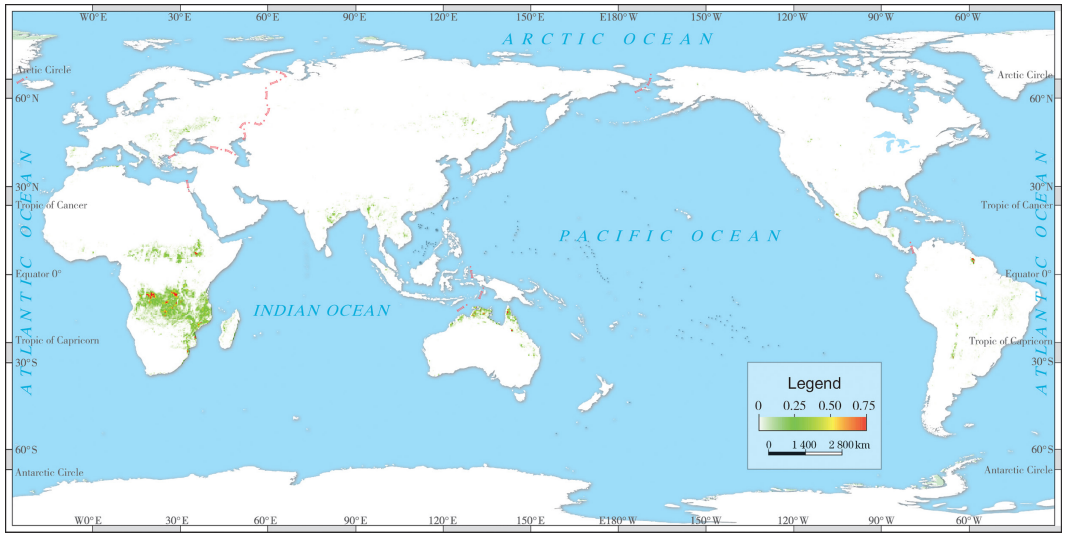

Figure 2. Spatial distribution of global burned forest area in 2000.

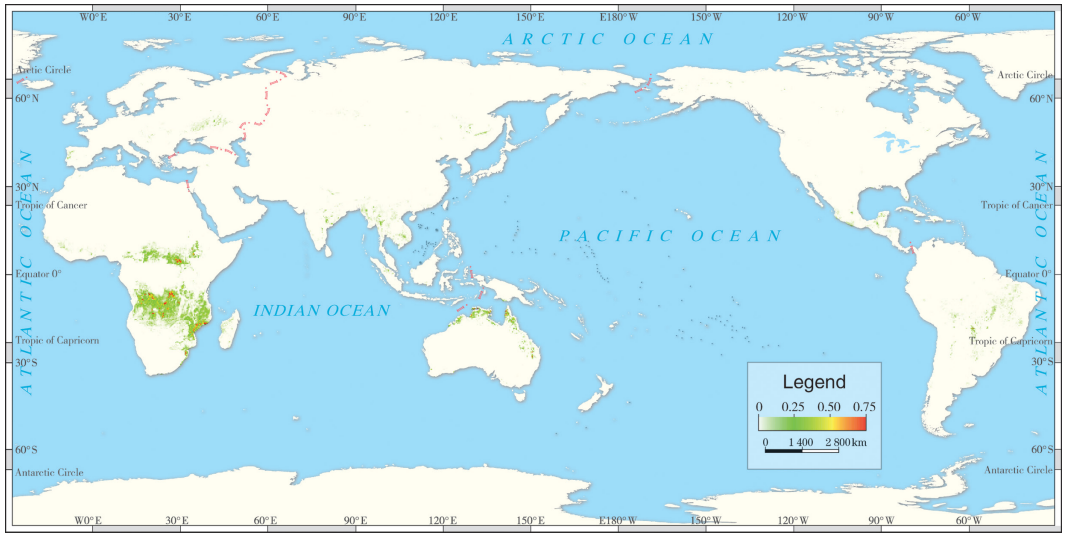

Figure 3. Spatial distribution of global burned forest area in 2005.

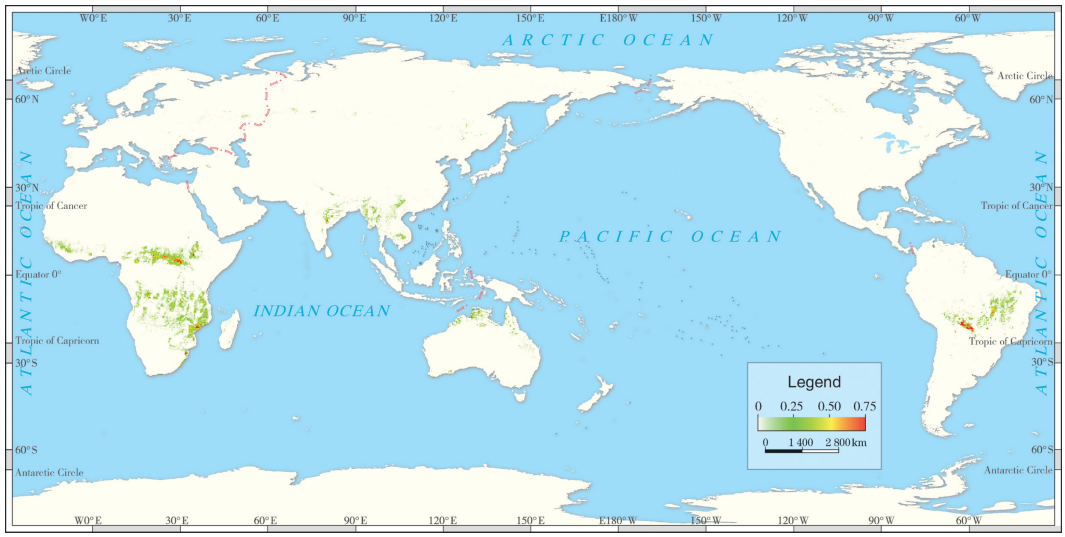

Figure 4. Spatial distribution of global burned forest area in 2010.

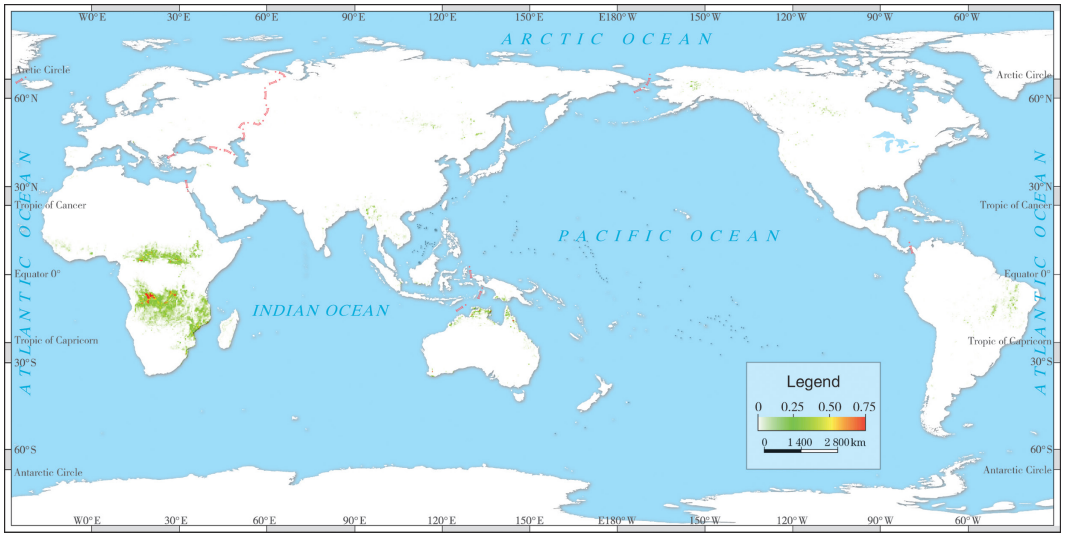

Figure 5. Spatial distribution of global burned forest area in 2015.

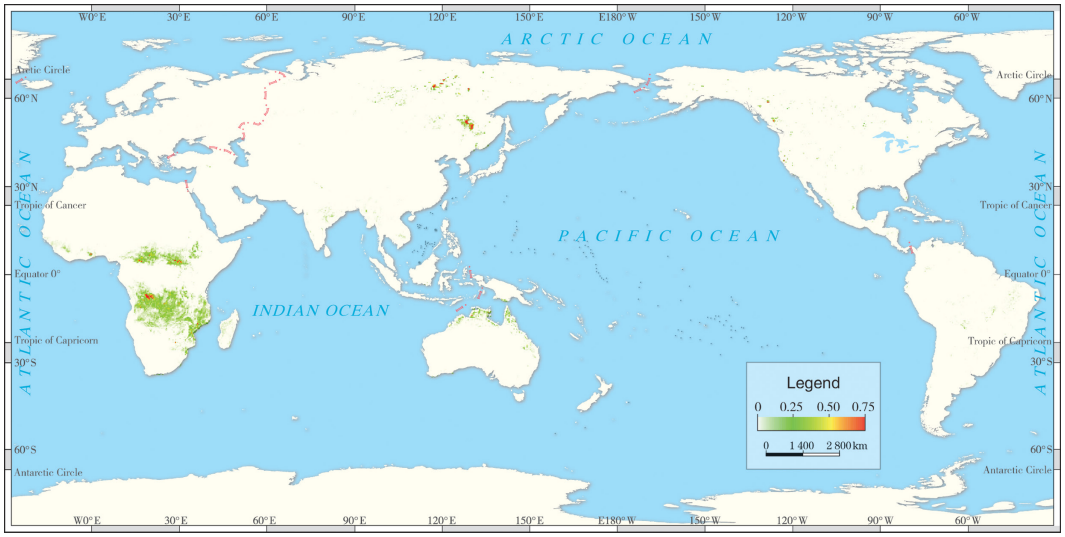

Figure 6. Spatial distribution of global burned forest area in 2018.

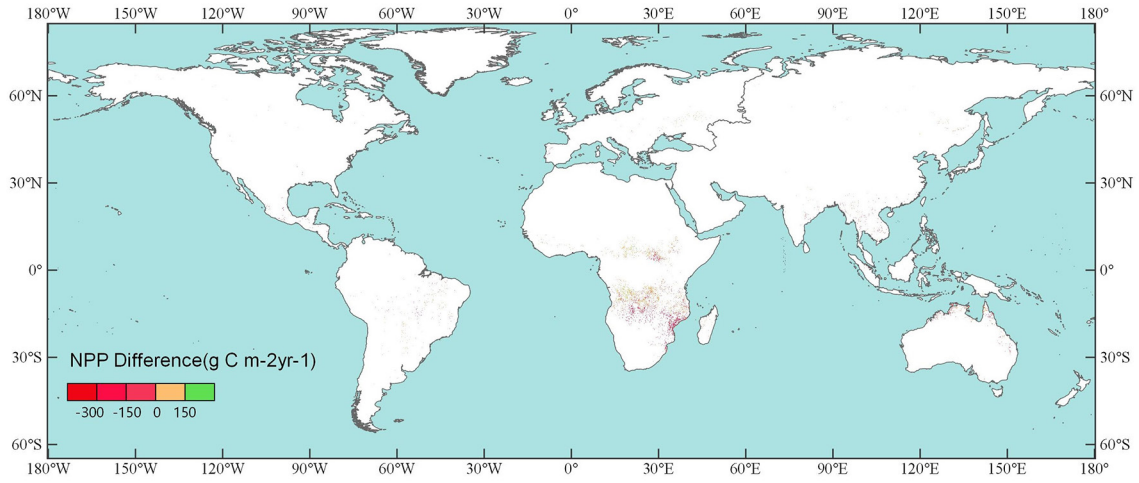

Figure 8. NPP difference between 2005 and 2004 in the burned forest area of 2005.

climates in 2018 was abnormally large (5.66 million hm²) (see Table 2) mainly due to the large forest fires in the Far East of Russia and Northeast China (the red areas in Figure 6).

Burned Forest Area Changes Among Different Years

The global burned forest areas varied considerably from year to year (Figure 7). As shown in Table 1, the global burned forest area was largest in 2005 (about 96.65 million hm²) and smallest in 2010 (about 59.52 million hm²). The difference between them was 37.13 million hm², a decrease of 38.42%. Interannual changes of global burned forest areas may be caused by multiple factors, including El Niño–Southern Oscillation and other climate modes. Influenced by the strong La Niña phenomenon in 2010, rainfall in central and southern Africa, Southeast Asia, Eastern Australia, Central, and Southeastern Europe increased abnormally. Increased precipitation led to high moisture content of inflammable materials and reduced risk of wildfires. Central and southern Africa were the most concentrated areas of forest fire in the world. The increase in rainfall led to a significant reduction of forest fires in central and southern Africa in 2010, resulting in a sharp decline of global burned forest area in 2010. Also affected by the strong La Niña phenomenon in 2010, South America suffered from a large area of severe drought, with forest fires occurring frequently, and the burned forest area more than doubled compared with the other four years (Table 1).

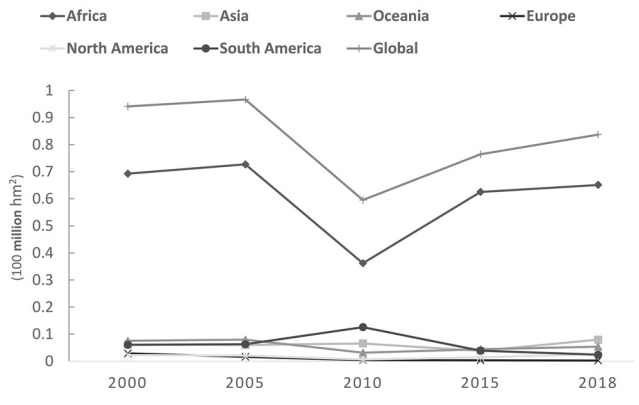

Figure 7. Interannual changes of burned forest areas on each continent and the globe.

It can be seen from Figure 7 that the interannual change characteristics of African burned forest areas were highly consistent with that of the global areas. Since the burned forest area in Africa accounted for more than 60% of the world, the interannual change of African burned forest areas largely determined that of the global areas. As explained above, we can see an evident peak in burned forest areas in South America in 2010.

Analysis of the Impact of Fire on Forest Net Primary Production (NPP)

In order to analyze the effect of fire on the production activity or growth of forests, as an example, MODIS Net Primary Production (NPP) products (MOD17A3H Version 6) (Running, Mu, Zhao 2019) of 2005 and 2004 were employed to detect the forest NPP changes caused by forest fire in 2005. The MOD17A3H Version 6 product provides information about annual NPP at 500 meter pixel resolution. The NPP difference between 2005 and 2004 was computed, then the resampled and reprojected NPP difference map was spatially intersected with the global burned forest area map of 2005. As demonstrated in Figure 8, fire exerted serious influences on forest NPP. Statistics show NPP declined in 91.90% of the burned forest area in 2005; while NPP in the remaining areas remained unchanged or increased slightly, which may be due to the difference in spatial resolution of the MOD17A3H (500 m) and GABAM (30 m) products or the rapid recovery of vegetation in tropical or subtropical areas.

Discussion

In this study, novel multiyear 30 meter resolution global burned forest area products were generated and released using Landsat time series data. Based on these products, spatial distribution patterns of global burned forest areas were investigated across different continents and climatic domains. Multiyear global burned forest area dynamics were also studied, and reasons for burned forest area changes among different years were analyzed. Although this study obtained some useful conclusions, there are several limitations to be improved in the future.

First, the GABAM product only uses Landsat time series data; the quality of the GABAM products may be affected by clouds due to the relatively low revisit frequency of the Landsat observation, and cloud detection is important (Shao *et al.* 2017a; Shao *et al.* 2019b). One solution to resolve this problem is to use multisource satellite images, such as the fusion of Landsat-8 and Sentinel-2 images (Shao and Cai 2018; Shao *et al.* 2019a). A recent study in southern Africa show that burned areas can be obtained with a higher accuracy when both the Landsat-8 and Sentinel-2 sensors are used than the single Sentinel-2 or Landsat sensor (Roy *et al.* 2019). In addition to using optical satellite sensors, burned areas can also be generated by taking advantage of integrating different earth observation techniques to strengthen the discrimination of burned pixels and reduce both omission and commission errors. Integrated analysis of lidar and passive optical sensors have been performed for BA mapping (Goetz *et al.* 2010; Sankey *et al.* 2017). Other earth observation techniques, such as radar (Imperatore *et al.* 2017; Lohberger et al.2018) and Unmanned Aerial Vehicles (Sankey *et al.* 2017; Sudhakar *et al.* 2020) also proved to be useful in BA detection.

The GABAM product can effectively depict the spatial-temporal patterns of fire-affected forest areas. In the section "Analysis of the Impact of Fire on Forest Net Primary Production (NPP)", it was found that the NPP in burned forest areas were seriously influenced. A better evaluation of the impact of fire on forest ecosystems would require pre- and postfire forest biomass. With pre- and postfire biomass values, it is possible to estimate the biomass loss caused by forest fire. Fortunately, remote sensing-based forest aboveground biomass estimation technology has made substantial progress over the past ten years (Shao and Zhang 2016; Shao, Zhang, Wang 2017b; Zhang *et al.* 2019; Wallis *et al.* 2019), which provides a bright future to analyze the fire effects on global forest conditions.

Conclusions

In this study, 30 meter resolution global burned forest area products were generated and released using Landsat time series data. Spatial distribution patterns of global forest fire activities were examined based on these products. It was found that burned forest areas varied obviously across different continents and climatic domains. In the years of 2000, 2005, 2010, 2015, and 2018, the global burned forest area was 94.14 million hm², 96.65 million hm², 59.52 million hm², 76.42 million hm², and 83.70 million hm², respectively, and the average value was 82.09 million hm², of which approximately 74.51% and 92.72% occurred in Africa and the tropical climatic domain. As indicated by the multiyear data products, global burned forest areas changed significantly from year to year in response to climate patterns, e.g., the La Niña phenomenon.

Acknowledgments

This research was funded by the National Key Research and Development Program of China (grant numbers 2016YFA0600302, 2016YFB0501502), the National Natural Science Foundation of China (grant number 61731022), and the Strategic Priority Research Program of the Chinese Academy of Sciences (grant number XDA19090300).

References

Chuvieco, E., C. Yue, A. Heil, F. Mouillot, I. Alonso-Canas, M. Padilla, J. M. Pereira, D. Oom and K. Tansey. 2016. A new global burned area product for climate assessment of fire impacts. *Global Ecology and Biogeography* 25:619–629.

Chuvieco, E., J. Lizundia-Loiola, M. L. Pettinari, R. Ramo, M. Padilla, K. Tansey, F. Mouillot, P. Laurent, T. Storm, A. Heil and S. Plummer. 2018. Generation and analysis of a new global burned area product based on MODIS 250 m reflectance bands and thermal anomalies. *Earth System Science Data* 10:2015–2031.

Chuvieco, E., F. Mouillot, G. R. Van der Werf, J. San Miguel, M. Tanase, N. Koutsias, M. García, M. Yebra, M. Padilla, I. Gitas, A. Heil, T. J. Hawbaker and L. Giglio. 2019. Historical background and current developments for mapping burned area from satellite Earth observation. *Remote Sensing of Environment* 225:45–64.

FAO (Food and Agriculture Organization of the United Nations). 2012. *Global Ecological Zones for* FAO *Forest Reporting: 2010 Update. Forest Resources Assessment Working Paper 179*. Rome, Italy: FAO. <www.fao.org/docrep/017/ap861e/ap861e00.pdf>. Accessed day Month year.

FRAAO. 2015. *Global Forest Resources aAssessment 2015 Desk Reference*. Rome, Italy: FAO. <http://www.fao.org/3/a-i4808e.pdf> Accessed day Month year

Giglio, L., J. T. Randerson and G. R. Werf. 2013. Analysis of daily, monthly, and annual burned area using the fourth generation global fire emissions database (GFED4). *Journal of Geophysical Research: Biogeosciences* 118:317–328.

Giglio, L., L. Boschetti, D. P. Roy, M. L. Humber and C. O. Justice. 2018. The collection 6 MODIS burned area mapping algorithm and product. *Remote Sensing of Environment* 217: 72–85.

Goetz, S. J., M. Sun, A. Baccini and P. S. Beck. 2010. Synergistic use of spaceborne lidar and optical imagery for assessing forest disturbance: An Alaska case study. *Journal of Geophysical Research: Biogeosciences* 115.

Hansen, M. C., R. S. DeFries, J.R.G. Townshend, M. Carroll, C. Dimiceli and R. A. Sohlberg. 2003. Global percent tree cover at a spatial resolution of 500 meters: First results of the MODIS vegetation continuous fields algorithm. *Earth Interact* 7:1–15.

Imperatore, P., R. Azar, D. S. Fabiana Cal'o, P. A. Brivio, R. Lanari and A. Pepe. 2017. Effect of the vegetation fire on backscattering: an investigation based on Sentinel-1 observations. *IEEE Journal of Selected Topics in Applied Earth Observations and Remote Sensing* 10:4478–4492.

Keenan, R. J., G. A. Reams, F. Achard and J. V. de Freitas. 2015. Dynamics of global forest area: Results from the FAO global forest resources assessment 2015. *Forest Ecology and Management* 352:9–20.

Lierop, P., E. Lindquist, S. Sathyapala and G. Franceschini. 2015. Global forest area disturbance from fire, insect pests, diseases and severe weather events. *Forest Ecology and Management* 352:78–88.

Lohberger, S., M. Stangel, E. C. Atwood and F. Siegert. 2018. Spatial evaluation of Indonesia's 2015 fire-affected area and estimated carbon emissions using Sentinel-1. *Global Change Biology* 24:644–654.

Long, T. F., Z. M. Zhang, G. J. He, W. Jiao, C. Tang, B. Wu, X. Zhang, G. Wang and R. Yin. 2019. 30 m resolution global annual burned area mapping based on Landsat images and Google Earth engine. *Remote Sensing* 11:489–519.

MacDicken, K. G. 2015. Global Forest Resources assessment 2015: What, why and how? *Forest Ecology and Management* 352:3–8.

Mouillot, F., M. G. Schultz, C. Yue, P. Cadule, K. Tansey, P. Ciais and E. Chuvieco. 2014. Ten years of global burned area products from spaceborne remote sensing—A review: Analysis of user needs and recommendations for future developments. *International Journal of Applied Earth Observation and Geoinformation* 26:64–79.

Roy, D. P., H. Y. Huang, L. Boschetti, L. Giglio, L. Yan, H. H. Zhang and Z. Lia. 2019. Landsat-8 and Sentinel-2 burned area mapping—A combined sensor multi-temporal change detection approach. *Remote Sensing of Environment* 231:111254.

Running, S., Q. Mu and M. Zhao. 2019. MOD17A3HGF MODIS/Terra net primary production yearly gap-filled L4 Global 500 m SIN Grid v006 [data set]. NASA EOSDIS Land Processes Distributed Active Archive Center. <https://doi.org/10.5067/MODIS/MOD17A3HGF.006> Accessed 6 May 2020.

Sankey, T., J. Donager, J. McVay and J. Sankey. 2017. UAV lidar and hyperspectral fusion for forest monitoring in the southwestern USA. *Remote Sensing of Environment* 195:30–43.

Shao, Z. F. and J. J. Cai. 2018. Remote sensing image fusion with deep convolutional neural network. *IEEE Journal of Selected Topics in Applied Earth Observations and Remote Sensing* 11 (5):1656–1669.

Shao, Z. F., J. J. Cai, P. Fu, L. Q. Hu and T. Liu. 2019a. Deep learning-based fusion of Landsat-8 and Sentinel-2 images for a harmonized surface reflectance product. *Remote Sensing of Environment* 235:111425.

Shao, Z. F., J. Deng, L. Wang, Y. W. Fan, N. Sumari and Q. M. Cheng. 2017a. Fuzzy Autoencode based cloud detection for remote sensing imagery. *Remote Sensing* 9:311.

Shao, Z. F., Y. Pan, C. Y. Diao and J. J. Cai. 2019b. Cloud detection in remote sensing images based on multiscale features-convolutional neural network. *IEEE Transactions on Geoscience and Remote Sensing* 57 (6):4062–4076.

Shao, Z. F. and L. J. Zhang. 2016. Estimating forest aboveground biomass by combining optical and SAR data: A case study in Genhe, Inner Mongolia, China. *Sensors* 16 (6):834.

Shao, Z. F., L. J. Zhang and L. Wang. 2017b. Stacked sparse Autoencoder modeling using the synergy of airborne LiDAR and satellite optical and SAR data to map forest above-ground biomass. *IEEE Journal of Selected Topics in Applied Earth Observations and Remote Sensing* 10 (12):5569–5582.

Simon, M., S. Plummer, F. Fierens, J. J. Hoelzemann and O. Arino. 2004. Burnt area detection at global scale using ATSR-2: The GLOBSCAR products and their qualification. *Journal of Geophysical Research: Atmospheres* 109 (D14S02):1–16. <https://doi.org/10.1029/2002JD003622>.

Sudhakar, S., V. Vijayakumar, C. Kumar, V. Priya, L. Ravi and V. Subramaniyaswamy. 2020. Unmanned Aerial Vehicle (UAV) based forest fire detection and monitoring for reducing false alarms in forest-fires. *Computer Communications* 149:1–16.

Tansey, K., J. M. Gregoire, D. Stroppiana, A. Sousa, J. Silva, J. M. Pereira, L. Boschetti, M. Maggi, P. A. Brivio, R. Fraser, S. Flasse, D. Ershov, E. Binaghi, D. Graetz and P. Peduzzi. 2004. Vegetation burning in the year 2000: Global burned area estimates from SPOT VEGETATION data. *Journal of Geophysical Research: Atmospheres* 109 (D14S03): 2–22.<https://doi.org/10.1029/2002JD003598>.

Tansey, K., J. M. Gregoire, P. Defourny, R. Leigh, J. F. Peckel, E. V. Bogaert and J. E. Bartholome. 2008. A new, global, multi-annual (2000–2007) burnt area product at 1 km resolution. *Geophysical Research Letters* 35:L01401. <https://doi.org/10.1029/2007GL03156>.

Plummer, S., O. Arino, M. Simon and W. Steffen. 2006. Establishing an Earth observation product service for the terrestrial carbon community: The Globcarbon initiative. *Mitigation and Adaptation Strategies for Global Change* 11:97–111.

Randerson, J. T., Y. Chen, G. R. van der Werf, B. M. Rogers and D. C. Morton. 2012. Global burned area and biomass burning emissions from small fires. *Journal of Geophysical Research* 117:G04012, doi:10.1029/2012JG002128.

Roy, D., Y. Jin, P. Lewis and C. Justice. 2005. Prototyping a global algorithm for systematic fire-affected area mapping using MODIS time-series data. *Remote Sensing of Environment* 97:137–162.

Van der Werf, G. R., J. T. Randerson, L. Giglio, T. T. van Leeuwen, Y. Chen, B. M. Rogers, M. Mu, M.J.E. van Marle, D. C. Morton, G. J. Collatz, R. J. Yokelson and P. S. Kasibhatla. 2017. Global fire emissions estimates during 1997–2016. *Earth System Science Data* 9:697–720.

Wallis, C., J. Homeier, J. Pena, R. Brandl, N. Farwig and J. Bendix. 2019. Modeling tropical montane forest biomass, productivity and canopy traits with multispectral remote sensing data. *Remote Sensing of Environment* 225:77–92.

Zhang, L. J., Z. F. Shao, J. C. Liu and Q. M. Cheng. 2019. Deep learning based retrieval of forest aboveground biomass from combined LiDAR and Landsat 8 data. *Remote Sensing* 11 (12):1459.

Zhang, X. M., T. F. Long, G. J. He, Y. Guo, R. Yin, Z. Zhang, H. Xiao, M. Li and B. Cheng. 2020. Rapid generation of global forest cover map using Landsat based on the forest ecological zones. *Journal of Applied Remote Sensing* 14 (2):022211.

Mapping Understory Invasive Plants in Urban Forests with Spectral and Temporal Unmixing of Landsat Imagery

Kunwar K. Singh and Josh Gray

Abstract

Successful eradication and management of invasive plants require frequent and accurate maps. Detection of invasive plants is difficult at moderate resolution because target species are often located in the forest understory among other vegetation types, and so produce mixed spectral signatures. Spectral unmixing approaches can help to decompose these spectral mixtures; however, they are typically applied to only one or a few images, and thus neglect phenological variability that may improve invasive species discrimination. We compared two approaches to multiple endmember spectral mixture analysis for detecting Ligustrum sinense in the southeastern United States: the use of temporal signatures of endmembers from full and select-date normalized difference vegetation index time series, and conventional spectral unmixing using a single image date. Our results suggest that using temporal signatures from all available imagery may be a good choice, with minimal impact to achievable accuracy, if a priori information on phenological differences between endmembers is unavailable, or imagery for periods of high phenological difference are unavailable.

Introduction

Invasive plants often negatively affect ecological integrity and the delivery of ecosystem services (Ehrenfeld 2010; Liebhold *et al.* 2017) by impacting forest regeneration (Wardle and Peltzer 2017), native species composition (Hejda, Pyšek, and Jarošík 2009), and species richness and abundance (Wilcox and Beck 2007). A variety of invasive plants have invaded vast areas of many forested landscapes worldwide (Bradley, Early, and Sorte 2015). Successful eradication and management of invasive plants requires frequently produced, accurate maps of their geographic distribution (Simberloff *et al.* 2013). Field-based efforts to map invasive plants are time and resource intensive, which limits the frequency and spatial extent at which maps can be produced. Mapping with remotely sensed satellite imagery is the only method capable of producing the data necessary for invasive plants management at the required temporal and spatial scales. However, invasive plants are often located in the forest understory among other plant types, and therefore express mixed spectral signatures that make invasive plants detection and mapping difficult with remotely sensed imagery (Asner and Vitousek 2005). For example, *Ligustrum sinense* (hereinafter *L. sinense*), commonly known as Chinese privet, has spread over one million hectares of forest understory across the southeastern United States (Miller, Chambliss, and Oswalt 2008). Both forest characteristics (e.g., canopy closure, canopy shadow, the density of invasive plants, heterogeneity, and terrain variability) and plant biophysical properties (e.g., height and evergreen versus deciduous leaves) contribute to the mixed spectral signature problem, thus making it harder to track the spread of *L. sinense* at both the desired scale and cost. This requires the development of plant-specific methodologies that rely on remote sensing products (e.g., vegetation indices–VI) and methods (e.g., mixed-pixel classification) that are capable of overcoming these mixed pixel challenges for unmixing understory invasive plant from other native vegetation over large scales.

A few studies have attempted to map the geographic distribution of *L. sinense* across small spatial extents using remotely sensed imagery (Gavier-Pizarro *et al.* 2012; Singh, Davis, and Meentemeyer 2015). Gavier-Pizarro *et al.* (2012) applied a nonparametric, support vector machine (SVM) classifier to monitor the spread of *Ligustrum lucidum* in urban landscapes of Córdoba, Argentina using six summer Landsat images. SVM analysis produced an overall Kappa of 0.88 with very low omission and commission errors. Cash, Anderson, and Marzen (2020) suggested using an adaptive process for developing training polygons, and tested remotely sensed imagery from multiple sources and classification algorithms to achieve better results. Lemke and Brown (2012) developed ensemble models to combine predictions of logistic regression and maximum entropy models developed using Landsat-derived variables to obtain a more robust prediction estimate of three invasive plants, including *L. sinense*. Native vegetation often leaf-out and senesce at different times compared to invasive plants. The results of Singh *et al.* (2018) suggested that multispectral remote sensing data obtained during a period when phenological differences between *L. sinense* and other native forest types are maximized can improve detection and mapping performance. Previous investigations have sought to exploit these periods of phenological difference to map invasive plants using unmixing schemes applied to spectral and/or VI (e.g., normalized difference vegetation index (NDVI), enhanced vegetation index, etc.) time series of brief duration (Singh and Glenn 2009; Somers and Asner 2013). However, the use of more complete temporal VI signatures (i.e., phenological signatures) in unmixing schemes for the detection and mapping of understory invasive plants has received less attention.

Time series VI have allowed for the characterization of plant phenological patterns (e.g., start and end of seasons) and revealed phenological differences among species that have been helpful in distinguishing understory invasive plants (Bradley

Kunwar K. Singh is with Global Research Institute, AidData, The College of William and Mary, 427 Scotland Street, Williamsburg, VA 23185 (ksingh@aiddata.wm.edu, kksingh@wm.edu).

Kunwar K. Singh and Josh Gray are with the Center for Geospatial Analytics and the Department of Forestry & Environmental Resources, North Carolina State University, Raleigh, North Carolina 27695.

Photogrammetric Engineering & Remote Sensing
Vol. 86, No. 8, August 2020, pp. 509–518.
0099-1112/20/509–518

doi: 10.14358/PERS.86.8.509

2014). This has been achieved using various classification algorithms applied to a single image corresponding to the time of maximum phenological difference (Noonan and Chafer 2007), multiple images that capture seasonal variation (Somers and Asner 2013), or multi-temporal image differencing (Wilfong, Gorchov, and Henry 2009). Singh *et al.* (2018) used NDVI time series from Landsat to identify the date of maximum phenological difference between *L. sinense*, deciduous, and evergreen forests, and used that single image date with elevation data (e.g., elevation, slope, soil moisture index, etc.) and the Random Forest algorithm to map *L. sinense* in the North Carolina Piedmont. Given these previous successes in using phenological information to map invasive species, it is reasonable to speculate on whether using fuller temporal information (i.e., full VI time series rather than single dates selected to maximize phenological difference) would further improve the discrimination of *L. sinense.* However, the fact that invasive plants like *L. sinense* typically occur in the forest understory amongst other vegetation types, and thus produce mixed and indistinct spectral signatures, is a substantial challenge to any attempt to map these species with moderate resolution remotely sensed imagery. Spectral mixture analysis (SMA) may offer a productive way to overcome mixed signatures effects.

SMA estimates subpixel fractions of scene components using spectral signatures (i.e., endmembers) derived from homogeneous pixels, field measurements, or reference databases (Roberts *et al.* 1998). SMA models multispectral observations in a single pixel as the fractionally weighted sum of endmembers, and the goal of an SMA analysis is to estimate these endmember fractions (Adams 1993; Roberts, Smith, and Adams 1993; Settle and Drake 1993). The performance of SMA depends on the representativeness of selected spectral endmembers (Roth, Dennison, and Roberts 2012), and the spectral variability of imagery constituents (Roberts *et al.* 1998; Song 2005). However, a conventional SMA fails to account for temporal and spatial variability between and among endmembers (Somers *et al.* 2011). Multiple endmember spectral mixture analysis (MESMA) improves upon the simple SMA approach by allowing for spectral variability in endmembers (Roberts *et al.* 1998; Song 2005). MESMA has been used to map urban impervious surfaces (Fan and Deng 2014), urban vegetation dynamics (Gan *et al.* 2014), wetland vegetation (Michishita *et al.* 2012), drought-induced change in a pinyon-juniper woodland (Brewer *et al.* 2017), vegetation phenology and species type (Dennison and Roberts 2003), and forest burn severity (Quintano *et al.* 2017). The potential of MESMA to map invasive species fractions has also been demonstrated for bamboo (*Dendrocalamus sp.*) and slash pine (*Pinus elliottii*) (Amaral *et al.* 2015), as well as invasive trees in a montane rainforest (Somers and Asner 2013). Multi-temporal information has been shown to improve MESMA results in certain conditions. Somers and Asner (2013) used MESMA to map invasive species in Hawaiian rainforests using six *Hyperion* images that captured seasonal variation and species phenological differences, and demonstrated a clear advantage of multi-temporal MESMA compared to single date imagery. Diao and Wang (2016) performed unmixing of time-series NDVI and spectral signatures drawn from Landsat imagery to monitor the abundance of plant species in spatially heterogeneous landscapes. Studies like these demonstrate that temporal variation can complement spectral information in pixel unmixing schemes, but the more general case of using fully realized temporal, rather than spectral signatures, has received less attention, especially for the case of mapping invasive understory species such as *L. sinense*.

The objective of this study is to compare the performance of MESMA for mapping *L. sinense* using temporal (i.e., NDVI time series) rather than spectral signatures. Specifically, we sought to answer the question: Do phenological endmember signatures from dense NDVI time series improve the mapping of *L. sinense* over traditional, single-date spectral signatures?

Material and Methods

Study Area

We focused on forested landscapes in Mecklenburg County (1415 km^2) in the Piedmont of North Carolina, United States (Figure 1). Forests in this region are a mix of secondary growth oak-hickory-pine forests that have regenerated on former timber plantation sites and abandoned farmlands (Singh *et al.* 2012). The establishment and spread of *L. sinense* in this area is due to a humid subtropical climate, frequent disturbance, and forest fragmentation (Merriam 2003).

L. sinense is an evergreen understory shrub with a height range of 1–5 m (Figure 2), occasionally reaching heights of 10 m (https://plants.usda.gov). It is a prolific seed producer with a high germination rate that tolerates a wide variety of climatic and environmental conditions (e.g., sunlight, moisture, soil quality, etc.), making it an aggressive spreader and amplifying its threat to natural ecosystems (Hanula, Horn, and Taylor 2009). Frequent forest disturbance and fragmentation establishes several pathways in urbanizing forests for the movement of *L. sinense* and provides an appropriate environment for their colonization. Aesthetic use of *L. sinense* in urban areas has also been a primary reason for its spread (Davis *et al.* 2016). The destructive impacts of *L. sinense* on native flora and fauna are pervasive, making it an invasive plant of extreme concern in the southeastern United States (Hanula and Horn 2011; Wilcox and Beck 2007). *L. sinense* has outcompeted small woody species and herbaceous plants in drier conditions along stream and riparian zones in Memphis, Tennessee (Foard *et al.* 2016). It has threatened to displace endangered Miccosukee gooseberry (*Ribes echinellum*) in Florida (Langeland and Burks 1998), and has pushed Schweintz's sunflower (*Helianthus schweinitzii*), an endangered species in the Piedmont of the Carolinas, closer to extinction (Isaac 2001).

Field Measurements

Field observations of *L. sinense* presence/absence and abundance from two sources were used to evaluate the MESMA performance (Table 1). We collected data at 346 randomly distributed field plots within 75 forest sites from 2009 to 2012. Data at 139 field plots were collected during the leaf-on season of 2009 and 2010, and at 207 field plots during the leaf-off season of 2012. At each site, we established a 10 × 10-m plot by defining a center point and recording coordinates using a Garmin GPSMAP 62s device. We recorded presence and absence of *L. sinense*. If *L. sinense* was present and covered more than 10% of a plot, we also estimated percent cover (e.g., 20%, 40%, 60%, 80%, and 100%) (Davis *et al.* 2016). We also used field survey data available from the Division of Nature Preserves and Natural Resources, Mecklenburg County Park and Recreation (MCPR) for augmenting the spatial distribution of *L. sinense* presence/absence and abundance in the study area. In 2005, MCPR established permanent 0.4 ha plots using a tagged, rebar center stake in the forested areas of nature preserves for collecting forest assessment data every 10 years. Field survey results included the percent cover of *L. sinense* (e.g., 1–4%, 5–24%, 25–49%, 50–74%, and 75–100%). We used 2012 high-resolution Digital Globe imagery from Google Earth to visually verify field plots and associated parameters for assuring data quality. For example, we excluded field plots if associated forest cover changed (i.e., removed/dieback some or all the existing vegetation) due to either human modification or natural disturbances. This also excluded field plots from the analysis if the percent cover of *L. sinense* was missing in the dataset. After screening data, we added eight field observations from the MCPR dataset collected in 2005 with presence/absence of *L. sinense* information. Figure 3 provides an overview of the entire analysis that we describe in detail in the following sections.

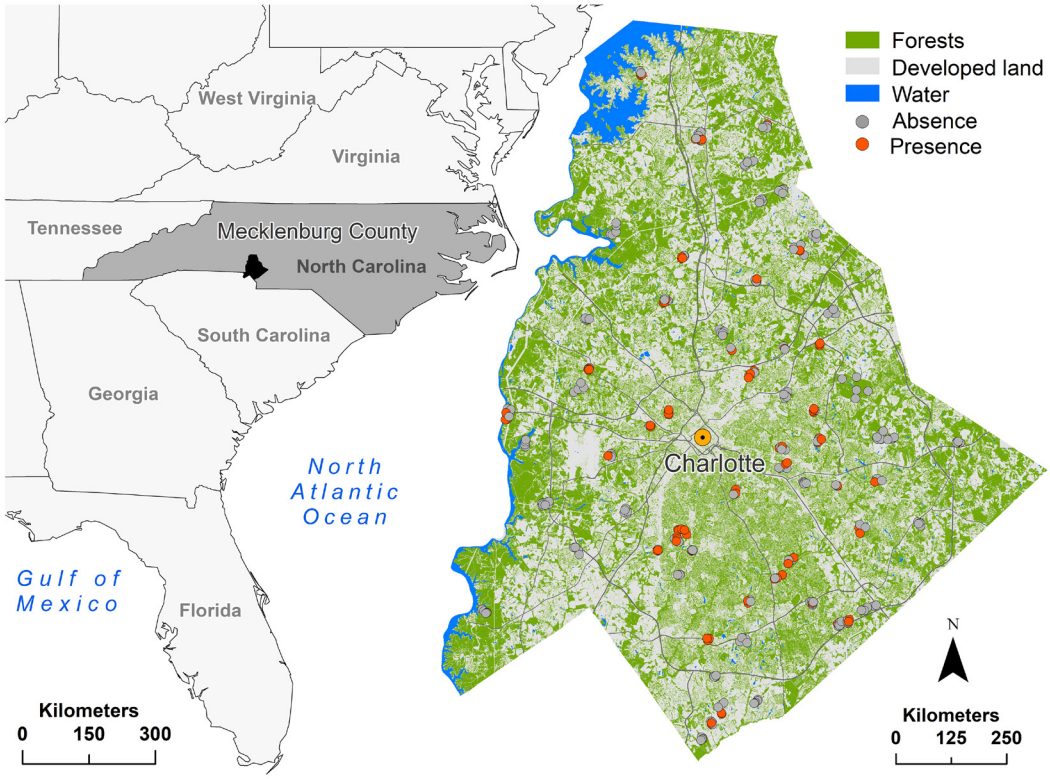

Figure 1. The location of Mecklenburg County within North Carolina, U.S.. The detailed lidar-derived map shows the distribution of forests across urbanizing landscapes in the Charlotte metropolitan area and field plots used in the study (Singh, Davis, and Meentemeyer 2015).

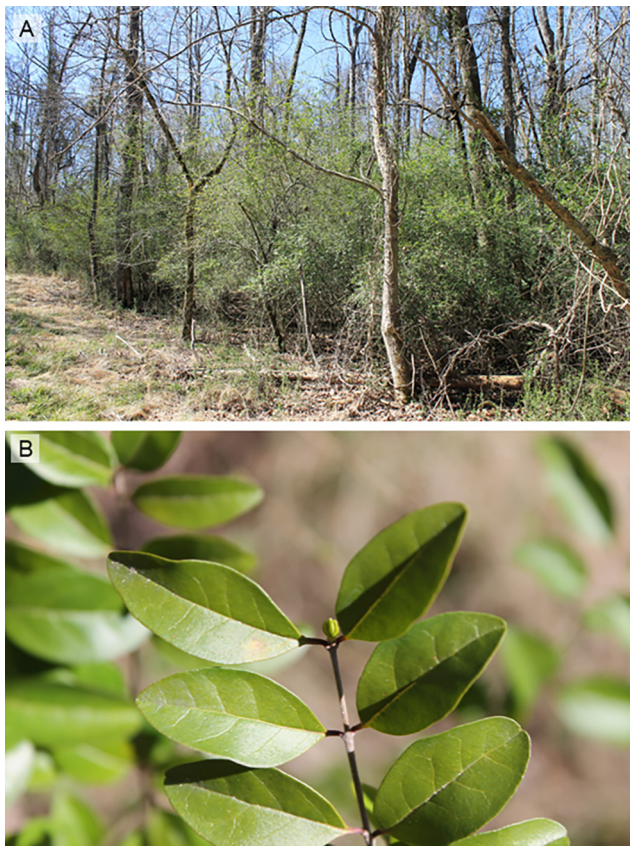

Figure 2. (a) A dense stand of *L. sinense* invasive shrub in forest understory at the forest edge next to a riparian area and (b) a typical foliage that exhibits thick leaves with a glossy upper surface and light green lower surface.

Table 1. *L. sinense* presence/absence attributes from our own field observations (2009, 2010, and 2012) and from Mecklenburg County Park and Recreation sites (2005).

Year	Presence	Absence	Total
2005	8	0	8
2009	21	75	96
2010	9	34	43
2012	96	111	207
Total	134	220	354

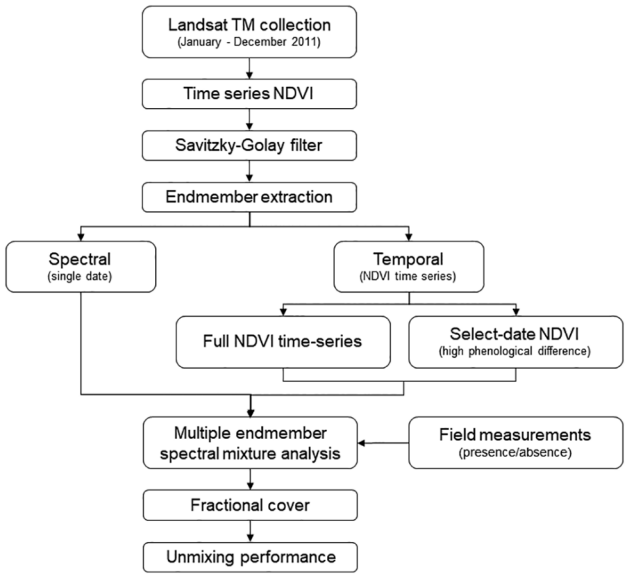

Figure 3. Schematic of analytical framework.

Remote Sensing Data Acquisition and Processing of Vegetation Index

Landsat Thematic Mapper Collection 1 surface reflectance data from January to December 2011 with less than 10% cloud cover for path 17 and rows 35–36 were acquired from the Land Processes Distributed Active Archive Center of United States Geological Survey. No imagery was available for January, May, or September due to high cloud cover. We mosaicked a portion of rows 35 and 36 images close to nadir for each time step to cover the study area, and then reprojected to the North Carolina State Plane Coordinate system. We used red and near-infrared bands to calculate NDVI for each mosaicked image (Tucker 1979). While Collection 1 surface reflectance products contain minimal geometric and atmospheric distortions, we applied a Savitzky-Golay filter to remove residual noise from the annual NDVI time series (Figure 4). The Savitzky-Golay filter uses a simplified least squares method to remove noise from data with a minimal loss of original information (Chen *et al.* 2004).

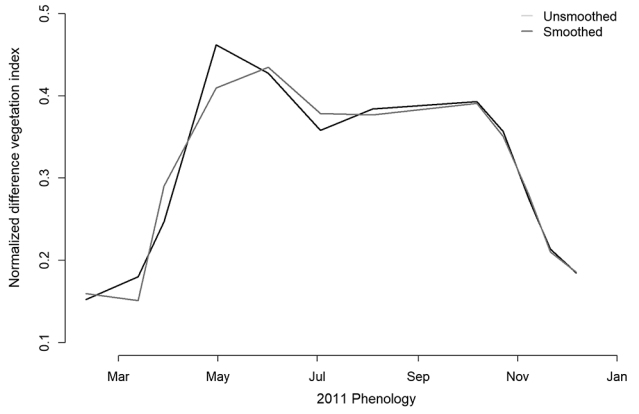

Figure 4. Raw 2011 Landsat NDVI time series mean and its Savitzky-Golay smoothed counterpart for all pixels within the study area.

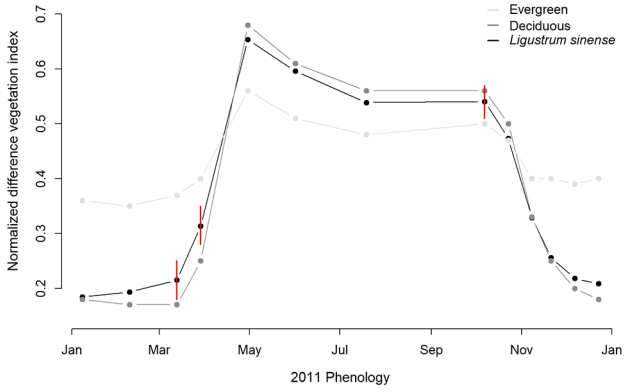

Figure 5. 2011 Landsat NDVI time series for *L. sinense*, deciduous, and evergreen forest types. Red segments show the dates of peak phenological difference between *L. sinense*, deciduous, and evergreen forest types used for the select-date temporal unmixing scheme.

Endmember Extraction and MESMA Unmixing Schemes

The performance of MESMA to detect *L. sinense* was tested with two types of endmembers: temporal signatures derived from NDVI time series, and traditional spectral signatures derived from a single Landsat image (Table 2). Both fully resolved (i.e., with the maximum available observations) and select-date versions of the temporal signatures were evaluated (Table 2). Selected dates were 13 March, 29 March, and 7 October 2011. These dates were selected via visual interpretation to coincide with the timing of maximum phenological difference between *L. sinense* and other image constituents (Figure 5). Typically, endmembers (i.e., spectrally unique and pure signature of objects) are derived from homogeneous pixels, field measurements, or reference databases. We created a multi-temporal NDVI image stack to extract both the select-date and fully resolved endmembers that we refer to as temporal signatures (Gong, Cui, and Gong 2014). We also derived traditional, single-date multispectral signatures for all Landsat image dates.

We used the VIPER Tools package, an ENVI add-on, to develop endmember libraries from NDVI time series and Landsat imagery. This tool creates an endmember library using regions of interest (i.e., ROIs) of target features in an image. VIPER extracts pixels within each selected ROI and saves it as a unique spectrum in the library. The advantage of MESMA over simple SMA is in accounting for signature variability among endmembers. Therefore, it is essential to capture the full spectral/temporal variability in endmembers across the application domain. We acquired temporal and spectral endmembers by selecting up to 20 constituents through visual analysis of land use and cover types common in the study area to account for both inner- and outer-class variability. Inner- and outer-class variability refers to the difference of spectral signatures in the same and between constituents types, respectively (Fan and Deng 2014). Later, we merged some potential constituents to minimize inner-class variability, maintain a high ratio between endmembers and input NDVI data/spectral bands, and mainly to concentrate on dominant land-cover types in the analysis. For example, we obtained endmembers for impervious surfaces, quarry, and buildings, but due to low inner-class variability among these constituents, we grouped these as an impervious surface endmember. In the end, eight endmembers were selected: *L. sinense*, deciduous, evergreen, farmland, golf course, water, soil, and impervious surfaces (Figure 6). We used three field plots from two forest sites that had >95% *L. sinense* coverage as an ROI for developing pure *L. sinense* spectral and NDVI signatures. These steps resulted into three different sets of endmembers: single-date spectral (unique for each time step), full NDVI time-series temporal, and select-date NDVI temporal.

We used the RStoolbox package's implementation of MESMA in R (version 3.5) to decompose each pixel for selected endmembers (Leutner and Horning 2018; R Core Team 2018). This package's implementation of MESMA uses a non-negative least square regression to compute probabilities by fitting non-negative model parameters linearly to remote sensing data

Table 2. Multiple endmember spectral mixture analysis (MESMA) schemes of temporal signatures (i.e., full- and select-date NDVI-normalized difference vegetation index) and spectral signatures of a single-date Landsat imagery for mapping spatial distribution of *L. sinense*.

Endmember types	Unmixing scheme	Description
Temporal	Select-date	NDVI signatures from three dates chosen to have high phenological differences (13 March, 29 March, and 7 October 2011)
	Full	NDVI signatures from all available image dates in 2011
Spectral	Single date	Multispectral signatures collected from each available Landsat image date

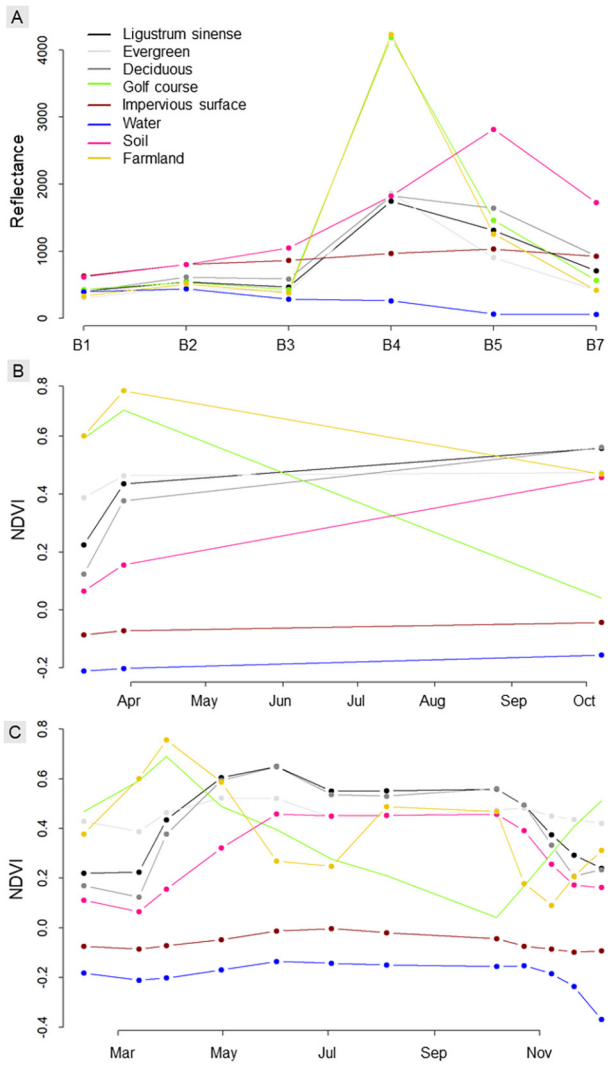

Figure 6. Spectral and temporal NDVI endmembers for dominant land-cover types including *L. sinense* used in the three unmixing schemes: (a) spectral single date, (b) select-date temporal NDVI, and (c) full temporal NDVI.

(Franc, Hlavac, and Navara 2005). We used output fractional cover images to derive quantitative estimates and maps of the geographic distribution of *L. sinense*.

Evaluation of Unmixing Performance

The MESMA estimated fractional cover of *L. sinense* was compared with field-observed fractional cover to evaluate unmixing performance. We resampled Landsat-scale maps of *L. sinense* fractional cover to 10 m resolution using nearest neighbor resampling in order to match the 10 × 10 m plot used for field data collection. The field-reported percent *L. sinense* cover along with the recorded presence of *L. sinense* were used to compute fractional cover.

The accuracy of the MESMA results were evaluated in two ways: direct comparison of modeled and observed *L. sinense* fractional cover using the correlation coefficient, and *L. sinense* presence/absence accuracy using traditional accuracy metrics computed from confusion matrices. We transformed the MESMA *L. sinense* fractional cover estimates to presence/absence via fractional cover thresholds determined with receiver operating characteristic (ROC) curves. Unmixing performance was assessed with overall accuracy (proportion of ground observed presences classified as *L. sinense* present), sensitivity and specificity, and the area under the ROC curve (AUC) (Sing *et al.* 2005). Sensitivity, also known as the true positive rate, measures the proportion of pixels flagged as "presence" that contained *L. sinense*. Specificity, also known as the true negative rate, is the proportion of pixels flagged as "absence" that are without *L. sinense*. The ROC curve provides a visual depiction of model performance where the proportion of true positive in presence cases (sensitivity) is plotted on the Y-axis against specificity (the proportion of true negative in absence cases) on the X-axis over multiple values of a parameter (in this case, the fractional abundance threshold). An ROC curve shows the tradeoff between sensitivity and specificity. Therefore, the closer the ROC curve follows the left-hand border (i.e., sensitivity) and then the top border of the ROC space, the higher the overall accuracy of the test. We selected an optimized cutoff point on the ROC curve that produces the highest accuracy by choosing the point nearest to the top left most corner of the ROC curve along with a default 0.5 cutoff point. While ROC curves are typically used to balance sensitivity and specificity, an unbalanced model may be more desirable contexts. For instance, if the penalty for missing true presences is high (as it may be in the case of harmful and prolifically spreading invasive plants s such as *L. sinense*), it may be desirable to maximize sensitivity at the cost of specificity. However, since the goal of our investigation was to compare the performance among various unmixing schemes, choosing an optimized fractional threshold which produces the highest accuracy allowed for a more interpretable and defensible comparison.

Results

The use of full and select-date temporal signatures did not improve the performance of MESMA in detection and mapping of *L. sinense* compared to using spectral signatures from single-date images where phenological difference among image constituents was high (Figure 7). All three MESMA models were positively correlated with ground observed fractional cover measures but the correlation coefficient was lower for MESMA using the full temporal signature (R = 0.51) when compared with select-date temporal signature (R = 0.64), and the best performing single-date (29 March 2011) spectral signature (R = 0.78)(Figure 8). The 29 March 2011 Landsat imagery exhibited the maximum phenological difference. These outcomes suggest that including observations for periods when phenological differences between *L. sinense* and other vegetation types are low can be counterproductive in a temporal signature-unmixing scheme.

In terms of accuracy in determining *L. sinense* presence/absence using an optimized fractional abundance threshold, the average overall accuracy of the full and select-date temporal signatures was 3.7% lower than the single-date (29 March 2011) spectral signatures of the maximum phenological difference (Table 3). The full temporal signature produced an overall accuracy of ~62%, which is ~3% lower than the select-date temporal signature. While the full temporal signature approach did not perform as we expected, results from the select-date temporal signatures suggests the contribution of phenological differences between *L. sinense* and other vegetation types to detection and mapping of *L. sinense*. For example, NDVI datasets for the select-date temporal signatures produced 65% overall accuracy with an AUC of 0.53 (95% CI, 0.60–0.70). The AUC value of full, select-date temporal signatures, and single date spectral signatures of the maximum phenological difference were 0.57, 0.53, and 0.67, respectively. AUC = 1 represents a perfect separation while AUC = 0.5 means model has no class separation capacity. Select-date temporal signatures produced ~25% higher sensitivity and ~10% lower specificity compared to the full temporal signatures, while the cutoff values for the fractional cover were similar in both (~0.9) (Table 3).

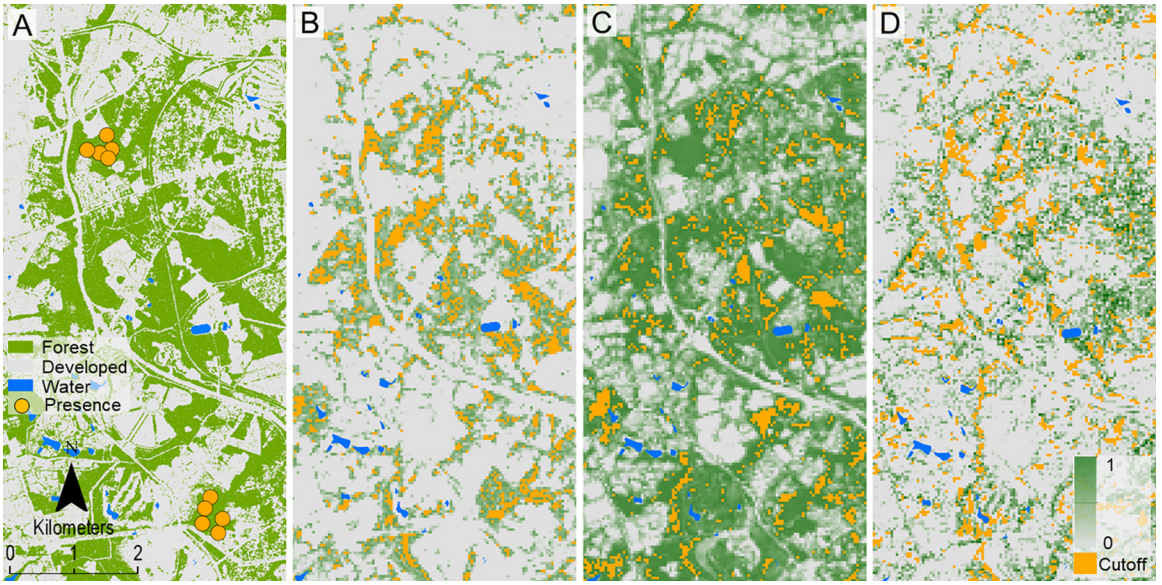

Figure 7. The distribution of forest cover, developed land, and water across the county with overlays of locations of field plots (a) along with the spatial distribution of *L. sinense* from MESMA schemes where (b)–(d) illustrates *L. sinense* fractional cover overlaid with the spatial distribution developed using ROC-optimized fractional abundance thresholds. (b) Spectral unmixing from a single-date Landsat imagery (29 March 2011) showed the highest performance, while (c) the temporal signature from the select-date and (d) full NDVI time-series resulted into the lowest performance.

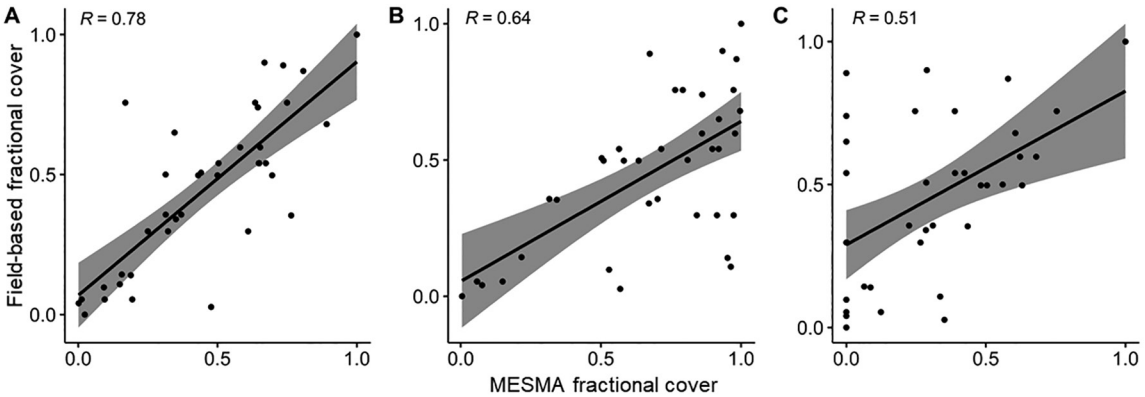

Figure 8. Scatterplots and associated R ($p < 0.001$) for the MESMA modeled estimates of: (a) spectral signatures from a single-date Landsat imagery (29 March 2011) that exhibited the maximum phenological difference, (b) temporal signatures from select-date NDVI (13 March, 29 March, and 7 October), and (c) the temporal signatures from full NDVI time-series.

Overall accuracy results of mapping *L. sinense* presence/absence were similar for in-common 0.5 fractional abundance thresholds compared to optimized variants. The overall accuracy difference between full and select-date temporal signature and between temporal and spectral schemes were 5% but the single-date maximum phenological difference (29 March 2011) produced the highest overall accuracy of 66.1%. Trends in sensitivity and specificity were opposite. For example, sensitivity accuracies using a naïve 0.5 fractional abundance threshold compared to the optimized variants were higher while specificity accuracies were lower except for January single-date temporal signatures. Only the select-date temporal signatures and March 2011 spectral signatures produced the highest sensitivity score and overall accuracy. Landsat imagery of 29 March 2011 produced the highest overall accuracy (68% with an optimized fractional abundance threshold of 0.7) among single-date spectral signature schemes (Table 3 and Figure 9). Sensitivity and specificity were 11% higher and 3% lower, respectively, compared to the select-date temporal signatures. Both *L. sinense* fractional cover and overall accuracy measures for the three unmixing schemes suggests that if a priori knowledge of dates of a maximum phenological difference is not available, or images for those time periods are unavailable, using as many image dates as possible can improve the performance of MESMA. In fact, using all available imagery might be a better solution to achieve higher performance than randomly selecting a cloud-free, single image date.

Using optimized fractional abundance thresholds did improve overall accuracy measures compared to the naïve value of 0.5, but inconsistently across unmixing variants. Among single-date spectral signatures, overall accuracies were, on average, 10% higher for optimal thresholds. However, the difference in overall accuracy was lower for the best single-date spectral signature scheme (1.5% difference on 29 March) and for select-date and full temporal NDVI signatures (4% and 6%, difference, respectively). This may suggest that the difference in overall accuracy between using an optimal and a typical 0.5 cutoff values decreases as the phenological difference in Landsat imagery and temporal NDVI increases. It should be noted that sensitivity scores for ROC-optimized thresholds were quite low, particularly for the full temporal signature variant. Overall, these results indicate that optimization of threshold

Table 3. Accuracy metrics for the unmixing models with overall accuracy, specificity, and sensitivity, and the area under the receiver-operating characteristic curve (AUC) with 95% confidence intervals (CI).

Data inputs	Unmixing scheme	Cutoff±	Predicted Yes/No	Yes	No	Accuracy	Sensitivity	Specificity	AUC (CI)
Spectral single date	8 January	0.37	Yes	42	93	64.7	0.32	0.85	0.549 (0.59–0.70)
			No	32	187				
		0.50	Yes	12	123	61.0	0.09	0.93	0.549 (0.56–0.66)
			No	15	204				
	9 February	0.66	Yes	10	125	63.8	0.08	0.99	0.557 (0.59–0.69)
			No	3	216				
		0.50	Yes	33	102	61.0	0.24	0.84	0.557 (0.55–0.66)
			No	36	183				
	13 March	0.69	Yes	23	11	66.8	0.18	0.94	0.652 (0.62–0.72)
			No	104	208				
		0.50	Yes	62	63	63.0	0.49	0.71	0.652 (0.58–0.68)
			No	65	156				
	29 March	0.58	Yes	55	83	67.5	0.39	0.85	0.675 (0.61–0.73)
			No	32	184				
		0.50	Yes	77	58	66.1	0.57	0.72	0.675 (0.60–0.71)
			No	62	157				
	30 April	0.77	Yes	20	115	63.8	0.15	0.94	0.636 (0.58–0.69)
			No	13	206				
		0.50	Yes	79	56	60.7	0.59	0.62	0.636 (0.55–0.66)
			No	83	136				
	1 June	0.97	Yes	1	134	62.2	0.01	1.00	0.469 (0.57–0.67)
			No	0	219				
		0.50	Yes	121	14	38.4	0.89	0.07	0.469 (0.33–0.44)
			No	204	15				
	19 July	0.64	Yes	0	135	61.9	0.39	0.55	0.443 (0.56–0.67)
			No	0	219				
		0.50	Yes	92	43	39.8	0.68	0.22	0.443 (0.35–0.45)
			No	170	49				
	4 August	0.85	Yes	2	133	62.2	0.02	0.99	0.518 (0.57–0.67)
			No	1	218				
		0.50	Yes	31	104	57.1	0.23	0.78	0.518 (0.51–0.62)
			No	48	171				
	7 October	0.86	Yes	9	126	63.3	0.07	0.98	0.475 (0.58–0.68)
			No	4	215				
		0.50	Yes	78	57	44.6	0.58	0.37	0.475 (0.39–0.50)
			No	139	80				
	8 November	0.84	Yes	11	124	62.2	0.08	0.95	0.488 (0.57–0.67)
			No	10	209				
		0.50	Yes	55	80	48.6	0.41	0.53	0.488 (0.43–0.54)
			No	102	117				
	23 December	0.68	Yes	22	113	64.9	0.17	0.95	0.556 (0.59–0.70)
			No	11	208				
		0.50	Yes	55	80	57.9	0.41	0.69	0.556 (0.52–0.63)
			No	69	150				
Temporal	Select-date temporal NDVI	0.85	Yes	38	97	65.3	0.28	0.88	0.531 (0.60–0.70)
			No	26	193				
		0.50	Yes	36	102	61.6	0.26	0.84	0.531 (0.32–0.42)
			No	34	182				
	Full temporal NDVI[¥]	0.90	Yes	3	132	62.4	0.02	0.99	0.574 (0.57–0.67)
			No	1	218				
		0.50	Yes	27	108	56.5	0.20	0.79	0.574 (0.51–0.62)
			No	46	173				

* 13 March, 29 March, and 7 October of 2011 with the peak phenology differences.
[¥] Excluded NDVI for the months of January, May and September 2011 due to the high cloud cover.

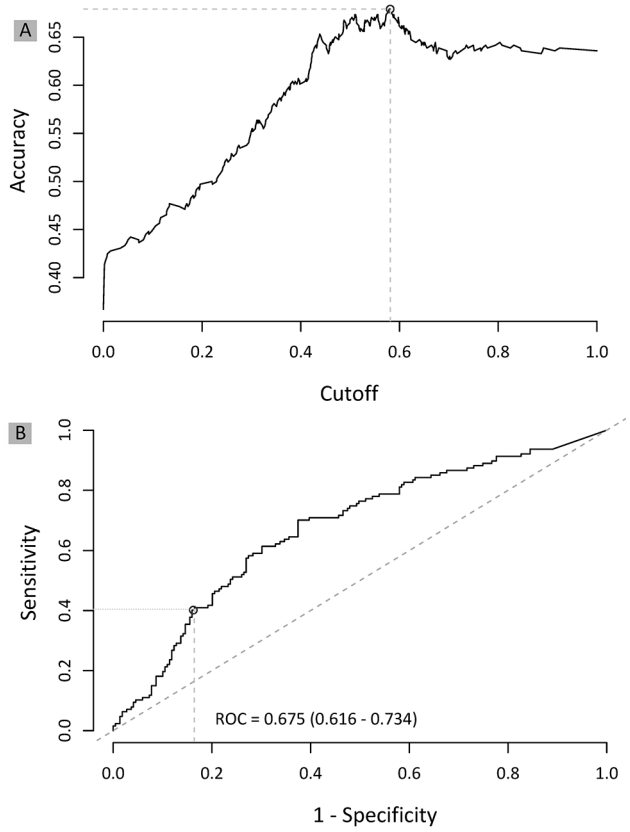

Figure 9. The performance of single-date, 29 March 2011 MESMA unmixing scheme: (a) accuracy-cutoff curve for the peak accuracy across a range of cutoffs and (b) ROC curve and AUC value.

values may marginally improve accuracy for high performing unmixing schemes, but the sensitivity and specificity tradeoffs must be evaluated in the context of a particular problem.

Discussion

Relatively low performance of unmixing schemes using temporal signatures has been reported in other studies (Diao and Wang 2016; Fan and Deng 2014; Somers and Asner 2013). This might be explained by the fact that MESMA equally weights differences among particular data points in endmember signatures, such that adding additional data points where signatures are similar may degrade unmixing performance. Adding many indistinct but equally weighted data lessens the influence of the few highly distinct time periods. Additionally, several studies have reported the effects of the number of unique endmembers and their selection procedure on the performance of subpixel unmixing (Quintano *et al.* 2017). Because the number of potential combinations increases with the number of endmembers, unmixing with many endmember possibilities tends to reduce accuracy while incurring a higher computational burden (Pal and Foody 2010; Tane *et al.* 2018). Likewise, Thorp, French, and Rango (2013) observed that MESMA results were sensitive to the characteristics of the image spectra and endmember spectra. Typically, in an unmixing technique, the selected endmembers types (n) cannot exceed the number of imagery bands. We used eight endmembers, more than the recommended endmembers for unmixing, for all the unmixing schemes including single-date scheme with Landsat imagery. Therefore, the selected eight endmembers could also be a potential cause for the lower performance of unmixing schemes, even though we selected endmembers for only dominant land-cover types and *L. sinense*.

While the lower performance of temporal signatures compared to single-date spectral signatures was unexpected, the gap in overall accuracies between temporal and spectral signatures were low, suggesting that each approach might be productively used to create maps of *L. sinense* or any other understory invasive plants. The high similarity in overall accuracy suggests that the documented performance differences may originate from factors specific to site and/or study design rather than a general principle that would favor spectral over temporal endmember signatures. In fact, it should be noted that even the single-date spectral signature approach contained implicit phenological information through the a priori selection of a date for which phenological differences were maximized. At a minimum, this suggests that phenological information should be considered when conducting unmixing analyses, even if traditional, single-date spectral signatures are used. Specifically, these results support the recommendation of Singh *et al.* (2018) to select remote sensing data for a period when phenological differences between invasive plant and forest types are at their peak (Figure 4). These results suggest that if periods of high phenological difference are not known a priori, or if those time periods are not represented in the available imagery, then using all available imagery in a temporal signature unmixing scheme may be preferred to randomly selecting a single image date from which to acquire multispectral signatures. Phenology differences between *L. sinense* and the dominant deciduous forest overstory are higher during the senescence and dormant phases (i.e., leaf-off season), which tends to increase inner-class variability in temporal and spectral signatures. Therefore, a low inner-class variability in temporal signatures from the leaf-on season NDVI data also might have led to poor performance. Other studies reported better performances from select-date unmixing but suggested a further evaluation of the contribution of temporal signatures. For example, Diao and Wang (2016) observed an improved abundance estimation accuracy using temporal signatures compared to the traditional single-date-optimal-spectral signature, and recommended a further evaluation of the role of temporal signatures in temporal partial unmixing before it can be generalized to other plant species.

We converted the *L. sinense* fractional cover results to binary presence/absence maps using two thresholds: a naïve 0.5 threshold and an ROC-optimized value. Several methods exist to achieve lower misclassification rates but since there was no preference between sensitivity and specificity, we attempted to maximize higher accuracy estimates. We observed that the difference in overall accuracy between using a typical 0.5 and an optimal threshold value decreased as the phenological difference in Landsat imagery and temporal NDVI increased. This also includes improved sensitivity values. Additionally, the full and select-date temporal signatures provided similarly high accuracies as the single-date spectral signatures from Landsat imagery of leaf-off season except March 2011, and substantially better than most of the single-date spectral schemes without threshold optimization. These observations suggest the general utility of using temporal signatures to estimate fractional cover of invasive plants if it is impractical to determine a priori the dates of maximum phenological difference. Usually, a reported low sensitivity value in the presence of a higher specificity indicates that the cutoff point might have been too stringent, and that sensitivity was sacrificed for obtaining high specificity. However, since we attempted to maximize overall accuracy, the very low sensitivity scores for the full temporal signatures may be due to the way MESMA operates, i.e., adding many indistinct but equally weighted data lessens the influence of the few highly distinct time periods. Besides, several factors, such as complexity of landscapes, range of deviance from normal, and homogeneity of the surveyed population may have contributed to lower sensitivity and higher specificity. The AUC estimate also indicates poor

overall performance, regardless of the method, including the 29 March 2011 single date spectral signatures (AUC = 0.675). Mismatch between the field-plot size (i.e., 10 × 10 m) and spatial resolution of Landsat (i.e., 30 × 30 m) and using more than the recommended endmembers for unmixing may have contributed to the overall poor performance.

While the correlation coefficient and traditional accuracy metrics computed from confusion matrices pointed out the same high performing MESMA models (e.g., single-date—29 March 2011), the latter approach produced a lower difference among temporal and the top performing single-date spectral signatures (29 March 2011) models. We also observed a lower performance of the traditional accuracy assessment (e.g., 29 March 2011—overall accuracy 67.5%) compared to correlation coefficient analysis (e.g., 29 March 2011—correlation coefficient 74%) of the top three MESMA models. The ROC-optimization may have contributed to the lower difference and the overall performance. Results from the ROC-optimized value indicate that threshold optimization may marginally improve accuracy for high performing unmixing schemes, but users must evaluate the sensitivity and specificity trade-offs in the context of a particular application.

The viability of time-series NDVI for mapping *L. sinense* using MESMA might not be as effective as spectral data (e.g., Landsat bands), but these results suggest the overall potential of MESMA for the mapping of invasive plants over large spatial extents. Improvement in the selection of endmembers may also help improving detection as discussed above. This also includes a comparative analysis of spectral data from multiple sources using both full- and select-date time-series. Since we examined only the difference in phenology and spectral signatures in unmixing pixels, a study using multispectral temporal signatures may improve mapping performance with higher accuracy estimates, as time series of multispectral values would include both sources of information. A comparative analysis between Landsat imagery and hyperspectral data from the peak senescence/dormant phase could lead to a better understanding whether the spectral resolution holds a clue to the higher accuracies of *L. sinense* mapping. Quintano *et al.* (2017) recommended environmental variables, such as elevation, topographic moisture, and solar radiation index along with a reclassification of fraction surface developed using MESMA technique for higher mapping accuracies. Overall, our results suggest that unmixing of remotely sensed images can be a productive means of mapping *L. sinense* presence over large spatial extents, and while spectral information is critical for constructing endmember signatures, phenological information of invasive plants can help to maximize it. Spectral signatures may be more advantageous than temporal signatures, but only if they can be retrieved for a time period of maximum phenological difference.

Conclusions

Remote sensing methods (e.g., phenological or spectral unmixing) that can offer frequent and accurate maps of the geographic distribution of invasive plants at large extents are indispensable for their successful eradication and management. Our results indicate similar overall accuracies for approaches that used single-date spectral or temporal endmember signatures for unmixing, and positive correlations between mapped and observed fractional cover for *L. sinense*. Findings suggest that optimization of threshold values may marginally improve accuracy for high performing unmixing schemes, but users must evaluate the sensitivity and specificity trade-offs following a particular problem. Single-date spectral signatures for time periods of high phenological difference performed slightly better than other approaches, supporting the idea that the addition of extra endmember signature information that is indistinct negatively affects unmixing performance. However, our single-date, spectrally based signatures contained implicit phenological information, and thus serves to highlight the importance of considering phenological information when unmixing remotely sensed imagery. Moreover, our results suggest using as many image dates as possible to improve the performance of MESMA if there is no a priori information about the dates of maximum phenological difference, or if those image dates are unavailable. The transformation of the MESMA-derived fractional cover to binary maps of presence/absence makes it suitable for ecological applications and management decision-making processes.

Acknowledgment

The National Aeronautics and Space Administration grant (NNX16AL68G) supported this research. We thank fellow researchers from the Center for Geospatial Analytics at North Carolina State University for their comments and feedback on the manuscript.

References

Adams, J. B. 1993. Imaging spectroscopy: Interpretation based on spectral mixture analysis. In *Remote Geochemical Analysis: Elemental and Mineralogical Composition*,145–166.

Amaral, C. H., D. A. Roberts, T.I.R. Almeida and C. R. Souza. 2015. Mapping invasive species and spectral mixture relationships with neotropical woody formations in southeastern Brazil. *ISPRS Journal of Photogrammetry and Remote Sensing* 108:80–93.

Asner, G. P. and P. M. Vitousek. 2005. Remote analysis of biological invasion and biogeochemical change. *Proceedings of the National Academy of Sciences of the United States of America* 102 (12):4383–4386.

Bradley, B. A. 2014. Remote detection of invasive plants: A review of spectral, textural and phenological approaches. *Biological Invasions* 16 (7):1411–1425.

Bradley, B. A., R. Early and C.J.B. Sorte. 2015. Space to invade? Comparative range infilling and potential range of invasive and native plants. *Global Ecology and Biogeography* 24 (3):348–359.

Brewer, W. L., C. L. Lippitt, C. D. Lippitt and M. E. Litvak. 2017. Assessing drought-induced change in a pinon-juniper woodland with Landsat: A multiple endmember spectral mixture analysis approach. *International Journal of Remote Sensing* 38 (14):4156–4176.

Cash, J. S., C. J. Anderson and L. Marzen. 2020. Evaluating free and simple remote sensing methods for mapping Chinese privet (Ligustrum sinense) invasions in hardwood forests. *SN Applied Sciences* 2:1–11.

Chen, J., P. Jonsson, M. Tamura, Z. H. Gu, B. Matsushita and L. Eklundh. 2004. A simple method for reconstructing a high-quality NDVI time-series data set based on the Savitzky-Golay filter. *Remote Sensing of Environment* 91 (3–4):332–344.

Davis, A.J.S., K. K. Singh, J. C. Thill and R. K. Meentemeyer. 2016. Accounting for residential propagule pressure improves prediction of urban plant invasion. *Ecosphere* 7 (3).

Dennison, P. E. and D. A. Roberts. 2003. The effects of vegetation phenology on endmember selection and species mapping in southern California chaparral. *Remote Sensing of Environment* 87 (2–3):295–309.

Diao, C. Y. and L. Wang. 2016. Temporal partial unmixing of exotic salt cedar using Landsat time series. *Remote Sensing Letters* 7 (5):466–475.

Ehrenfeld, J. G. 2010. Ecosystem consequences of biological invasions. *Annual Review of Ecology, Evolution, and Systematics* 41:59–80.

Fan, F. L. and Y. B. Deng. 2014. Enhancing endmember selection in multiple endmember spectral mixture analysis (MESMA) for urban impervious surface area mapping using spectral angle and spectral distance parameters. *International Journal of Applied Earth Observation and Geoinformation* 33:290–301.

Foard, M., D. J. Burnette, D.R.L. Burge and T. D. Marsico. 2016. Influence of river channelization and the invasive shrub, Ligustrum sinense, on oak (*Quercus spp.*) growth rates in bottomland hardwood forests. *Applied Vegetation Science* 19 (3):401–412.

Franc, V., V. Hlavac and M. Navara. 2005. Sequential coordinate-wise algorithm for the non-negative least squares problem. Pages 407–414 in *Proceedings of the International Conference on Computer Analysis of Images and Patterns*.

Gan, M. Y., J. S. Deng, X. Y. Zheng, Y. Hong and K. Wang. 2014. Monitoring urban greenness dynamics using multiple endmember spectral mixture analysis. *Plos One* 9 (11).

Gavier-Pizarro, G. I., T. Kuemmerle, L. E. Hoyos, S. I. Stewart, C. D. Huebner, N. S. Keuler and V. C. Radeloff. 2012. Monitoring the invasion of an exotic tree (*Ligustrum lucidum*) from 1983 to 2006 with Landsat TM/ETM plus satellite data and Support Vector Machines in Cordoba, Argentina. *Remote Sensing of Environment* 122:134–145.

Gong, Z., T. Cui and H. Gong. 2014. Estimating wetland vegetation abundance based on spectral mixture analysis: A comparison between LSMA and FCM classification methods. *International Journal of Remote Sensing* 35 (1):189–203.

Hanula, J. L., S. Horn and J. W. Taylor. 2009. Chinese privet (*Ligustrum sinense*) removal and its effect on native plant communities of riparian forests. *Invasive Plant Science and Management* 2 (4):292–300.

Hanula, J. L. and S. Horn. 2011. Removing an invasive shrub (Chinese privet) increases native bee diversity and abundance in riparian forests of the southeastern United States. *Insect Conservation and Diversity* 4 (4):275–283.

Hejda, M., P. Pyšek and V. Jarošík. 2009. Impact of invasive plants on the species richness, diversity and composition of invaded communities. *Journal of Ecology* 97 (3):393–403.

Isaac, S. 2001. Chinese privet: A Case Study of the Problem of Invasive Species. <http://www.ibiblio.org/ecoaccess/info/wildlife/pubs/chineseprivet.html> Accessed 11 January 2012.

Langeland, K. A. and K. C. Burks. eds. 1998. *Identification and Biology of Non-Native Plants in Florida's Natural Areas*, p. 165. Gainesville, Fla.: University of Florida.

Lemke, D. and J. A. Brown. 2012. Habitat modeling of alien plant species at varying levels of occupancy. *Forests* 3 (3):799–817.

Leutner, B. and N. Horning. 2018. RStoolbox: Tools for remote sensing data analysis. *CRAN–Package RStoolbox*. <https://cran.r-project.org/web/packages/RStoolbox/index.html> Accessed 19 June 2018.

Liebhold, A., E. G. Brockerhoff, S. Kalisz, M. A. Nunez, D. A. Wardle and M. J. Wingfield. 2017. Biological invasions in forest ecosystems. *Biological Invasions* 19 (11):3437–3458.

Merriam, R. W. 2003. The abundance, distribution and edge associations of six non-indigenous, harmful plants across North Carolina. *Journal of the Torrey Botanical Society* 130 (4):283–291.

Michishita, R., Z. B. Jiang, P. Gong and B. Xu. 2012. Bi-scale analysis of multitemporal land cover fractions for wetland vegetation mapping. *ISPRS Journal of Photogrammetry and Remote Sensing* 72:1–15.

Miller, J. H., E. B. Chambliss and C. M. Oswalt. 2008. Maps of occupation and estimates of acres covered by nonnative invasive plants in southern forests using SRS FIA data. Accessed 11 February 2012.

Noonan, M. and C. Chafer. 2007. A method for mapping the distribution of willow at a catchment scale using bi-seasonal SPOT5 imagery. *Weed Research* 47 (2):173–181.

Pal, M. and G. M. Foody. 2010. Feature selection for classification of hyperspectral data by SVM. *IEEE Transactions on Geoscience and Remote Sensing* 48 (5):2297–2307.

Quintano, C., A. Fernandez-Manso and D. A. Roberts. 2017. Burn severity mapping from Landsat MESMA fraction images and land surface temperature. *Remote Sensing of Environment* 190:83–95.

R Core Team. 2018. R: A language and environment for statistical computing. R Foundation for Statistical Computing, Vienna, Austria.

Roberts, D. A., M. O. Smith and J. B. Adams. 1993. Green vegetation, nonphotosynthetic vegetation, and soils in aviris data. *Remote Sensing of Environment* 44 (2–3):255–269.

Roberts, D. A., M. Gardner, R. Church, S. Ustin, G. Scheer and R. O. Green. 1998. Mapping chaparral in the Santa Monica Mountains using multiple endmember spectral mixture models. *Remote Sensing of Environment* 65 (3):267–279.

Roth, K. L., P. E. Dennison and D. A. Roberts. 2012. Comparing endmember selection techniques for accurate mapping of plant species and land cover using imaging spectrometer data. *Remote Sensing of Environment* 127:139–152.

Settle, J. J. and N. A. Drake. 1993. Linear mixing and the estimation of ground cover proportions. *International Journal of Remote Sensing* 14 (6):1159–1177.

Simberloff, D., J. L. Martin, P. Genovesi, V. Maris, D. A. Wardle, J. Aronson, F. Courchamp, B. Galil, E. Garcia-Berthou, M. Pascal, P. Pysek, R. Sousa, E. Tabacchi and M. Vila. 2013. Impacts of biological invasions: What's what and the way forward. *Trends in Ecology & Evolution* 28 (1):58–66.

Sing, T., O. Sander, N. Beerenwinkel and T. Lengauer. 2005. ROCR: Visualizing classifier performance in R. *Bioinformatics* 21 (20):3940–3941.

Singh, K. K., A. J. Davis and R. K. Meentemeyer. 2015. Detecting understory plant invasion in urban forests using LiDAR. *International Journal of Applied Earth Observation and Geoinformation* 38:267–279.

Singh, K. K., Y.-H. Chen, L. Smart, J. Gray and R. K. Meentemeyer. 2018. Intra-annual phenology for detecting understory plant invasion in urban forests. *ISPRS Journal of Photogrammetry and Remote Sensing* 142:151–161.

Singh, N. and N. F. Glenn. 2009. Multitemporal spectral analysis for cheatgrass (*Bromus tectorum*) classification. *International Journal of Remote Sensing* 30 (13):3441–3462.

Singh, K. K., Vogler, J. B., Shoemaker, D. A., & Meentemeyer, R. K., 2012. LiDAR-Landsat data fusion for large-area assessment of urban land cover: Balancing spatial resolution, data volume and mapping accuracy. *ISPRS Journal of Photogrammetry and Remote Sensing*, 74, 110-121.

Somers, B., G. P. Asner, L. Tits and P. Coppin. 2011. Endmember variability in spectral mixture analysis: A review. *Remote Sensing of Environment* 115 (7):1603–1616.

Somers, B. and G. P. Asner. 2013a. Invasive species mapping in Hawaiian rainforests using multi-temporal hyperion spaceborne imaging spectroscopy. *IEEE Journal of Selected Topics in Applied Earth Observations and Remote Sensing* 6 (2):351–359.

Somers, B. and G. P. Asner. 2013b. Multi-temporal hyperspectral mixture analysis and feature selection for invasive species mapping in rainforests. *Remote Sensing of Environment* 136:14–27.

Song, C. H. 2005. Spectral mixture analysis for subpixel vegetation fractions in the urban environment: How to incorporate endmember variability? *Remote Sensing of Environment* 95 (2):248–263.

Tane, Z., D. Roberts, S. Veraverbeke, A. Casas, C. Ramirez and S. Ustin. 2018. Evaluating endmember and band selection techniques for multiple endmember spectral mixture analysis using post-fire imaging spectroscopy. *Remote Sensing* 10 (3).

Thorp, K. R., A. N. French and A. Rango. 2013. Effect of image spatial and spectral characteristics on mapping semi-arid rangeland vegetation using multiple endmember spectral mixture analysis (MESMA). *Remote Sensing of Environment* 132:120–130.

Tucker, C. J. 1979. Red and photographic infrared linear combinations for monitoring vegetation. *Remote Sensing of Environment* 8 (2):127–150.

Wardle, D. A. and D. A. Peltzer. 2017. Impacts of invasive biota in forest ecosystems in an aboveground–belowground context. *Biological Invasions* 19 (11):3301–3316.

Wilcox, J. and C. W. Beck. 2007. Effects of *Ligustrum sinense Lour.* (Chinese privet) on abundance and diversity of songbirds and native plants in a southeastern nature preserve. *Southeastern Naturalist* 6 (3):535–550.

Wilfong, B. N., D. L. Gorchov and M. C. Henry. 2009. Detecting an invasive shrub in deciduous forest understories using remote sensing. *Weed Science* 57 (5):512–520.

SUSTAININGMEMBERS

Aerial Services, Inc.
Cedar Falls, Iowa
www.AerialServicesInc.com
Member Since: 5/2001

Airbus Defense and Space
Chantilly, Virginia
www.intelligence-airbusds.com
Member Since: 11/2018

Ayres Associates
Madison, Wisconsin
www.AyresAssociates.com
Member Since: 1/1953

Bohannan Huston, Inc.
Albuquerque, New Mexico
www.bhinc.com
Member Since: 11/1992

Dewberry
Fairfax, Virginia
www.dewberry.com
Member Since: 1/1985

Esri
Redlands, California
www.esri.com
Member Since: 1/1987

GeoWing Mapping, Inc.
Richmond, California
www.geowingmapping.com
Member Since: 12/2016

Global Science & Technology, Inc.
Greenbelt, Maryland
www.gst.com
Member Since: 10/2010

GPI Geospatial Inc.
formerly Aerial Cartographics of America, Inc. (ACA)
Orlando, Florida
www.aca-net.com
Member Since: 10/1994

Green Grid Inc.
San Ramon, California
www.greengridinc.com
Member Since: 1/2020

Kucera International
Willoughby, Ohio
www.kucerainternational.com
Member Since: 1/1992

L3Harris Corporation
Broomfield, Colorado
www.harris.com
Member Since: 6/2008

Pickett and Associates, Inc.
Bartow, Florida
www.pickettusa.com
Member Since: 4/2007

Quantum Spatial, Inc.
Sheboygan Falls, Wisconsin
www.quantumspatial.com
Member Since: 1/1974

Sanborn Map Company
Colorado Springs, Colorado
www.sanborn.com
Member Since: 10/1984

T3 Global Strategies, Inc.
Bridgeville, Pennsylvania
https://t3gs.com/
Member Since: 6/2020

Towill, Inc.
San Francisco, California
www.towill.com
Member Since: 1/1952

Trimble
Munich, Germany
www.trimble.com/geospatial
Member Since: 4/1942

Wingtra
Zurich, Switzerland
https://wingtra.com/
Member Since: 6/2020

Woolpert LLP
Dayton, Ohio
www.woolpert.com
Member Since: 1/1985

SUSTAININGMEMBER**BENEFITS**

Membership

- ✓ Provides a means for dissemination of new information
- ✓ Encourages an exchange of ideas and communication
- ✓ Offers prime exposure for companies

Benefits of an ASPRS Membership

- Complimentary and discounted Employee Membership*
- E-mail blast to full ASPRS membership per year*
- Professional Certification Application fee discount for any employee
- Discounts on *PE&RS* Classified Ad
- Member price for ASPRS publications
- Discount on group registration to ASPRS virtual conferences
- Sustaining Member company listing in ASPRS directory/website
- Hot link to company website from Sustaining Member company listing page on ASPRS website
- Press Release Priority Listing in *PE&RS* Industry News
- Priority publishing of Highlight Articles in *PE&RS* plus, 20% discount off cover fee, one per year
- Discount on *PE&RS* full-page advertisement
- Exhibit discounts at ASPRS sponsored conferences (exception ASPRS/ILMF)
- Free training webinar registrations per year*
- Discount on additional training webinar registrations for employees
- Discount for each new SMC member brought on board (Discount for first year only)

*quantity depends on membership level

PE&RS

PE&RS 2020 Advertising Rates

PHOTOGRAMMETRIC ENGINEERING & REMOTE SENSING

The official journal for imaging and geospatial information science and technology

Advertise in the #1 publication in the imaging and geospatial information industry!

asprs THE IMAGING & GEOSPATIAL INFORMATION SOCIETY

Impact Factor (2018): 3.15

PE&RS (Photogrammetric Engineering & Remote Sensing) is the official journal of the American Society for Photogrammetry and Remote Sensing—the Imaging and Geospatial Information Society (ASPRS). This highly respected publication is the #1 publication in the industry by a wide margin. Advertisers with a desire to reach this market can do no better than PE&RS. It delivers the right audience of professionals who are loyal and engaged readers, and who have the purchasing power to do business with you.

***PE&RS* Readership Highlights**

Circulation:	Total audience:
3,000	6,400*

Founded in 1934, the American Society for Photogrammetry and Remote Sensing (ASPRS) is a scientific association serving professional members throughout the world. Our mission is to advance knowledge and improve understanding of mapping sciences to promote the responsible applications of photogrammetry, remote sensing, geographic information systems (GIS), and supporting technologies.

Our members are analysts/specialists, educators, engineers, managers/administrators, manufacturers/ product developers, operators, technicians, trainees, marketers, and scientists/researchers. Employed in the disciplines of the mapping sciences, they work in the fields of Agriculture/Soils, Archeology, Biology, Cartography, Ecology, Environment, Forestry/Range, Geodesy, Geography, Geology, Hydrology/Water Resources, Land Appraisal/ Real Estate, Medicine, Transportation, and Urban Planning/Development.

RESERVE YOUR SPACE TODAY!

Bill Spilman, ASPRS Advertising, Exhibit Sales & Sponsorships
(877) 878-3260 toll-free
(309) 483-6467 direct
(309) 483-2371 fax
bill@innovativemediasolutions.com

	Corporate Member Exhibiting at a 2019 ASPRS Conference	**Corporate Member**	**Exhibitor**	**Non Member**
All rates below are for four-color advertisments				
Cover 1	$1,850	$2,000	$2,350	$2,500
In addition to the cover image, the cover sponsor receives a half-page area to include a description of the cover (maximum 500 words). The cover sponsor also has the opportunity to write a highlight article for the journal. Highlight articles are scientific articles designed to appeal to a broad audience and are subject to editorial review before publishing. The cover sponsor fee includes 50 copies of the journal for distribution to their clients. More copies can be ordered at cost.				
Cover 2	$1,500	$1,850	$2,000	$2,350
Cover 3	$1,500	$1,850	$2,000	$2,350
Cover 4	$1,850	$2,000	$2,350	$2,500
Advertorial	1 Complimentary Per Year	1 Complimentary Per Year	$2,150	$2,500
Full Page	$1,000	$1,175	$2,000	$2,350
2 page spread	$1,500	$1,800	$3,200	$3,600
2/3 Page	$1,100	$1,160	$1,450	$1,450
1/2 Page	$900	$960	$1,200	$1,200
1/3 Page	$800	$800	$1,000	$1,000
1/4 Page	$600	$600	$750	$750
1/6 Page	$400	$400	$500	$500
1/8 Page	$200	$200	$250	$250
Other Advertising Opportunities				
Wednesday Member Newsletter Email Blast	1 Complimentary Per Year	1 Complimentary Per Year	$600	$600

A 15% commission is allowed to recognized advertising agencies

THE MORE YOU ADVERTISE THE MORE YOU SAVE! *PE&RS* offers frequency discounts. Invest in a three-times per year advertising package and receive a 5% discount, six-times per year and receive a 10% discount, 12-times per year and receive a 15% discount off the cost of the package.

*Based on 2 readers per copy as well as online views| Source: *PE&RS* Readership Survey, Fall 2012

Digital Elevation Model Technologies and Applications: The DEM Users Manual, 3rd Edition

Edited by David F. Maune, PhD, CP
and Amar Nayegandhi, CP, CMS

To order, visit https://www.asprs.org/dem

The 3rd edition of the DEM Users Manual includes 15 chapters and three appendices. References in the eBook version are hyperlinked. Chapter and appendix titles include:

1. Introduction to DEMs
   David F. Maune, Hans Karl Heidemann, Stephen M. Kopp, and Clayton A. Crawford
2. Vertical Datums
   Dru Smith
3. Standards, Guidelines & Specifications
   David F. Maune
4. The National Elevation Dataset (NED)
   Dean B. Gesch, Gayla A. Evans, Michael J. Oimoen, and Samantha T. Arundel
5. The 3D Elevation Program (3DEP)
   Jason M. Stoker, Vicki Lukas, Allyson L. Jason, Diane F. Eldridge, and Larry J. Sugarbaker
6. Photogrammetry
   J. Chris McGlone and Scott Arko
7. IfSAR
   Scott Hensley and Lorraine Tighe
8. Airborne Topographic Lidar
   Amar Nayegandhi and Joshua Nimetz
9. Lidar Data Processing
   Joshua M. Novac
10. Airborne Lidar Bathymetry
    Jennifer Wozencraft and Amar Nayegandhi
11. Sonar
    Guy T. Noll and Douglas Lockhart
12. Enabling Technologies
    Bruno M. Scherzinger, Joseph J. Hutton, and Mohamed M.R. Mostafa
13. DEM User Applications
    David F. Maune
14. DEM User Requirements & Benefits
    David F. Maune
15. Quality Assessment of Elevation Data
    Jennifer Novac

Appendix A. Acronyms

Appendix B. Definitions

Appendix C. Sample Datasets

This book is your guide to 3D elevation technologies, products and applications. It will guide you through the inception and implementation of the U.S. Geological Survey's (USGS) 3D Elevation Program (3DEP) to provide not just bare earth DEMs, but a full suite of 3D elevation products using Quality Levels (QLs) that are standardized and consistent across the U.S. and territories. The 3DEP is based on the National Enhanced Elevation Assessment (NEEA) which evaluated 602 different mission-critical requirements for and benefits from enhanced elevation data of various QLs for 34 Federal agencies, all 50 states (with local and Tribal input), and 13 non-governmental organizations.

The NEEA documented the highest Return on Investment from QL2 lidar for the conterminous states, Hawaii and U.S. territories, and QL5 IfSAR for Alaska.

Chapters 3, 5, 8, 9, 13, 14, and 15 are "must-read" chapters for users and providers of topographic lidar data. Chapter 8 addresses linear mode, single photon and Geiger mode lidar technologies, and Chapter 10 addresses the latest in topobathymetric lidar. The remaining chapters are either relevant to all DEM technologies or address alternative technologies including photogrammetry, IfSAR, and sonar.

As demonstrated by the figures selected for the front cover of this manual, readers will recognize the editors' vision for the future – a 3D Nation that seamlessly merges topographic and bathymetric data from the tops of the mountains, beneath rivers and lakes, to the depths of the sea.

Co-Editors

David F. Maune, PhD, CP and
Amar Nayegandhi, CP, CMS

PRICING

Student (must submit copy of Student ID)	$50 +S&H
ASPRS Member	$80 +S&H
Non-member	$100 +S&H
E-Book (only available in the Amazon Kindle store)	$85

LEARN
DO
GIVE
BELONG

ASPRS

AMERICAN SOCIETY FOR PHOTOGRAMMETRY & REMOTE SENSING

ASPRS Offers

- » Cutting-edge conference programs
- » Professional development workshops
- » Accredited professional certifications
- » Scholarships and awards
- » Career advancing mentoring programs
- » *PE&RS*, the scientific journal of ASPRS

asprs.org